

https://dspace.org/

Rock strength domaining at Mogalakwena Mine, South Africa: An approach to on-site geometallurgical characterisation

Germiquet, Jason

2016-07-14
http://hdl.handle.net/10539/20586

Downloaded from a DSpace repository. https://dspace.org/

ROCK STRENGTH DOMAINING AT MOGALAKWENA MINE, SOUTH AFRICA

An Approach to On-Site Geometallurgical Characterisation

Jason Germiquet

(Student number: 675592)

School of Engineering and the Built Environment

University of the Witwatersrand

Johannesburg, South Africa.

A research report submitted to the Faculty of Engineering and the Built Environment, University of the Witwatersrand, Johannesburg, in partial fulfilment of the requirements for the degree of Master of Science in Engineering.

31 December 2015

DECLARATION

I declare that this research report is my own unaided work. The content covers research done at Mogalakwena Mine. It is being submitted for the Degree of Master of Science in Engineering by advanced coursework and research to the University of the Witwatersrand, Johannesburg. It has not been submitted before for any degree or examination to any other University.

……

Jason Germiquet

…….. day of …… year ……

ABSTRACT

The geometallurgical characteristics of ore are key drivers of value realisation when applied to the optimisation of mining and plant processing. The variability of ore strength and hardness has an impact on crushing, milling and liberation efficiency due to the method in which different rock behaves under stress and grinding. Mogalakwena Mine is exploiting the intrusive Platreef which forms part of the Northern Limb of the Bushveld Complex. This complex orebody exhibits areas of metasomatic alteration, metamorphism and sporadic mineralisation of the footwall and hanging wall. These different varieties of ore type have various hardness and strength characteristics. These variables must be known prior to processing in order to optimise recovery. Predictive modelling is vital before ore is mined and processed. Exploration core represents accurate geological data and this database was used to source rock strength information. The textural and grain size distribution of each rock type in the reef was investigated for the Overysel (OY) farm. Point load testing is done on core samples in each borehole and is converted to uniaxial compressive strength (UCS). The relationship between lithology, texture, grain size and UCS was examined. There is an inverse relationship between UCS and grain size for unaltered rocks while altered rocks do not exhibit this relationship. Strength and hardness mean results were compared with evidence that bond work index and UCS may be related. Drilling performance is linked to UCS and more accurate UCS values for blast patterns assists in scheduling. The grain size adjusted UCS values was applied to a 3D model for OY farm. The model represents rock strength changes across the ore body. The model can be updated at a smaller grid spacing using strength data generated by digitally recorded drilling measurements. The project forms part of establishing relevant data and data sources for a larger geometallurgical programme. The project reveals that ore categories can be tailored to represent variables which impact mining performance and, with more data, plant performance. The financial benefits of strength domaining are made clear in the use of autogenous milling.

Dedicated to Jean-Daniel (Dan) Germiquet

1949 - 2013

CONTENTS

ACKNOWLEDGEMENTS viii

LIST OF FIGURES ix

LIST OF TABLES xvi

LIST OF ABREVIATIONS xix

CHAPTER 1: INTRODUCTION 1

1.1 Mine Background 4

1.1.1 History 4

1.1.2 Mining – Drilling and Blasting 5

1.1.3 Mine Layout 8

1.1.4 Concentrator Plants 9

1.1.5 Exploration and Core Logging 10

1.1.6 Competitors 12

1.2 Aim 12

1.3 Objectives 15

1.4 Available Databases 15

1.4.1 Exploration Database 15

1.4.2 Blast hole Database 16

1.4.3 Rock Strength and Hardness 17

1.4.4 RockMa Database 18

1.4.5 Deswick 18

1.5 Project Area 19

1.6 Summary 20

CHAPTER 2: LITERATURE REVIEW 21

2.1 Introduction 21
2.2 Geometallurgy 21
2.2 Geology 26
2.2.1 Geological Setting 26
2.2.2 Lithological Classification System 32
2.2.3 Rock Types 34
2.2.4 Alteration 38
2.2.5 Texture 38
2.3 Rock Hardness and Strength 40
2.3.1 Texture, Grain Size and Strength Relationship 42
2.4 Hardness and Strength Tests 42
2.5 Drilling 43
2.5.1 Machine variables affecting drilling performance 44
2.6 Summary 48
CHAPTER 3: METHODOLOGY 49
3.1 Introduction 49
3.2 Textural Distribution of Major Rock Types 49
3.3 Rock Strength and Textural Distribution 51
3.4 Strength and Hardness Relationships 51
3.5 Drilling Performance and Rock Strength 51
3.6 Strength Modelling 52
3.7 Financial benefit Analysis 53
3.8 Summary 53
CHAPTER 4: RESULTS AND INTERPRETATION 54
4.1 Introduction 54
4.2 Textural Distribution of Major Rock Types 54

4.2.1 Lithology Distribution Analysis 56
4.2.2 Reef Distribution 58
4.2.3 Textural Distribution 59
4.2.4 Grain Size Distribution 62
4.2.5 Field Checks 86
4.3 Rock Strength and Textural Relationship 90
4.3.1 Strength, Texture and Grain Size 92
4.3.2 Field Tests -Validation Dataset 106
4.3.3 Summary of Grain Size Adjusted UCS 113
4.4 Strength and Hardness Relationships 115
4.4.1 BWI vs. UCS 116
4.5 Drilling Performance and Rock Strength 118
4.5.1 Penetration Rates and Rock Types 118
4.5.2 RockMa MWD Initiative 122
4.6 Rock Strength Modelling 127
4.7 Summary 129
CHAPTER 5: FINANCIAL BENEFITS OF ORE STRENGTH CHARACTERISATION 130
5.1 Introduction 130
5.2 South Plant 130
5.3 Financial Benefit Analysis 132
5.4 Proposed Feed Material Optimisation Plan 134
5.5 Summary 135
CHAPTER 6: DISCUSSION AND CONCLUSION 136
6.1 Introduction 136
6.2 Discussion 136

6.2.1 Textural Distribution 136
6.2.2 Rock Strength and Textural Relationship 139
6.2.3 Strength and Hardness Relationships 142
6.2.4 Drilling Performance and Rock Strength 143
6.2.5 Rock Strength Modelling 145
6.2.6 Potential Financial Benefits 146
6.3 Conclusion 147
6.4 Recommendations 150
REFERENCES 152
APPENDIX 159

ACKNOWLEDGEMENTS

Thanks to my supervisor, Richard Minnitt for his guidance and support of my efforts to venture widely in the area of research.

Thanks go to the following for their technical support, recommendations and assistance at Mogalakwena Mine; Trust Muzondo, Charles Radzivhoni, Deon Spies, Phutela Myeni, Mavis Lehutjo, Nosipho Kasa and Jacques du Toit. My gratitude goes to the Exploration Department staff at Mogalakwena Mine for allowing and assisting with the PLI test work, information on logging and access to the exploration database; James Winch, Fiona Stevens, Sakhile Befile and Herman Freysen. Special thanks to Lesibama Klimboy for assisting with the PLI test work. Thanks to the team at Anglo American Research for answering many questions, allowing me to visit the centre and highlighting potential areas that would add value to Mogalakwena Mine; Robert Schouwstra, Deryck de Vaux, Jacques Roberts, Doug Philips and Shauna McClutcheon.

A special thanks to Alan Bye for sharing his knowledge on the Platreef, rock mechanics and measurement while drilling technology. Thanks to Phil Piper for guidance on PLI testing and Calvin Morrison for the information covering the use of RockMa technology. Thanks to the drilling crew of PV149 for allowing me to spend several shifts with them and for sharing the invaluable truths of drilling in a production environment.

Thanks to Hendrik van Niekerk, MRM Manager, for endorsing the project. Thanks to the Human Resource Development department at Anglo American Platinum for approving the funding for the project.

Thanks to friends and family for their constant support. Finally, thanks to Claire Robartes for understanding that my excuses for working late were honourable.

LIST OF FIGURES

Figure 1: Mogalakwena Mine as part of Anglo American Platinum's portfolio. 5
Figure 2: Operational scenario at North Pit showing scale of mining equipment... 6
Figure 3: Three Atlas Copco 351 Pit Vipers drilling in North Pit. 6
Figure 4: Mogalakwena property with satellite image and farm names. Platreef outcrop indicated with red line. 8
Figure 5: View from Big Mike crusher over the North Concentrator. In the centre is the A-frame over the secondary cone crushers. 9
Figure 6: View from Big Bruce crusher over South Concentrator. 10
Figure 7: Prospecting and mining rights outlined. Exploration hole positions marked. (Source: Exploration Department) 11
Figure 8: Summary of aims of the project, the data used and the source of the data. 14
Figure 9: Geologist logging drill chips from a Pit Viper. The chip lithology is entered in SABLE Database Warehouse. 17
Figure 10: Current rock properties required in the SABLE database after chip logging. 17
Figure 11: Mogalakwena Mine with project area indicated with the insert showing the entire mine property. 19
Figure 12: North Pit production pit (looking south). 20
Figure 13: Replicating difference in UCS between pyroxenite and other rocks (Ziemski *et al*., 2010). 24
Figure 14: Plan view of Bushveld Complex. Insert is Northern Limb (modified after Cairncross & Dixon, 1995). 27
Figure 15: Geological map of the Platreef, Northern Limb with Mogalakwena pits marked (Holwell & McDonald, 2010) 29
Figure 16: Plan view of Mogalakwena Mine mining lease with rock types illustrated. 30
Figure 17: S-N Section view of mineral rights area. Operational pits only exist on Sandsloot, Zwartfontein and Overysel farms. 31

Figure 18: Generalised stratigraphy of the Platreef in relation to the Western Bushveld (Bye, 2003). 32
Figure 19: Ternary diagram of gabbroic rocks (Copyright 2014 by Andrew Alden, geology.about.com, reproduced under educational fair use). 35
Figure 20: Feldspathic pyroxenite (major reef rock type) showing cumulus pyroxene and intercumulus plagioclase. 36
Figure 21: Close up photograph of brecciated agmatite - termed granofels on site. 37
Figure 22: Granofels in the footwall showing distinct variation in composition. Changes in composition are irregular. 38
Figure 23: UCS vs. DWT (AxB) showing a good correlation (Bye, 2004). 43
Figure 24: Typical ROP vs. WOB response plot (Source: Osgouei, 2007) 45
Figure 25: Mean drilling penetration rate for 3 drill rig types per stratigraphic unit (Source: Du Toit, 2014) 46
Figure 26: 326-085 being drilled and the reporting of relative rock strength by PV149 48
Figure 27: Distribution of 754 exploration holes located on Overysel farm used for hardness data. 55
Figure 28: Stratigraphic distribution of OY exploration database. 57
Figure 29: Lithological distribution in the reef package at OY. 59
Figure 30: Textural distribution in the reef. 61
Figure 31: Textural distribution in the footwall. 62
Figure 32: Feldspathic pyroxenite - Textural distribution of feldspathic pyroxenite. 64
Figure 33: Feldspathic pyroxenite - Grain size distribution for each textural description. 65
Figure 34: Pyroxenite - Textural distribution of pyroxenite. 66
Figure 35: Pyroxenite - Grain size distribution for each textural description. 67
Figure 36: Serpentinite - Textural distribution of serpentinite. 68
Figure 37: Serpentinite - Grain size distribution for each textural description. 69
Figure 38: Serpentinised pyroxenite - Textural distribution of serpentinised pyroxenite. 70

Figure 39: Serpentinised pyroxenite - Grain size distribution for each textural description. 71
Figure 40: Serpentinised feldspathic pyroxenite - Textural distribution of serpentinised feldspathic pyroxenite. 72
Figure 41: Serpentinised feldspathic pyroxenite - Grain size distribution for each textural description. 73
Figure 42: Pegmatoidal feldspathic pyroxenite - Textural distribution of pegmatoidal feldspathic pyroxenite. 74
Figure 43: Pegmatoidal feldspathic pyroxenite - Grain size distribution for each textural description. 75
Figure 44: Parapyroxenite - Textural distribution of parapyroxenite. 76
Figure 45: Parapyroxenite - Grain size distribution for each textural description. 77
Figure 46: Serpentinised parapyroxenite - Textural distribution of serpentinised parapyroxenite. 78
Figure 47: Serpentinised parapyroxenite - Grain size distribution for each textural description. 79
Figure 48: Feldspathic parapyroxenite - Textural distribution of feldspathic parapyroxenite. 80
Figure 49: Feldspathic parapyroxenite - Grain size distribution for each textural description. 81
Figure 50: Calc-silicate - Textural distribution of calc-silicate. 82
Figure 51: Calc-silicate - Grain size distribution for each textural description. ... 83
Figure 52: Granofels - Textural distribution of granofels. 84
Figure 53: Granofels - Grain size distribution for each textural description. 85
Figure 54: Isolated area of mineralised Cr-rich feldspathic pyroxenite lying within barren hanging wall gabbronorite. 86
Figure 55: North Pit with bench outlines. The ore line is running N-S with the blue line showing the hanging wall contact. 326/063 is falling in the hanging wall. 87
Figure 56: 326/063 is within the expected hanging wall waste. The black line represents the presence of discordant reef material rich in Cr and PGEs. 87

Figure 57: Sharp contact between barren gabbronorite and feldspathic pyroxenite from 326/063. 88
Figure 58: Sharp contact between fine grained Cr-rich feldspathic pyroxenite and a medium grained feldspathic pyroxenite from 326/063. The Cr-rich component is higher in PGE content with a direct relationship with more mafic minerals. 89
Figure 59: A fine-grained serpentinite has a sharp contact with a coarse grained feldspathic pyroxenite. The feldspathic pyroxenite then becomes finer towards the bottom of the photograph. 89
Figure 60: A feldspathic pyroxenite which grades from medium to fine-medium grain size. A sharp contact with a fine grained chromitite seam is seen on the right. 90
Figure 61: UCS data per rock type - initial study. 92
Figure 62: Grain size and UCS for feldspathic pyroxenite using cumulus, varied and blank textures. 94
Figure 63: Grain size and UCS for feldspathic pyroxenite using cumulus, varied and blank textures (M-PEG grain size removed). 94
Figure 64: Grain size and UCS for pyroxenite using cumulus and blank textures. 95
Figure 65: Grain size and UCS for serpentinite using cumulus, homogeneous, recrystallised and blank textures..... 96
Figure 66: Grain size and UCS for serpentinised pyroxenite using cumulus, recrystallised and blank textures..... 97
Figure 67: Grain size and UCS for serpentinised feldspathic pyroxenite using cumulus, recrystallised and blank textures. 98
Figure 68: Grain size and UCS for pegmatoidal feldspathic pyroxenite using pegmatoidal texture..... 99
Figure 69: Grain size and UCS for pegmatoidal feldspathic pyroxenite using pegmatoidal texture. M grain size category has been removed. 100
Figure 70: Grain size and UCS for parapyroxenite using cumulus, recrystallised and blank textures. 101
Figure 71: Grain size and UCS for parapyroxenite using cumulus, recrystallised and blank textures. 102

Figure 72: Grain size and UCS for serpentinised parapyroxenite using cumulus, recrystallised and blank textures..... 103
Figure 73: Grain size and UCS for calc-silicate using cumulus, recrystallised and blank textures..... 104
Figure 74: Grain size and UCS f\or feldspathic pyroxenite using cumulus, varied and blank textures. 1984 samples..... 106
Figure 75: The 100 samples from 4 BHs. Samples were measured to 10cm and cut with a diamond core cutter. 107
Figure 76: Mr Lesibama Klimboy Teffo operating the Point Load equipment during the testing of the 100 samples. 107
Figure 77: Sample 25 from ZN981D0 exhibiting a fine-medium grained assemblage of euhedral clinopyroxene and orthopyrothene crystals with intercumulus anorthite. 108
Figure 78: Sample 25. 108
Figure 79: Sample 10 from ZN890D0. Sample was marked and cut before undergoing PL test. 108
Figure 80: Sample 10 from ZN890. 109
Figure 81: Sample 28 from ZN891D0 showing a pegmatitic texture. 109
Figure 82: Sample 28 with mica minerals..... 109
Figure 83: Grain size vs. UCS for feldspathic pyroxenite (validation dataset)... 111
Figure 84: Two distinct population groups defined by grain size and composition in granofels..... 112
Figure 85: OY1023 showing measured UCS (as calculated from PLI) and mean UCS for the rock type. 115
Figure 86: BWI vs. UCS for means for OY..... 116
Figure 87: BWI vs. UCS OY means excluding pyroxenite. 117
Figure 88: BWI vs. UCS from Zwartfontein means excluding pyroxenite. 117
Figure 89: 326/050 with drilling grid falls within the reef package. 118
Figure 90: Pattern 323/036 and 326/037 lying across the HW and Reef contact. Ore line lies on toe elevation. 119
Figure 91: 411-076 falls within the estimated HW stratigraphy. 119

Figure 92: Penetration rates vs. UCS results from exploration defaults and those calculated for entire stratigraphic units 120
Figure 93: Penetration rates vs. UCS from the exploration database using rock types (Average UCS). 121
Figure 94: Penetration rates vs. UCS from exploration using rock types. 122
Figure 95: Pattern 326/141in HW drilled by PV149. 123
Figure 96: Legend for rock strength in the RockMa system. 123
Figure 97: View looking East at Cut 8 on bench 8. Rock strength is greater in the North and decreases towards the South. Blue line is the length of the photograph 124
Figure 98: A view of the section marked in Figure 99; Fresh FW Granofels is seen on the left of the picture and becomes oxidised moving towards the right (South) (contact shown at the position of the dashed line). Bench 8 crest and toe indicated between two black lines. 124
Figure 99: View of all Cut 8 drilling patterns. Colours represent relative rock strength data reported by PV149. Patterns with no rock strength data were not drilled by PV149. Lines represent estimated reef zone (HW contact is blue and FW is red). 125
Figure 100: An oblique view of relative rock strength data for patterns in Cut 8. The red line shows the uneven dip of reef revealed through drilling through the FW contact. 126
Figure 101: PV149 planned drilling for February. Drilling time for 408/119 and 411/077 is proportional yet bench 408 is oxidised with a significantly higher ROP. 126
Figure 102: Rock strength legend: 138 - 300MPa 127
Figure 103: 3D rendered model. Blue line indicates HW contact and red line indicates FW contact. The lighter green colours within the reef indicate lower rock strengths. 128
Figure 104: Isosurface set at 220MPa. 129
Figure 105: View from Big Bruce crusher over South Plant conveyor system where coarse and fine crushed material is split at the 110mm grizzly. 131

Figure 106: Schematic diagram of South Plant crushing and milling for section A and B. Red block shows coarse material stockpile which can be optimised with improved ore strength feed. 131
Figure 107: South Plant milled tons for 2014 with potential increase in coarse material due to optimised ore feed. 133
Figure 108: Proposed modelling and stockpiling stage before primary crushing to South Plant using a 190Mpa division. 135

LIST OF TABLES

Table 1: Drilling results for the years 2011 to 2014 for all rigs. 7
Table 2: Exploration boreholes drilled in OY property. 11
Table 3: Generalised minerals in the common rocks of the Northern Limb (Nex *et al*., 2006). 33
Table 4: Textural associations of PGM (excluding Au/Ag alloys) in the variety of host-rock types and the percentage of grains (Source: Holwell *et al*, 2006) 39
Table 5: Grain size categories (Bell, 1983). 40
Table 6: Total percentage of rock types in the OY exploration database. 56
Table 7: Waste and ore production per year. 58
Table 8: Total reported waste and ore production from 2011 to 2013. 58
Table 9: Textural abbreviations and descriptions. 60
Table 10: Distribution of textures in the reef. 61
Table 11: Textural distribution in the footwall granofels. 62
Table 12: Grain size abbreviations and descriptions used in the report. 63
Table 13: Feldspathic pyroxenite - Grain sizes per texture and their occurrence in the exploration database in meters. Dominant grain sizes are highlighted in green. 65
Table 14: Pyroxenite - Grain sizes per texture and their occurrence in the exploration database in meters. Dominant grain sizes are highlighted in green. .. 67
Table 15: Serpentinite - Grain sizes per texture and their occurrence in the exploration database in meters. Dominant grain sizes are highlighted in green. .. 69
Table 16: Serpentinised pyroxenite - Grain sizes per texture and their occurrence in the exploration database in meters. Dominant grain sizes are highlighted in green. 71
Table 17: Serpentinised feldspathic pyroxenite - Grain sizes per texture and their occurrence in the exploration database in meters. Dominant grain sizes are highlighted in green. 73

Table 18: Pegmatoidal feldspathic pyroxenite - Grain sizes per texture and their occurrence in the exploration database in meters. Dominant grain sizes are highlighted in green. 75
Table 19: Parapyroxenite - Grain sizes per texture and their occurrence in the exploration database in meters. Dominant grain sizes are highlighted in green. .. 77
Table 20: Serpentinised parapyroxenite - Grain sizes per texture and their occurrence in the exploration database in meters. Dominant grain sizes are highlighted in green. 79
Table 21: Feldspathic parapyroxenite - Grain sizes per texture and their occurrence in the exploration database in meters. Dominant grain sizes are highlighted in green. 81
Table 22: Calc-silicate - Grain sizes per texture and their occurrence in the exploration database in meters. Dominant grain sizes are highlighted in green. .. 83
Table 23: Granofels - Grain sizes per texture and their occurrence in the exploration database in meters. Dominant grain sizes are highlighted in green. .. 85
Table 24: Rock tests from 1996 to 2006 (Source: Little, 2006)..... 90
Table 25: UCS data per rock type 91
Table 26: Grain size and UCS relationship for feldspathic pyroxenite 93
Table 27: Grain size and UCS relationship for pyroxenite. 95
Table 28: Grain size and UCS relationship for serpentinite. 96
Table 29: Grain size and UCS relationship for serpentinised pyroxenite. 97
Table 30: Grain size and UCS relationship for serpentinised feldspathic pyroxenite. 98
Table 31: Grain size and UCS relationship for pegmatoidal feldspathic pyroxenite. 99
Table 32: Grain size and UCS relationship for parapyroxenite. 101
Table 33: Grain size vs. UCS relationship for serpentinised parapyroxenite. 102
Table 34: Grain size vs. UCS relationship for feldspathic pyroxenite. 103
Table 35: Grain size vs. UCS for calc-silicate. 104
Table 36: Grain size vs. UCS relationship for granofels. 105
Table 37: Results for feldspathic pyroxenite from the validation PLI test dataset. 110

Table 38: UCS results for 2 components of granofels from the validation PLI test dataset..... 111
Table 39: Summary of grain size and UCS (MPa) relationship for all mineralised rock types. 113
Table 40: Mean UCS values used at Mogalakwena Mine based on these tests (Little, 2006)..... 114
Table 41: Penetration rate per stratigraphic unit from PV149. 120
Table 42: Penetration rate per rock type from PV149. 121
Table 43: Total downtime per month due to depletion of coarse feed material.. 132
Table 44: Total milled tons lost due to depletion of coarse material..... 132
Table 45: The assumptions used for the financial benefit calculation..... 133

LIST OF ABREVIATIONS

ARC	Anglo Platinum Research Centre (now Anglo American Technical Solutions)
BH	Borehole
BC	Bushveld Complex
BIF	Banded Iron Formation
BMS	Base Metal Sulphides
BWI	Bond Work Index
CAD	Computer Aided Design
CCIC	Caracle Creek International Consulting
CZ	Critical Zone
DWT	Drop Weight Test (A x b)
FW	Footwall
HW	Hanging Wall
IUGS	International Union of Geological Sciences
ISRM	International Society for Rock Mechanics
JCI	Johannesburg Consolidated Investment
LOM	Life of Mine
LZ	Lower Zone
MLA	Mineral Liberation Analyser
MWD	Measurement While Drilling
MZ	Main Zone
OY	Overysel farm
PGE	Platinum Group Elements (Pt, Pd, Rh, Ru, Ir and Os)
PGM	Platinum Group Minerals
PL	Point Load test
PLI	Point Load Index (Calculated Index)
PSD	Particle Size Distribution
PV	Pit Viper
R	Reef
RLS	Rustenburg Layered Suite
ROP	Rate of Penetration
RPM	Revolutions per Minute
SS	Sandsloot farm
UCS	Uniaxial Compressive Strength
UG2	Upper Group 2
ZN	Zwartfontein farm

CHAPTER 1: INTRODUCTION

The mineral resource is the primary asset of a mining company and remains constant throughout economic cycles. The continued study and understanding of this asset leads to greater potential for extractive efficiency. Mogalakwena Mine continuously strives towards world leading extractive practices. The aim of this project is to investigate the textural and strength characteristics of the Platreef orebody and relate them to rock strength. The integration of rock description, rock test methods and measurement while drilling technology into a geometallurgical modelling framework has the potential to unlock value in downstream processes such as drilling performance prediction and comminution.

Mogalakwena Mine is the flagship mine of Anglo American Platinum Ltd producing mainly platinum group element (PGE), copper and nickel. The mine is highly mechanised and boasts a good safety record. The life of mine (LOM) indicates that production volumes will be constant for at least 78 years on currently operational properties. Exploration has good coverage on the operational farm and is targeting expansion projects to the north. The optimisation of such an asset will have proportionately large financial benefits for the mine and company.

The Platreef is a complex PGE bearing Cu-Ni deposit of the Rustenburg Layered Sequence (RLS). The RLS in turn constitutes the mafic sequence of the parent Bushveld Complex (Johnson *et al.*, 2006). The multifaceted ore body has little in common with the well-known Merensky and Upper Group 2 (UG2) reefs (Johnson *et al.*, 2006; McDonald *et al,* 2005) and has been the site of many academic studies to this effect. Differences in ore type primarily occur along strike as footwall lithologies change (Maier *et al.*, 2007; Kinnaird *et al.*, 2010). Other influences on ore type differences include pervasive alteration, platinum group mineral (PGM) changes and the mineralisation of hanging wall and footwall lithologies (Maier *et al.*, 2007; Armitage *et al.*, 2002; Gloy, 2005).

The expansion of the mine along strike has resulted in the exploitation of different ore types. This would require continual test work on newly exposed rock types in order to accurately characterise the resulting plant feed. The plant has suffered sporadic drops in recovery due to the changing character of the ore. There is constant difficulty in providing the required geometallurgical characteristics before the ore is processed (Gloy & Hey, 2002). This is compounded by the incredibly high rate of production.

Geometallurgical projects require accurate and relevant input data in order to model the effects of mined material on mining equipment and downstream operations (Gloy & Hey, 2002). Comminution represents the most significant operating cost (Barrat & Doll, 2008). The potential to unlock value by optimising plant processes exists in any operation and continued investigation into plant effectiveness is needed (Burger *et al*., 2006). These projects aim to limit geometallurgical risk and improve efficiency and the effectiveness of mine and plant equipment (Chibaya, 2013). The key drivers of metallurgical response at the plant are primarily ore hardness and mineralogy (Radzivhoni *et al*., 2014). Each of these variables is determined by multiple factors including rock strength and composition. An accurate data set needs to be aligned to operational requirements for effective modelling (Barrat & Doll, 2008).

Rock strength and hardness, important geometallurgical variables, are influenced by a number of variables (Dhungana, 2013). Compositional proportions in rocks have shown conflicting results when used to describe rock strength (Ozturk *et al*., 2014). This can be attributed to complex grain relationships (Ozturk *et al*., 2014) and textural differences (Roberts & Reinecke, 2003). Applying standardised and mean strength parameters to ore based on lithological description alone is thus problematic.

Drilling performance is affected by rock characteristics with rock strength being a primary influence (Heinz, 2009; Bourgoyne *et al*., 1986). Production drilling rigs at Mogalakwena Mine display drilling parameters on the operator's screen. Only

depth and time per hole drilled was manually reported by operators. The possibility of expanding the amount of drilling data reported by operators was investigated by attempting to manually record drilling parameters. Initial results proved to include inaccuracies and could not be practically implemented. The advent of digitised real-time drilling parameter recording solved the problematic manual recording inaccuracies. This is termed measurement while drilling (MWD) technology. Drilling data accuracy has been achieved through the implementation of the RockMa digital logging system. The RockMa system was installed on all production drilling rigs during 2014. Strength proxies allow for the prediction of certain rock properties, machine specifications and operating conditions (Napier-Munn *et al*., 1999). The information reported by RockMa has opened a potential avenue for low cost ore strength characterisation through the potential to proxy drilling performance data. MWD strength data generated by production drilling and the RockMa software can be used to feed into a rock strength model per blast. Scheduling of drilling rigs can be more accurately achieved with the incorporation of mean penetration rates for the rock types expected in the pattern.

Strength domains can be delineated for geometallurgical needs which can be used for plant relevant hardness characterisation. This can be achieved while a blast pattern is still in the drilling phase. The modelled strength domains can be compared to plant relevant rock tests which replicate plant performance of ore. This can be achieved through correlating RockMa data to hardness test results in the mine database once the RockMa system is fully operational. This allows for the correlation of measured rock properties with process parameters in order to spatially model hardness domains. Additional ore variables can be compared to the RockMa data regression analyses. New technologies, such as MWD, are indicative of the future of mining involving real time data collection and usage.

The project forms part of the preliminary step of utilising MWD to model plant behaviour. The project will lead to a classification scheme for ore patterns based on the MWD results. The hardness characterisation could ultimately feed into a

greater geometallurgical programme to characterise plant feed as a proactive tool to approximate plant performance and eventually to the recovery of economic minerals. The characterisation of the feed material is needed to predict breakage characterisation in the plant. Rock type distributions including textural and grain size characterisation are necessary to add to the geometallurgical parameters per blast pattern.

In summary, the ultimate objective of this research is to combine continuous drilling data with ore hardness characterisation allowing real-time inputs into a geometallurgical domaining programme. It would be necessary to gain ore strength and possibly hardness data before or during mining efforts as a proactive approach to predicting comminution performance. The project aims to incorporate the rock strength database from exploration core to predict drilling performance in ore rocks and to predict crushing and milling efficiency. The increase in data accuracy, systems to collect data from chip logging and the MWD database allows for wider information gathering. The data will fill the geometallurgical need for accurate rock strength data and continuous feeding of information into fit for purpose models.

1.1 Mine Background

1.1.1 History

The Platreef was discovered by Dr Hans Merensky in 1924 (Allen, 1996). By 1925, eight shallow trenches, a 30m deep vertical shaft and an inclined winze had exposed the Platreef on Sandsloot, as well as two shafts on Zwartfontein and Vaalkop. In 1926 a treatment plant was set up and by 1928 1122 tons of concentrate had been produced after mining approximately 110 000 tons of ore. The 1930's financial depression and consequential fall in the platinum price resulted in the ceasing of mining operations. In 1968, bulk sampling was done in two exploratory winzes on Zwartfontein by Johannesburg Consolidated Investments (JCI). Sixty-eight boreholes were drilled in the current lease area by

the end of 1971. By 1975, it was identified that an open pit mining operation could be feasible. In 1976 soil sampling, mapping, geophysical surveys and percussion drilling identified five target areas for intensive diamond bit drilling. An underground exploration shaft was sunk in 1980 which allowed for the delineation of a broad Platreef stratigraphy (A, B & C Reef). After trial mining on Sandsloot and Tweefontein North in 1988, it was announced in September 1990 that the development of a major new open pit mine would commence. The first blast occurred on Sandsloot in February 1992.

1.1.2 Mining – Drilling and Blasting

Mogalakwena Mine (previously known as Potgietersrus Platinum Mine, PPL or PPRust) is the largest open cast platinum mine in the world and is situated on the Northern Limb of the Bushveld Complex (Figure 1). The mine is exploiting the PGE, Cu and Ni bearing Platreef. The open pit mine is fully owned and managed by Anglo American Platinum Ltd. and represents the largest producing mine in the company portfolio in both tons and ounces produced. The current LOM is 78 years for open pit mining. However, the option of underground mining remains once open pit mining has been concluded.

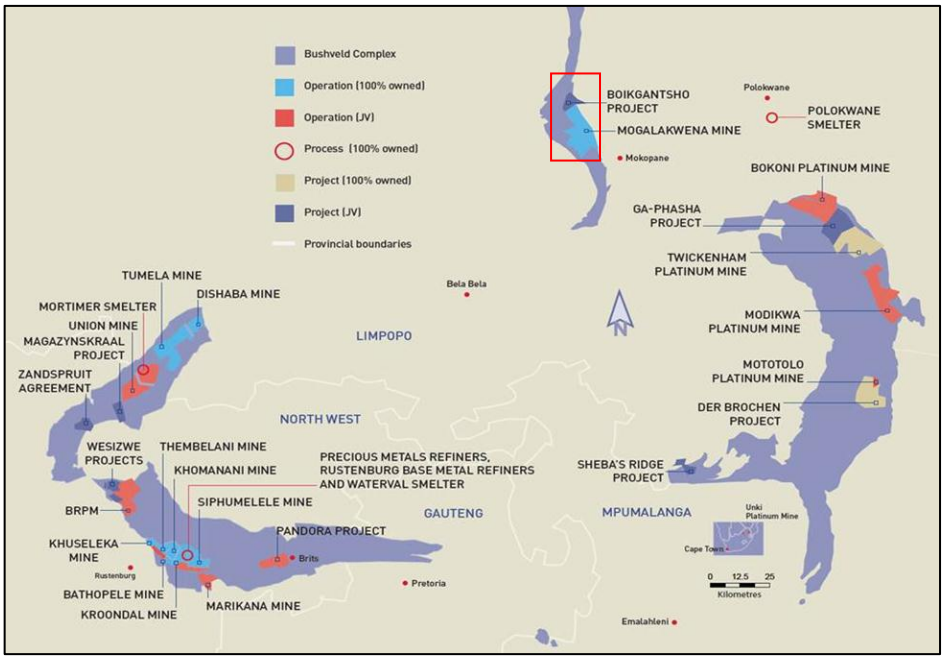


Figure 1: Mogalakwena Mine as part of Anglo American Platinum's portfolio.

Mogalakwena is a highly mechanised mine producing upwards of 250 000 tons per day (Figure 2 and Figure 3). Production monthly targets are in the range of 7.7 million tons. A stripping ratio of 5:1 is targeted across the property.



Figure 2: Operational scenario at North Pit showing scale of mining equipment.



Figure 3: Three Atlas Copco 351 Pit Vipers drilling in North Pit.

The Atlas Copco Pit Viper 351 constitutes the majority of production drilling (Figure 4). The drilling rigs use a top drive rotary mechanism with no percussive action. At the North Pit the Atlas Copco Pit Viper 351 is used to drill 250mm and 311mm rotary blast holes. Annual drilling production can be upwards to 1 million meters (Table 1). The 2014 monthly target for drilling is 134 483m.

Table 1: Drilling results for the years 2011 to 2014 for all rigs.

Year	Total Drilled Meters
2011	1 132 912
2012	841 805
2013	1 160 441
2014	1 366 193

Daily drilling targets for the Pit Viper (PV) fleet is in the range of 1,500m and represents a large amount of drilling data. Drilling represents a significant cost in the mining operation.

Blasting practices follow strict controls at Mogalakwena Mine. A mixture of ammonium nitrate porous prill, emulsion and gassing solution is pumped into blast holes and stemmed. Timing is standardised according to hole size and the major rock response is expected to realise optimal fragmentation for effective loading. Major challenges experienced include collapsing holes and misfires. Areas of potential improvement include blasting according to grade categories (separation of waste and ore by controlling throw direction) and optimising fragmentation for comminution processes.

1.1.3 Mine Layout

Five pits are located along the outcrop of the ore body striking NNW-SSE. The pits are located on the farms (from North to South) Overysel (OY), Zwartfontein (ZN) and Sandsloot (SS) (Figure 4Table 4).

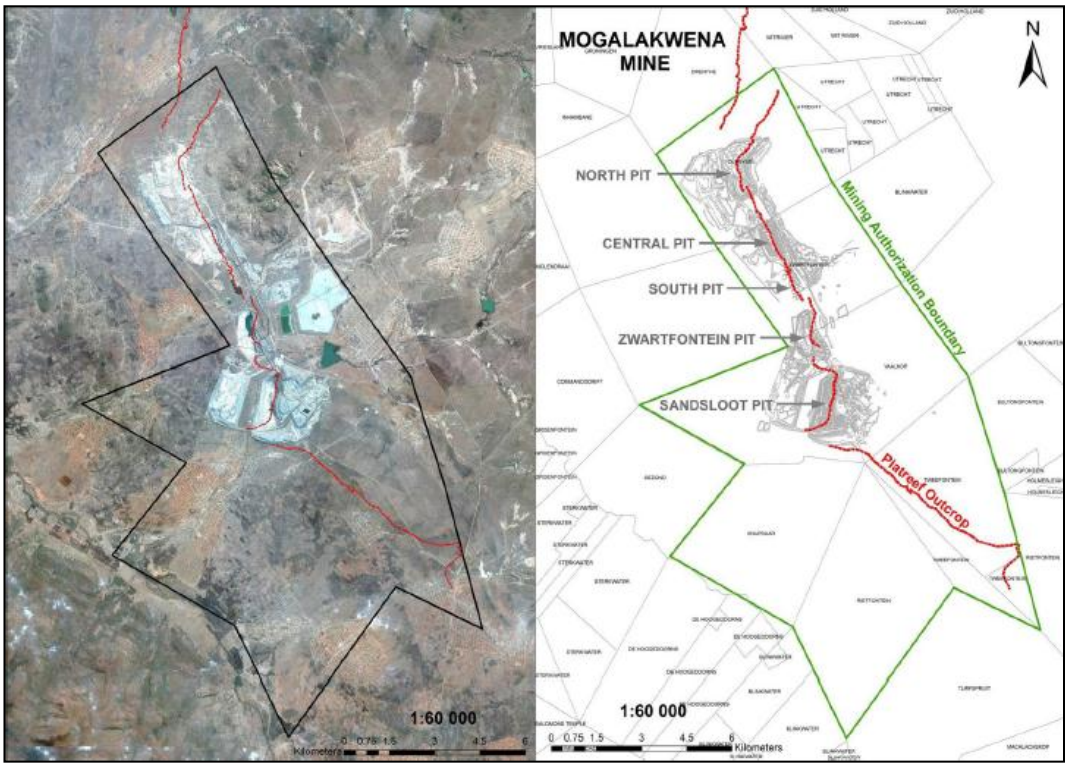


Figure 4: Mogalakwena property with satellite image and farm names. Platreef outcrop indicated with red line.

The North Pit is located on OY. This pit is the largest and contributes 80% of production at the mine. The pit forms the focus of this project. The North Pit is the site of the most recent exploration data and is the most densely covered by production drill rigs. The lithological variety is not as complex as the Southern portion of the property and will serve as a more simplistic test programme for comparing drilling performance to rock properties.

1.1.4 Concentrator Plants

Two crushers feed two separate plants resulting in 25,000 ounces (4E) being produced every month. The South Plant processes 400,000 tons of ore a month while the North Plant has a capacity of 600,000 tons per month. At Mogalakwena Mine, 2 primary gyratory crushers and secondary cone crushers feed material to either ball mills or autogenous mills.

1.1.4.1 North Plant

Big Mike crusher, the larger of the two crushers, is primarily fed material from OY farm averaging 25,000 tons of ore crushed daily and transported by conveyor belts to the North Concentrator (Figure 5).



Figure 5: View from Big Mike crusher over the North Concentrator. In the centre is the A-frame over the secondary cone crushers.

The primary crusher aims to crush ore to <185mm. The material is crushed by secondary jaw crushers to <45mm and then by cone crushers to <17mm. The material is then sent to the primary mills.

1.1.4.2 South Plant

Big Bruce is the primary crusher for the South Concentrator (Figure 6). The material fed to this crusher is sourced for the farms ZN and SS. Although South Concentrator has a significantly lower ton throughput (Figure 6), there is scope to stabilise increased performance.



Figure 6: View from Big Bruce crusher over South Concentrator.

The South Plant will be investigated further when the results of the research are applied in characterising the feed ore hardness to the plant.

1.1.5 Exploration and Core Logging

An extensive brownfields exploration project is managed on site. The project targets down dip resources and expansions between pits. The quantity of drilling over the history of the mine has created a large database. A total of 754 boreholes have been drilled in OY (Table 2).

Table 2: Exploration boreholes drilled in OY property.

BHs	**754**
Drilled meters	**315,022.35m**
Core loss meters	**7,347.99m**

The total number of exploration holes drilled since 1967 is upwards of 4,500m in the entire mine boundary (Figure 7). This amounts to a total of 1,034,497m to the end of 2013. The exploration drilling budget for 2014 is 45,000m.

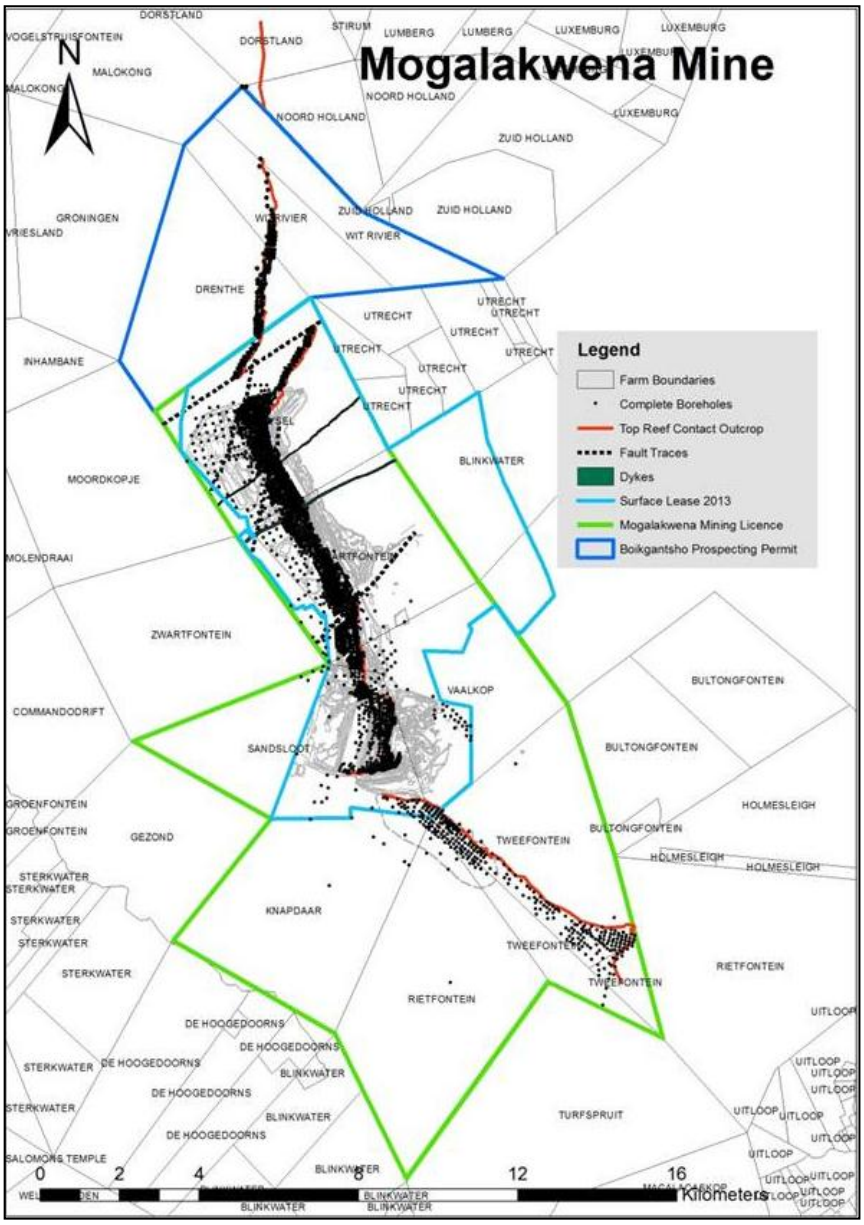


Figure 7: Prospecting and mining rights outlined. Exploration hole positions marked. (Source: Exploration Department)

Anglo American Platinum has recently acquired the exploration rights to the Boikgantsho farm north of the mining lease area which includes Drenthe and Witrivier farms. This farm will be explored for the potential of expanding mining operations northwards. Core logging is carried out at the exploration department by geologists from both Mogalakwena Mine and Caracle Creek International Consulting (CCIC).

1.1.6 Competitors

The Northern Limb has generally continuous PGE resources along its 130km strike length which stretches from Mokopane to Harriet's Wish. The shallow nature of available resources has garnered attention from a variety of large, mid and junior mining companies.

Ivanhoe Mining is currently sinking a bulk sampling shaft down dip from Mogalakwena and is planning to start production in late 2015. They have identified 2 tabular reefs locally named the Flatreef.

PTM is currently exploring and ramping up on decline shafts on their Waterberg project. Mineralisation occurs in Main Zone norites and gabbro-norites. The property is on the northern extremity of the Northern Limb.

Exploration projects owned by Sylvania and Lonmin (Akanani project) also exist on the Northern Limb.

1.2 Aim

The project aims to use cost effective means to understand the textural and hardness relationship. Correlating pre-existing data from various databases will allow mining processes to gain from cross referenced data analysis. The

information can be used to generate a strength model applicable to production and plant processes. The aims can be summarised as follows:

- Find simplistic method of categorisation of lithology, texture and grain size.

- Apply hardness data to lithology based on grain size from exploration database.

- Investigate the relationship between UCS to crushing and milling proxy tests (drop weight test (DWT) and bond work index (BWI) respectively).

- Investigate rock strength effects on drilling and the application of measurement while drilling UCS data.

- Model creation using UCS based on lithology and grain size.

- Investigate the financial benefits of achieving the required ore hardness to South Plant.

The aims are achieved in order since each aim relies on the previous one (Figure 8).

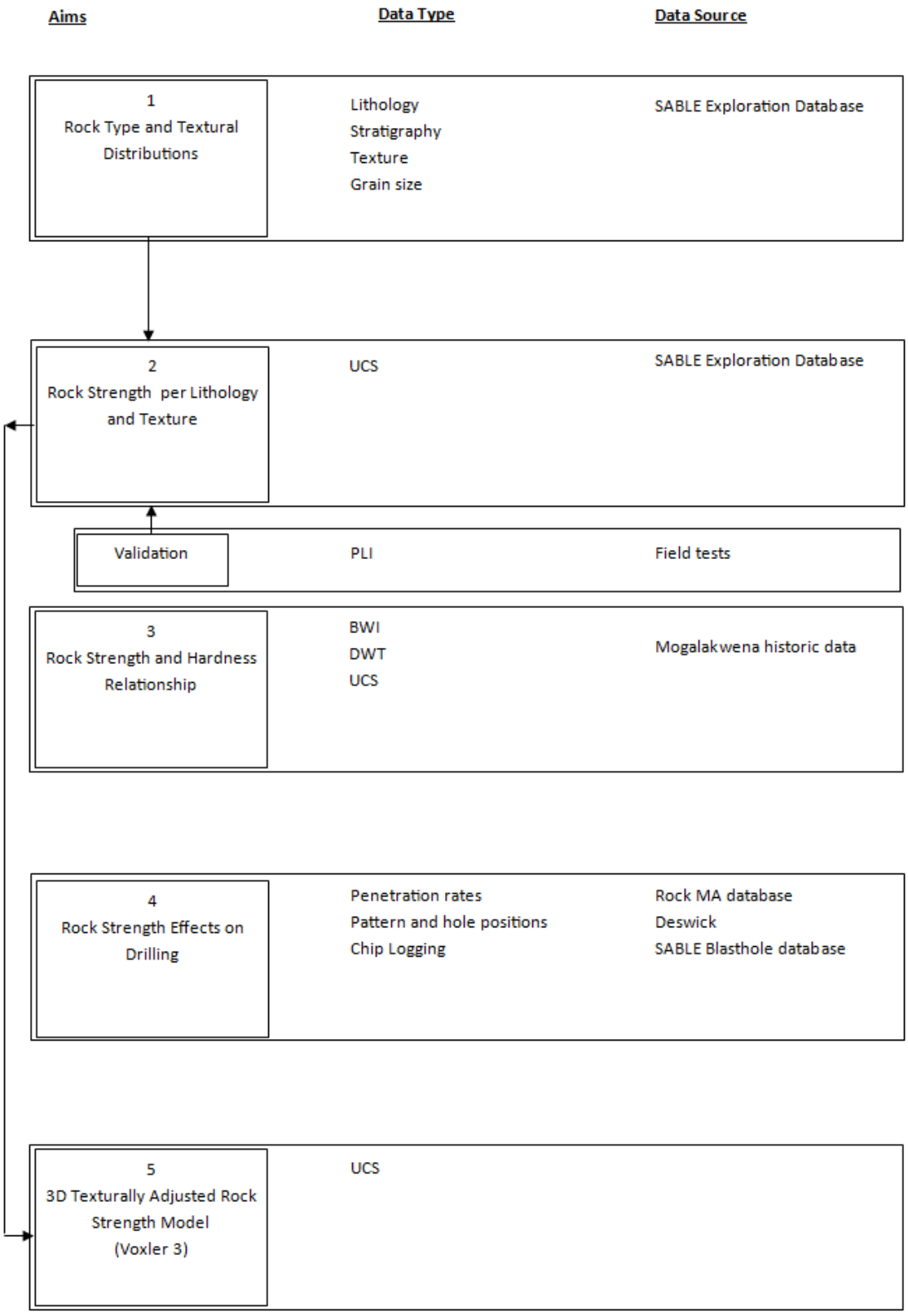


Figure 8: Summary of aims of the project, the data used and the source of the data.

1.3 Objectives

The objective of the report is to create a site specific hardness model which will accurately represent the UCS of diverse rock types. Drilling performance can be accurately predicted and planning can optimise drill rig use. MWD techniques can be calibrated to the data set and recorded data can update the hardness model. The model can be used to predict plant throughput due to the link to texture. This will be achieved in the following order:

i. Distribution of lithology and texture from exploration database.
ii. Determining the rock type texture and grain size relationship to UCS.
    a. Validation of relationship through PL test work dataset.
iii. Comparison between rock strength and hardness.
iv. Effects of rock type hardness on drilling rate of penetration.
v. Strength model creation.

1.4 Available Databases

Several databases exist at Mogalakwena Mine which can be utilised in the research.

1.4.1 Exploration Database

Mogalakwena Mine has a vast database of rock property information reported and gathered over many years through different methods. The exploration drilling data stored on the SABLE database holds the majority of the information in a structured, secure and easily accessible database.

The data includes:

- Lithology
- Stratigraphy
- Texture
- Grain size
- PL results for PL samples
- UCS as calculated from PLI
- Accepted UCS for rock type

The accepted UCS value has been attained from UCS test work and is independent of PL results. It is applied to lithological entries in the exploration database.

1.4.2 Blast hole Database

Mogalakwena Mine has a vast database of rock property information reported and gathered over many years through different methods. The exploration drilling data stored on the SABLE holds the majority of the information in a structured, secure and easily accessible database. Lithological classification (logging) through blasthole sampling has challenges. The many inaccuracies and allowances for errors in such a method of rock identification will not accurately identify lithologies over small widths but can be used to determine the main rock type over the entire blast hole depth. Therefore, such a method will assist in this study. The impact of difficulties in rock type classification on this study is that generalised zones cannot be accurately defined. Instead, blast hole by blast hole rock-type identification and ore-type domaining will need to be introduced in order to ensure appropriate accuracy.

The data includes:

- Lithology
- Stratigraphy

1.4.2.1 Chip logging

The drilling chips from production drill rigs are logged daily (Figure 9). The chips are taken from sampling RC drilling and blast holes.



Figure 9: Geologist logging drill chips from a Pit Viper. The chip lithology is entered in SABLE Database Warehouse.

Lithological data is entered into SABLE Database Warehouse (Figure 10). A limited range of rock parameters are recorded.

Sample ID	From	To	Sampled Width	Lithology Type	Stratigraphic Zone
317/137/367A	0.000	2.500	250.0	N	H
317/137/367B	2.500	5.000	250.0	N	H
317/137/367C	5.000	7.500	250.0	N	H
317/137/367D	7.500	10.000	250.0	N	H
317/137/367E	10.000	12.500	250.0	N	H
317/137/367F	12.500	15.000	250.0	N	H

Figure 10: Current rock properties required in the SABLE database after chip logging.

1.4.3 Rock Strength and Hardness

Historic rock strength and hardness tests have been carried out for UCS, DWT and BWI. The results have been used for a variety of mine improvement projects (Little, 2006), geotechnical modelling and concentrator construction planning (Bye, 2004). The relationship between these results was investigated.

The data includes:

- Mean UCS
- Mean BWI
- Mean DWT

1.4.4 RockMa Database

The new RockMa system records penetration rates for each hole for each rig on the mine. This database is sourced for the application of rock strength values to drilling performance through different lithologies.

The data includes:

- Position of blast hole
- Effective drilling time
- Depth of hole
- Penetration rate (calculated from effective drilling time and hole depth)

The relative rock strength data could not be exported at time of writing.

1.4.5 Deswick

Deswick is a computer aided design (CAD) software package used for pattern design and planning. The blast patterns are stored within the Deswick database and are viewed in the user interface.

Data includes:

- Pattern position
- Ore lines
- Drill hole positions

1.5 Project Area

Two operational areas, namely; North Pit and Cut 8, exist within the farm boundary (Figure 11). The project focused on the OY farm which includes North Pit. North Pit is the largest operational area at Mogalakwena accounting for roughly 80% of ore production. Cut 8 is an expansion project along strike to the south of North Pit.

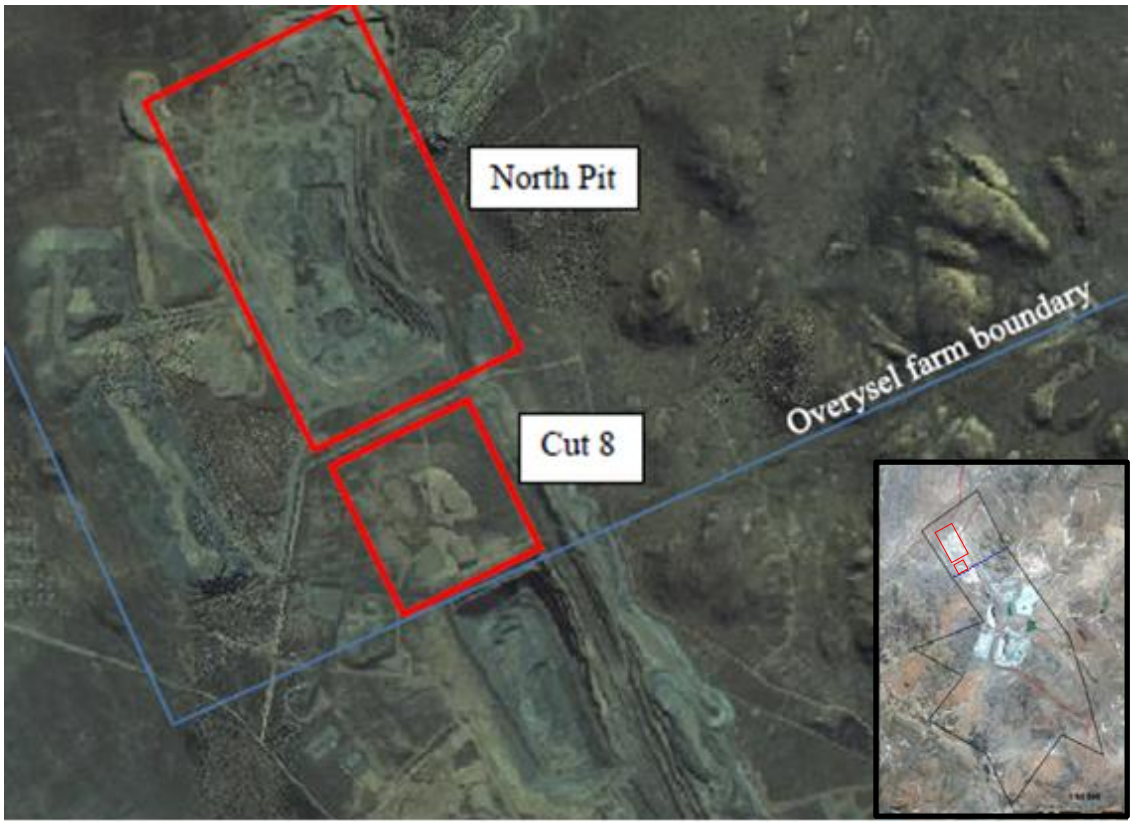


Figure 11: Mogalakwena Mine with project area indicated with the insert showing the entire mine property.

The North Pit represents the largest of the 5 pits at Mogalakwena Mine and 80% of total production (Figure 12).



Figure 12: North Pit production pit (looking south).

1.6 Summary

This introduction chapter has established the overview, aims, objectives, available databases and the project area. The foundation of the project has been laid and allows for a holistic view of the research purpose. The following chapter covers relevant work that has been previously completed at Mogalakwena Mine.

CHAPTER 2: LITERATURE REVIEW

2.1 Introduction

The previous chapter gave an overview of the project aims. This chapter investigates relevant research at Mogalakwena Mine and more broadly in the fields of geometallurgy and drilling. The findings in the literature review will guide the level of investigation and reveal areas in which geological understanding at Mogalakwena can be improved. A better understanding of the orebody will highlight the necessary changes required in drilling equipment selection and usage as well as downstream processing.

2.2 Geometallurgy

The greatest loss of PGEs occurs in the crushing, grinding and flotation stages. It is vital to understand this process and how rock properties affect these. The field of geometallurgy combines the characteristics of ore variables to mining process performance at various stages in the value chain. Geometallurgy has proven effective in the optimisation of plant processes and potential for cost reduction (McLean & Watt, 2009). Geometallurgical programmes have thus been an area of growing importance in the international mining industry and have been adding value to downstream processing.

Geometallurgy is defined as a branch of applied metallurgy and numerical analysis that places emphasis on the geological controls of mineral processing and prediction of process performance from multiple rock properties (Deutch, 2013).

Along with production forecasting, Geometallurgical studies quantify all material impacts on end recovery including; mineralogy, metallurgy, flotation response,

crushing and milling behaviour, texture and hardness (Deutch, 2013; Napier-Munn *et al*., 1999). Plants require regulated feed (Napier-Munn *et al*., 1999) and can be optimised to process a certain ore type at a certain time - which geometallurgical studies aim to categorise.

The relationship between rock properties and processing variables is complex (Deutch, 2013; Napier-Munn *et al*., 1999). One such property is ore hardness which is a geometallurgical variable that has a quantifiable impact on recovery performance due to its direct link to the milling stage (Napier-Munn *et al*., 1999). Rock properties must be modelled geostatistically and spatially. Increased uncertainty in the rock properties will undermine the certainty in the prediction of processing variables (Deutch, 2013). Spatially accurate ore hardness characterisation is required in a geometallurgical programme to indicate potential changes in comminution behaviour (Chibaya, 2013).

Tests on samples act as proxies to guide understanding when applied to the actual process that the testing is trying to replicate (Napier-Munn *et al*., 1999; Bye, 2004). For example, laboratory flotation tests cannot be guaranteed to exhibit the same response at a full scale concentration plant (Gloy & Hey, 2002). Test work results are used as guides and do not necessarily represent the actual rock response during processing. Continual validation of test work is needed through accurate equipment or process results.

2.1.1 Crushing and Comminution

The purpose of comminution processes is to break the ore to a size small enough to free or liberate the valuable components from gangue. Breakage characterisation and throughput is determined by ore properties. Milling rates can be optimised for different ores. Optimisation is the adjusting of machine and circuit variables to attain some improved operating condition (Napier-Munn *et al*., 1999). Optimised milling times minimise unnecessary costs. Thirty to fifty percent of total plant power drawn is used for comminution which represents the single most energy intensive operating unit on a mine. The energy usage can

increase by seventy percent for hard ores (Cohen, 1983). Flotation performance is affected by liberation which is usually linked to particle size distribution (PSD).

Milling is an energy intensive process and its optimisation by adjusting milling rates would lead to greater recovery and decreased costs (Cohen, 1983). The cohesion between grains provides the overriding power demand inside such mills (Doll *et al*., 2003). The concept of rock hardness must be clearly defined due to the large number of mechanical tests available (Heinz, 2009) and results must be fit for which ever purpose to which it is applied (Napier-Munn *et al*., 1999).

Cost saving and revenue increase potential lies in modelling ore hardness which can be linked to expected milling performance allowing milling rates to be adjusted. There is much to be gained from improving the practice of rock breakage. Therefore, value addition is unlocked by optimising the performance of comminution by ensuring that the installed capital asset is exploited as efficiently as possible in an economic sense (Napier-Munn *et al*., 1999).

Generally, crusher throughput increases when softer material (lower rock strength) is fed (McLean & Watt, 2009) resulting in higher crushing rates. This leads to the general rule that ore hardness has a quantifiable impact on recovery performance due to its direct link to comminution throughput (Napier-Munn *et al*., 1999).

In summary, benefits of rock breakage optimisation include:

- Reduced unit operating cost (R/ton treated).
- Increased throughput.
- Improved downstream process performance as a result of an optimised feed size.

A 2008 study investigating the effect of ore type on plant throughput showed significant differences in plant throughput for varying rock types found in the orebody (Figure 13) (Ziemski *et al*., 2010). This behaviour was confirmed in the

data compile for actual performance observed in the plant from an earlier study (Bye *et al*., 2008).

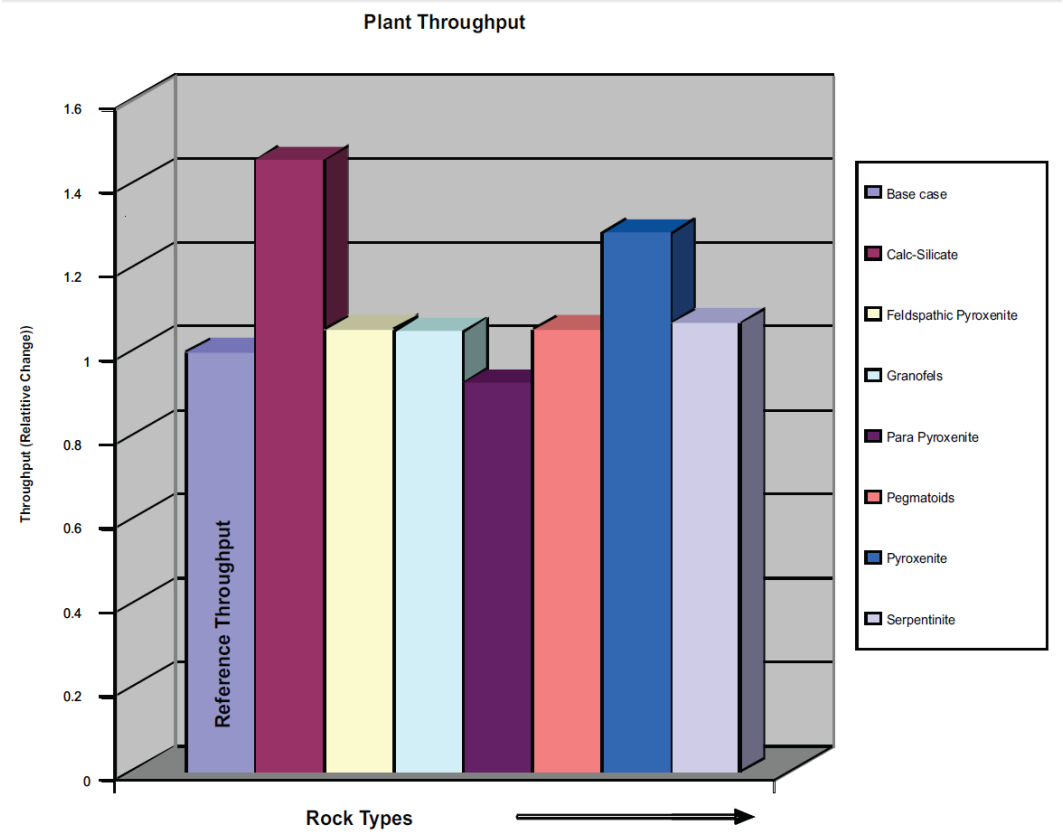


Figure 13: Replicating difference in UCS between pyroxenite and other rocks (Ziemski *et al*., 2010).

In an ARC report (Gloy & Hey, 2002), the differences in mineralogy of altered and unaltered ore was investigated. The following positive correlations were determined:

- Head grade and recovery.
- Head grade and mass pull.
- Base metal sulphide (BMS) content and recovery.

The following negative correlations were determined:

- Recovery with alteration mineral content (serpentine, chloritisation and talc).
- Enstatite and feldspar with alteration minerals.

Alteration is not the full story of poor recoveries, as shown by Gloy and Hey (2002). Alteration caused the PGEs to become mobile and migrate locally. The primary and secondary mineralisation styles of the PGEs are associated with silicates, tellurides or sulphides and this has an influence on recovery (Holwell *et al*., 2006).

Bye (2005) investigated hardness and mineralogical characteristics of blast 138-055 in Sandsloot mine. The findings included a shift from enstatite to diopside from unaltered to altered ores in Sandsloot. This indicates a more calcium oxide (CaO) rich chemistry. Schouwstra and de Vaux (2013) reported that altered ores are higher in CaO and showed a positive correlation between DWT and CaO content of samples. These studies show that mineralogy and hardness are closely linked.

Geometallurgical variables are therefore sourced from a wide range of data sets. Each variable will have differing responses to different processes. It is important to identify the role of each variable and be able to source accurate data for modelling.

2.1.2 Geometallurgical modelling

Models can be created to guide the necessary stages in mining to achieve an optimised mine to mill process. Geometallurgical modelling enables mining operations to effectively predict the potential value of an economic deposit. Planning, business strategies and management decisions are dependent on correct models. Accurate information is vital in modelling to reduce mining risk (Bye, 2004; Deutch, 2013). Models add value to the mine to mill process by allowing corrective loading practices and milling rates (Little, 2006). Models can be used as a primary tool for mineral resource management.

Geotechnical block models specifically, use rock properties to describe rock masses, slope angle, blastability index, energy factor and associated costs (Little,

2006). The data used include, but are not limited to, UCS and PLI. They can be thought of as a subset to a geometallurgical model.

Bye (2004) developed geotechnical block models for fragmentation and slope stability. The fragmentation model was used for predicting the correct quantity of explosives to be used to achieve the needed fragmentation size for hauling and crushing.

The model needs to describe 2 elements of the problem:

- Breakage properties of the rock – the breakage which occurs as a result of the application of a given amount of specific energy.
- The features of the comminution machine – the amount and nature of energy applied, and the transport of the rock through the machine.

2.2 Geology

Rock properties are essential in understanding mining related effects and downstream processes. Consistency in classification is essential for common terminology use between different projects. This chapter covers the geological overview of the Northern Limb, Platreef and common rock types at Mogalakwena Mine. The textural distribution per rock type is investigated to guide the formulation of a representative hardness vs. texture relationship for each rock type.

2.2.1 Geological Setting

The Bushveld Complex (BC) represents the largest preserved layered mafic intrusion in the world. The intrusion has been dated at 2060Ma (Walraven *et al.*, 1990) and generally intruded into Transvaal Supergroup sediments. The complex consists of 5 limbs each varying slightly in regard to stratigraphic composition (Figure 14). The aptly named Western, Eastern and Northern limbs are the most economically significant. The BC is divided into a felsic sequence and an

ultramafic sequence which is traced across the limbs. The ultramafic sequence is termed the Rustenburg Layered Suite (RLS) and is host to the most voluminous deposits of Platinum Group Elements, vanadium and chromium in the world (Johnson *et al*., 2006). The RLS is subdivided into zones which vary according to compositional proportions of mafic and felsic minerals. The Upper Zone (UZ), Main (MZ) and Lower Zone (LZ) extend throughout the complex and are identified in the Northern Limb. The Critical Zone (CZ) is recognised as the most abundant in PGE, Cu and Ni of which the Merensky and Upper Group 2 (UG2) reefs of the Western and Eastern Limbs are part. The CZ in the Northern Limb shows a marked difference to that found in the other limbs. The Northern Limb CZ does not show the clear layering and tabular reefs of the Western and Eastern Limbs.

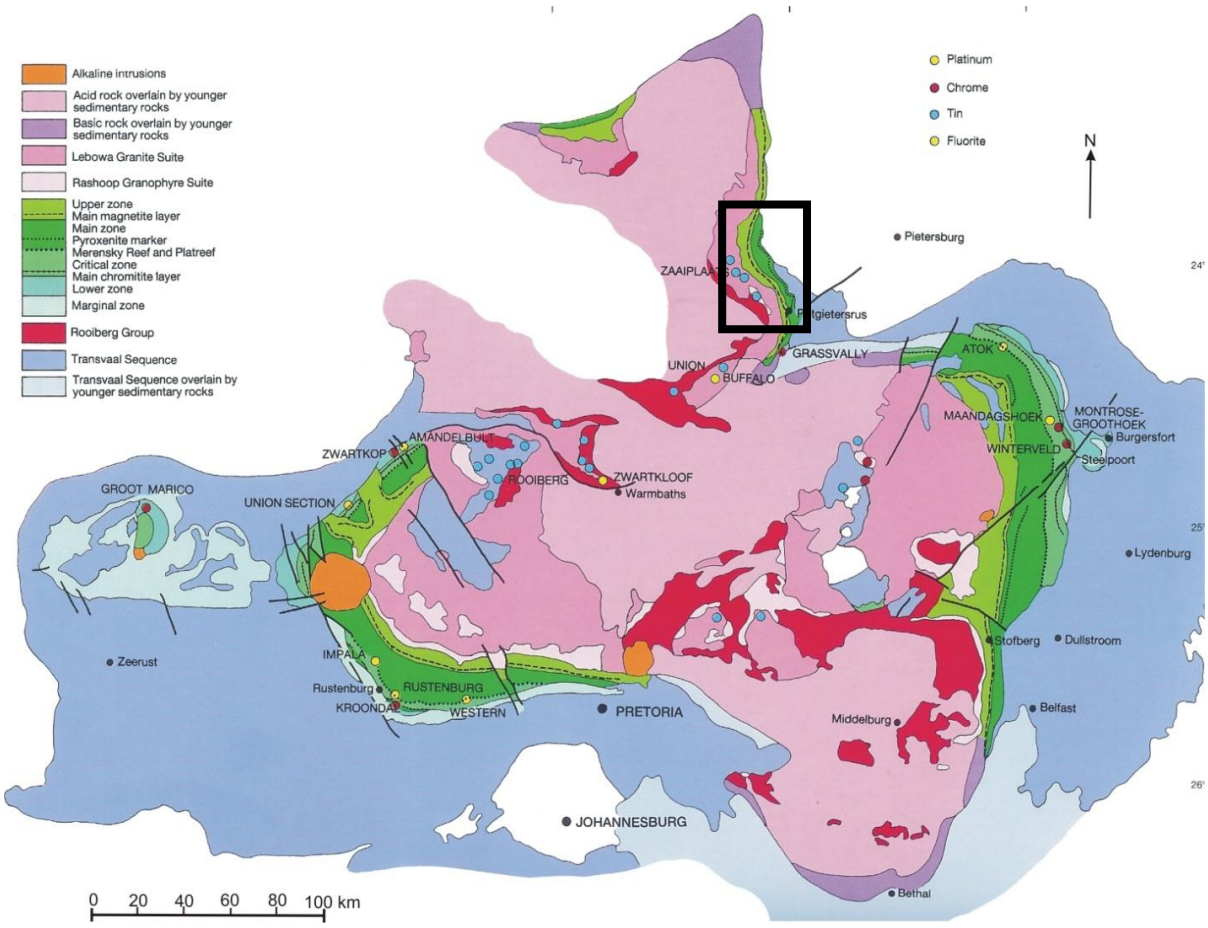


Figure 14: Plan view of Bushveld Complex. Insert is Northern Limb (modified after Cairncross & Dixon, 1995).

The Platreef is considered an orthomagmatic PGE-rich Cu-Ni sulphide deposit (Holwell, 2010). The host rock is primarily pyroxenite containing varying quantities of feldspar overlain by MZ norites and gabbro-norites and underlain by the LZ, Archean granite and Transvaal Supergroup sediments.

The Platreef comprises a set of sills which occurred as magmatic impulses. Three to four Platreef packages with varying mineralisation and grade can be recognised along strike. The unaltered reef is dominated by feldspathic pyroxenite but includes pyroxenite successions. The footwall rocks change over the North-South strike of the orebody in the mine property rights (Figure 15) and have been cited as the source of hydrothermal interaction and assimilation.

Fluid interaction related to contact metamorphism, related metasomatic and assimilation can disguise lithological distinctions (Kinnaird *et al.*, 2010; Holwell *et al., 2006).* Alteration in the form of serpentinisation, chloritisation and epidotisation overprints the primary lithologies throughout the orebody and in varying degrees.

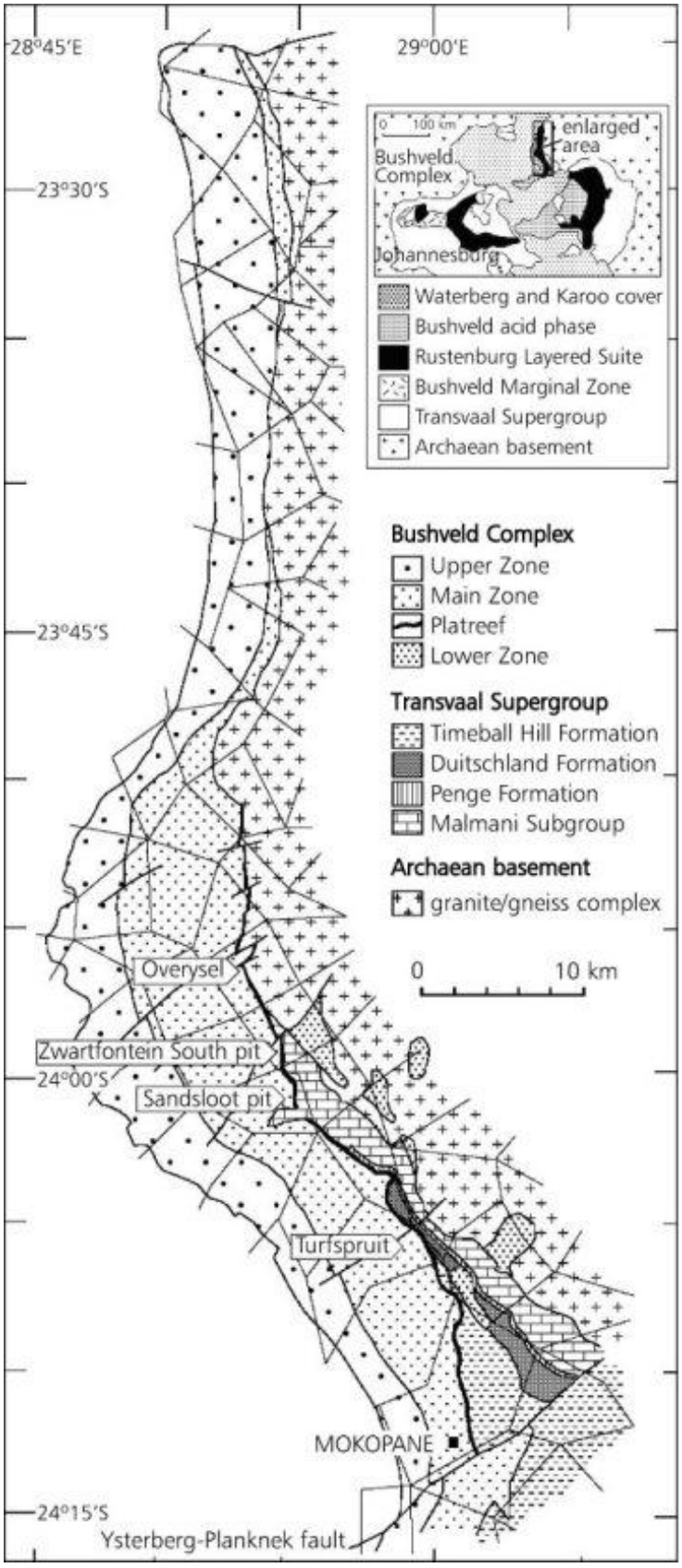


Figure 15: Geological map of the Platreef, Northern Limb with Mogalakwena pits marked (Holwell & McDonald, 2010) .

In the Northern sector, the Platreef irregularly overlies the Utrech granite and Hout Rivier gneisses. Interaction between the Platreef and footwall has established an anhydrous gneiss middling referred to as granofels located between the Archean basement and the Platreef (Figure 16). Limited fluid interaction and PGE distribution is controlled by the behaviour of sulphide liquids producing a PGE-BMS association (Kinnaird and Naldrett, 2010). However, even within one farm or pit area, considerable variation in BMS association exists (Kinnaird and Naldrett, 2010). The Platreef package of coarse grained pyroxenite with varying proportions of plagioclase can vary from 25m to 100m thick overlying the Archean granites. The variation in thickness is purported to be due to topographical differences in the footwall. Chromitite seams occur irregularly within the reef. Two such seams can be traced fairly consistently in the study area at 5-7m and 23-25m from the Platreef – Main seam contact (Kinnaird and Naldrett, 2010).

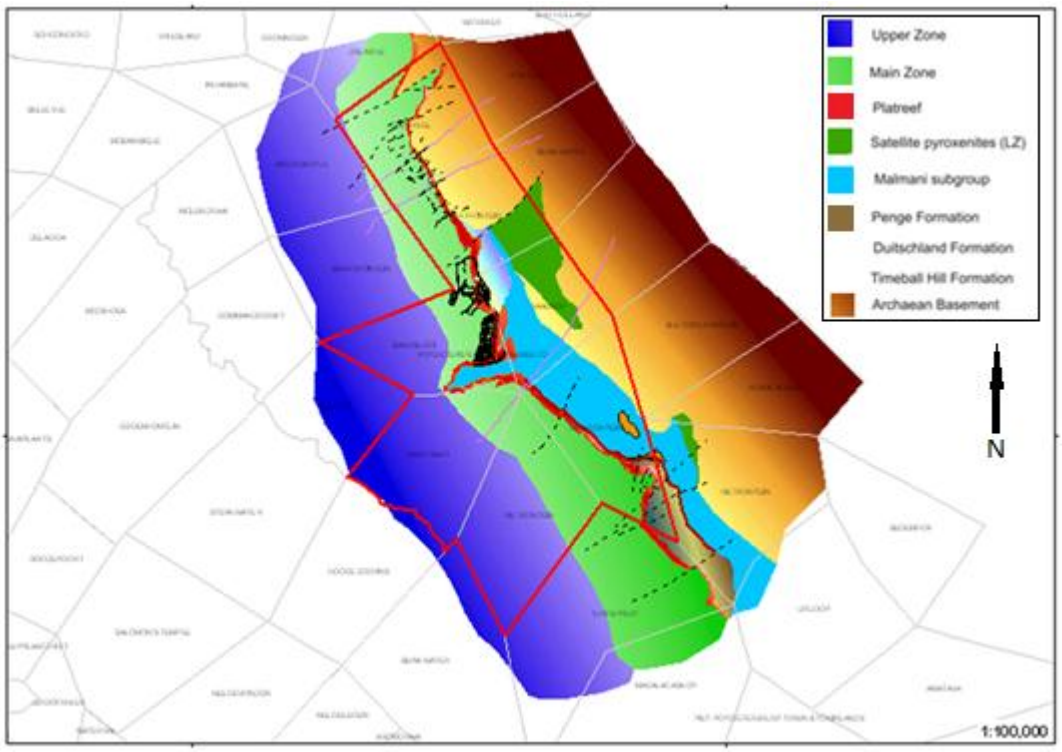


Figure 16: Plan view of Mogalakwena Mine mining lease with rock types illustrated.

The banded iron formation (BIF) and quartzites of the Duitsland and Penge formations occur as the footwall in the southern farms Tweefontein, Turfspruit and Macalacaskop. These farms are not part of the project area (Figure 17). The footwall changes from dolomite of the Malmani Group to granite of the Archean basement from South to North (Figure 17). The change has implications for mineralogy and mineralisation style of Platreef rocks in contact with the footwall. Xenolith distribution of calc-silicate predominates in the SS farm. The xenoliths are described as rafts of dolomite sourced from the footwall and carried into the reef magma during the intrusive event. Parapyroxenite is a metasomatic alteration of pyroxenite and feldspathic pyroxenite occurring in close proximity to calc-silicate xenoliths and dolomite footwall. Parapyroxenite and calc-silicate become less common toward the north. Alteration in the form of serpentinisation, chloritisation and the formation of talc occurs throughout the farms OY, ZN and SS.

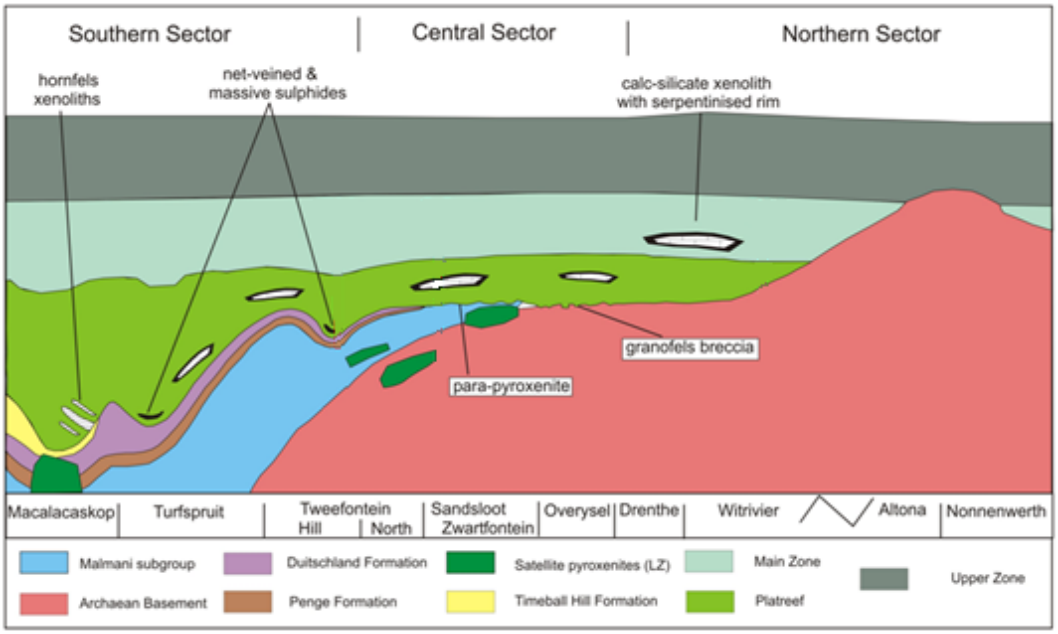


Figure 17: S-N Section view of mineral rights area. Operational pits only exist on Sandsloot, Zwartfontein and Overysel farms.

2.2.2 Lithological Classification System

The Platreef, as mined at Mogalakwena Mine, was classified into 3 units, A, B and C type reefs (Figure 18) based on host lithology and vertical correlation. This has proved overly simplistic and is redundant when attempting to implement classification regimes to optimise recoveries due to high levels of sporadic alteration indiscriminately affecting the Platreef rocks.

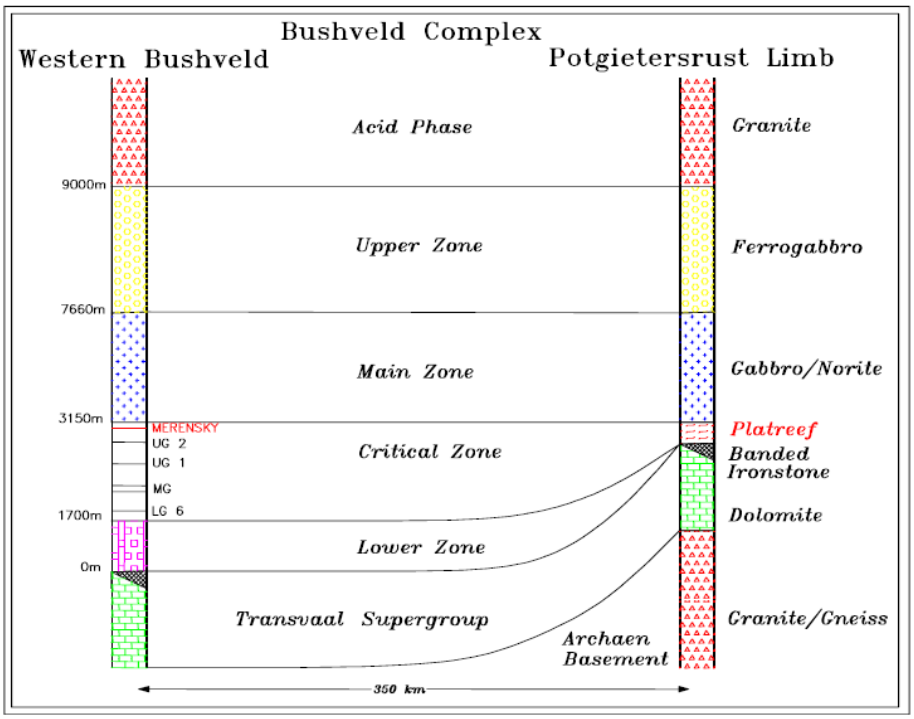


Figure 18: Generalised stratigraphy of the Platreef in relation to the Western Bushveld (Bye, 2003).

The Platreef contains a multitude of igneous and metamorphic rocks greater in diversity than the rest of the Bushveld Complex (Nex *et al.*, 2006). Multiple sill intrusions, differing footwall lithologies and late stage recrystallisation due to fluid involvement (Kinnaird *et al.*, 2010) are such processes amounting to the observed complexity.

The unaltered BC rocks of Mogalakwena Mine all contain varying proportions of plagioclase, pyroxene and olivine which fall within a single ternary diagram

(Figure 19). A study to simplify rock type name usage was carried out by Nex *et al*. (2006).The study aimed at providing a standardised classification scheme for core logging and rock identification at Mogalakwena. The study was based on definitions from the 3rd Edition of Glossary of Geology published by American geological Institute, the IUGS classification scheme and with reference to classifications stipulated by the British Geological Survey. The study by Nex *et al*. (2006) forms the foundation of rock type classification for this research.

Northern Limb rocks are similar in mineralogy but differ in mineral proportions. The specific mineral occurrences are widely documented (Table 3).

Table 3: Generalised minerals in the common rocks of the Northern Limb (Nex *et al*., 2006).

Mineral Group	**Mineral**	**Ideal Chemical Formula**
Orthopyroxene	Enstatite	$MgSiO_3$
	Ferrosilite	$FeSiO_3$
Clinopyroxene	Diopside	$MgCaSi_2O_6$
Olivine	Fosterite	Mg_2SiO_4
	Fayalite	Fe_2SiO_4
Plagioclase	Anorthite	$CaAl_2Si_2O_8$
Accessory Minerals	Biotite	$K(Mg,Fe)_3AlSi_3O_{10}(F,OH)_2$
	Chromite	$(Fe,Cr)_2O_4$
	Magnetite	Fe_3O_4
	Sulphides	$(Cu,Fe,Ni)S_{1-2}$
Alteration Minerals	Serpentine	$(Mg,Fe)_3Si_2O_5(OH)_4$
	Talc	$Mg_3Si_4O_{10}(OH)_2$
	Chlorite	$((Mg,Fe)_5Al)(AlSi_3)O_{10}(OH)_8$

2.2.3 Rock Types

Below is a summary of rock types that will be used in the study based on mentions in literature reviews. The rocks listed do occur as mineralised but vary greatly in PGE grade. These rock types can all occur as mineralised and are representative of the vast majority of reef rock types and direct hanging wall and footwall rock. These rocks are representative of the Main, Critical and Lower Zone in addition to metamorphosed and fluid interaction derived rocks abutting the footwall. These rock types are used within the exploration database. A full description of each rock type can be found in the appendix (Appendix 1). A list of abbreviations used in the exploration database for rock types, texture and grain size can be found in the appendix (Appendix 2). OY farm is considered less altered and more representative of the primary magma (Holwell *et al*., 2006) which makes this farm ideal for the study of rock type strength behaviour.

2.2.3.1 Hanging wall

Hanging wall rocks are confined to the Main and Upper Zone stratigraphic units. The rocks are generally noritic and gabbroic. The range of plagioclase percentage in these rocks is identified using the terms leuco and mela (Figure 19). Variants of anorthosite exist with the most prominent being the poikalitic anorthosite marker commonly identified immediately above the reef. These rocks are unmineralised except on rare occasions. The distinction between orthopyroxene and clinopyroxene is important in the accurate classification of hanging wall rocks accurately. Bushveld rocks generally exhibit visual differences between the two pyroxene groups (Nex *et al*., 2006). Gabbroic rocks are extremely rare within the Platreef itself and, if they occur, are assumed to be hanging wall intrusive inter-fingering (Nex *et al*., 2006).

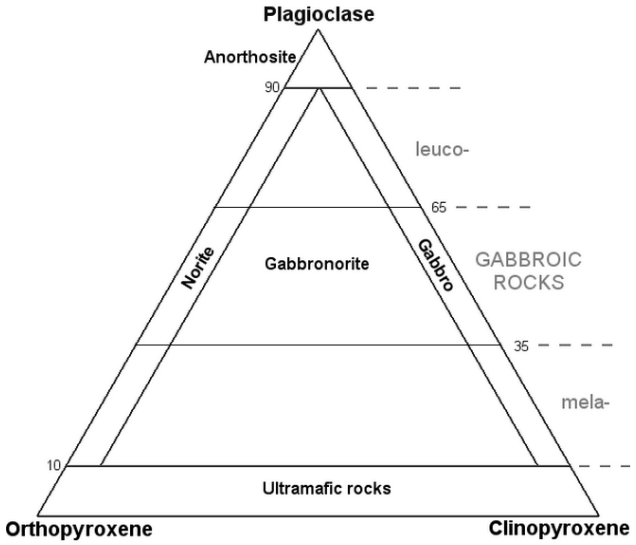


Figure 19: Ternary diagram of gabbroic rocks (Copyright 2014 by Andrew Alden, geology.about.com, reproduced under educational fair use).

2.2.3.2 Reef

The reef is dominated by pyroxenite and its variants. Variants include differing plagioclase content and a degree of hydrous alteration in the form of Serpentinisation, chloritisation and the formation of talc. The immediately recognisable transition from hanging wall to reef is the increase in pyroxene content and the change of plagioclase from cumulus to intercumulus. Pyroxene grains are generally euhedral with a cumulus texture. Clinopyroxene can occur in an oikocrystic texture as seen in the barren pyroxenite directly below the hanging wall contact. Accessory minerals include interstitial sulphides; pyrrhotite, chalcopyrite, pentlandite and pyrite. Sporadic disseminated chromite can be identified with reef lithologies. The locally used term feldspathic pyroxenite is used to distinguish pyroxenite from a more plagioclase-rich pyroxenite with intercumulus grains which would otherwise be described as a mela-gabbronorite (Figure 20).

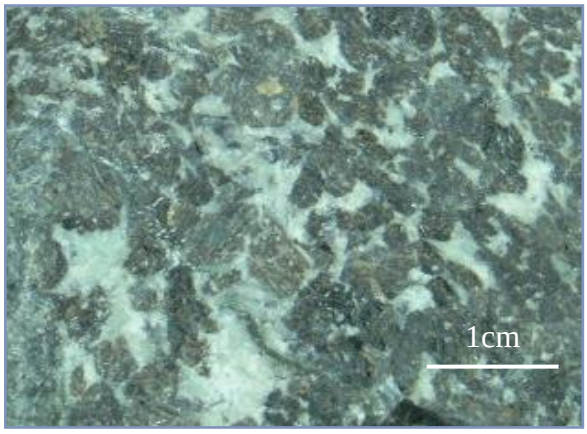


Figure 20: Feldspathic pyroxenite (major reef rock type) showing cumulus pyroxene and intercumulus plagioclase.

Pyroxenites which have undergone hydrothermal alteration display a darker black-green colour. The alteration occurs due to the hydration of ferromagnesian minerals (olivines and pyroxenes). Serpentine minerals include antigorite, chrysotile and lizardite (Nex *et al*., 2006). Minor amounts of chlorite and talc are also present. The rock is termed a serpentinite if alteration has completely overprinted the original texture and minerals beyond visual recognition. Feldspathic pyroxenite makes up 80% of the reef. Grain sizes vary from fine to pegmatoidal. Finer grained rocks are normally located directly below the HW contact. Calc-silicates are metamorphosed dolomite xenoliths entrained in the mafic melt during the intrusion. These are occasionally found at OY farm and can be mineralised. Parapyroxenites are a subject of great interest and, on occasion, great debate. Parapyroxenites occur in close proximity to calc-silicates and are formed by the addition of volatiles and water from the adjacent xenolith into the crystallising mafic melt. They are thus identified by their proximity to calc-silicate, varying texture and highly altered appearance.

2.2.3.3 Footwall

The footwall changes from dolomite on farms SS and ZN to granofels and granite on OY farm (Figure 17 and Figure 18).

Granofels is a term used for footwall agmatites, breccia and agmatitic breccia containing two igneous components developed at the footwall contact (Figure 21). Fine grained pyroxenite fragments occur within a granitic matrix (Nex *et al*., 2006). The leucocratic and granitic matrix contains plagioclase and quartz from an unknown origin – presumably assimilated Archean granite (Cawthorn *et al*., 1985). Pyroxenite fragments are identified as irregular and angular blocks of varying size between the cross cutting leucocratic veins. The pyroxenite component has a similar geochemistry to LZ pyroxenites but does contain entrained Platreef material (Nex *et al*., 2006). LZ pyroxenites are also found as satellite intrusions within the Archean basement (Figure 16).

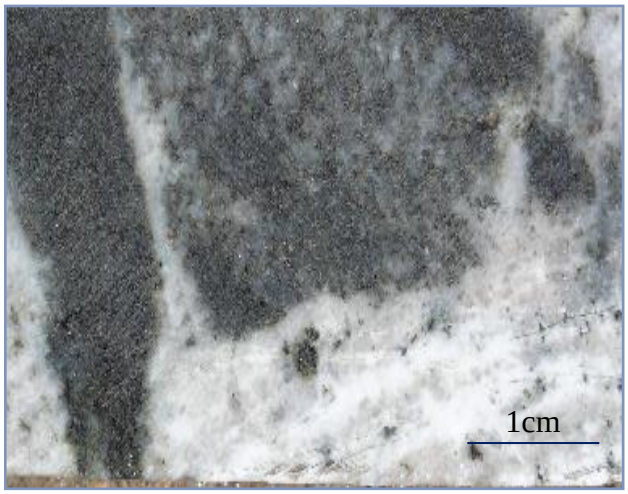


Figure 21: Close up photograph of brecciated agmatite - termed granofels on site.

Granitic veins are also found crosscutting this lithology (Cawthorn *et al*., 1985). Granofels is commonly mineralised at the reef contact with occasional sulphide back-veining occurring. This rock type, exclusively within the footwall, can be described as an ore (Figure 22).



Figure 22: Granofels in the footwall showing distinct variation in composition. Changes in composition are irregular.

2.2.4 Alteration

Examples exist of core samples originally logged as being unaltered, while in reality, they have pervasive alteration (Gloy, 2005) Visual estimation of alteration did not correlate to measured alteration. This emphasises the difficulty in a visual estimation of alteration in rocks (Gloy, 2005).

Hydrous alteration is widespread. Areas of serpentinisation occur throughout the Platreef and can extend within the dolomitic footwall. Serpentinisation is generally used to describe hydrous alteration of ferromagnesian minerals. Resultant minerals include serpentine (antigorite, chrysotile and lizardite) in addition to chlorite, talc and magnetite as formed through parallel processes. Isolated chloritisation occurs in the HW and FW rocks in immediate contact with the Platreef. Chloritised HW norites, which are often associated with recrystallisation, are termed hybrid norites and occur in direct contact with the reef.

2.2.5 Texture

Texture is defined as the degree of crystallinity of component grains and their mutual arrangement (Williams *et al*, 1982; Bell, 1983). The majority of unaltered rocks in the Rustenburg Layered suite contain one to four cumulus minerals

(Johnson *et al*., 2006). Texture does have downstream influences (Roberts and Reinecke, 2003) and such variables need to be categorised firstly by lithology (Ozturk *et al*., 2014). Texture is a secondary attribute to the more important compositional property of rocks and may be meaningfully linked to mineralisation style, PGE and base metal distribution (Holwell *et al*., 2006).

Rock breakage preferentially occurs along lines of structural weakness such as grain boundaries, pyroxene cleavage planes, hairline fractures and serpentine veins. This was markedly seen on unaltered North pit pyroxenite ore during the early stages of coarse crushing and grinding. Rock breakage disrupts the original textural fabric of the rock and results in the early liberation of PGMs. (Roberts & Reinecke, 2003). A study by Holwell *et al*. (2006) investigated the relationship between rock type and PGM association with BMS and silicate minerals. The results show that the dominant host relationship of PGMs differs across stratigraphy and rock type (Table 54).

Table 4: Textural associations of PGM (excluding Au/Ag alloys) in the variety of host-rock types and the percentage of grains (Source: Holwell *et al*, 2006)

All PGM, Au, Ag phases Association:	HW	PXT	PEG	ORR	CPX	FRH	FWP	CS	PSP	TSP
Enclosed in BMS (%)	10.3	12.6	9.1	8.2		77.8	10.4	6.4	21.2	
BMS-silicate contact (%)	29.9	38.1	16.9	49.0	30.4	11.1	27.6	14.9	60.6	11.5
Enclosed in silicate (%)	59.8	49.3	74.0	42.8	69.6	11.1	62.0	78.7	18.2	88.5
Pt-dominant phases Association:	HW	PXT	PEG	ORR	CPX	FRH	FWP	CS	PSP	TSP
Enclosed in BMS (%)	23.1	8.4	11.9	6.5			9.8	4.3		
BMS-silicate contact (%)	53.8	37.3	26.2	41.3			14.8	8.7	67.6	7.4
Enclosed in silicate (%)	23.1	54.2	61.9	52.2	100.0	100.0	75.4	87.0	32.4	92.6
Pd-dominant phases Association:	HW	PXT	PEG	ORR	CPX	FRH	FWP	CS	PSP	TSP
Enclosed in BMS (%)	8.0	8.5	3.1	6.1		72.2	10.5	8.7	29.2	
BMS-silicate contact (%)	22.7	34.1	3.1	51.0	40.0	16.7	34.7	21.7	55.6	16.1
Enclosed in silicate (%)	69.3	57.3	98.8	42.9	60.0	11.1	54.8	69.6	15.3	83.9

2.2.5.1 Grain size

A grain size description is a subsection of texture. It is an important aspect of texture due to its indication of recrystallisation processes. It can be quantified by measuring the major and minor axis, perimeter and area (Ozturk *et al*., 2014). Detailed measurements require much effort and expense. Hand held rulers are used to measure grain sizes in core at Mogalakwena Mine. The accurate identification of grain size is difficult in rock types exhibiting multiple grain sizes. Normally a ranged value is used to describe such occurrences (i.e. fine – coarse) based on visual description and physical measurement (Table 5). Automated grain size quantification is available at a higher cost with the use of an automated mineralogical technique and would ensure more consistent results.

Table 5: Grain size categories (Bell, 1983).

Term	Particle Size (mm)
Very Coarse	>60
Coarse	2-60
Medium	0.06-2
Fine	0.002-0.06
Very fine	<0.002

2.3 Rock Hardness and Strength

Rock strength is the resistance to breakage forces (Dhungana, 2013). This depends on the properties of intact rock material along with the character of discontinuities. Rock strength has important implications to underground and surface mine design (Ozturk *et al*., 2014), drilling performance (Heinz, 2009) and comminution (Adeyemo & Olaleye, 2012).

Rock strength depends on a number of rock properties or variables (Dhungana, 2013; Napier-Munn *et al*., 1999; Ozturk *et al*., 2014). The properties affecting

rock strength include; mineral composition, density, rock porosity, fabric, texture, moisture content and the degree of alteration or weathering Prikryl, 2001; Dhungana, 2013; Ozturk *et al*., 2014). Rock breakage is controlled by the distribution of flaws available to initiate breakage under stress. This includes geological jointing and faulting (discontinuities) on macro scales to dislocations in crystal structure at the micro scale (Napier-Munn *et al*., 1999). Rock strength is affected by discontinuities occurring in the mass as described above (Heinz, 2009; Ozturk *et al*., 2014).

Rock strength and rock hardness are occasionally used as synonyms. There is a distinct correlation between rock material strength, as measured by UCS, and rock hardness (Heinz, 2009). Heinz (2009) recommends that the term "strength" be retained for the description of the entire rock mass while "hardness" be used as suggestive of the strength of the rock material (Heinz, 2009) and its resistance to permanent deformation (Dhungana, 2013). Rock strength is usually of prime interest for mining. Hardness is more readily and consistently described using simple mechanical tests (Heinz, 2009).

Compressive strength, specifically, is the capacity of a material to withstand directed forces (Dhungana, 2013). The uses of such data include the creation of a hardness index and can be used to predict rock strength in a mining block (Dhungana, 2013). A higher UCS value is strongly correlated to a higher difficultly in crushing the rock (Adeyemo & Olaleye, 2012). The relationships between strength (UCS) and hardness (DWT) have shown some correlation while a low correlation between UCS and BWI exists (Bye, 2004). Both DWT and BWI tests are used to describe breakage characterisation for comminution processes.

For a meaningful classification of rock types, quantitative data is necessary (Palmstrom, 1995). Quantitative data is sourced from various test work compiled on Mogalakwena Mine ores.

2.3.1 Texture, Grain Size and Strength Relationship

Grain size is well known to influence rock strength (Ozturk *et al*., 2014). With large grain sizes there would be more flaws available to initiate breakage with the inverse being true as grain sizes reduce (Paterson & Wong, 2005). In addition, inter-grain cohesion and angular relationships of differently sized grains impact strength. Developing the relationship between strength, texture and grain size is difficult because of the many properties which obscure the effects of any one variable. A thorough investigation of texture would require digital quantification of geometrical relationship of grains and matrix (Ozturk *et al*., 2014).

2.4 Hardness and Strength Tests

Strength characteristics of ore must be specified by using fit for purpose test methods. There is a distinct correlation between rock material strength, as measured by UCS, and rock hardness (Heinz, 2009). However, there is generally limited to no correlation between UCS and BWI (Doll *et al*., 2003). The data used in the study by Doll *et al* (2003) covered 11 mines and there was a failure to link the energy required to factor rocks inside a mill to the rock strength as measured in MPa.

A trend was established between DWT and UCS at Mogalakwena Mine by Bye (2004) (Figure 23).

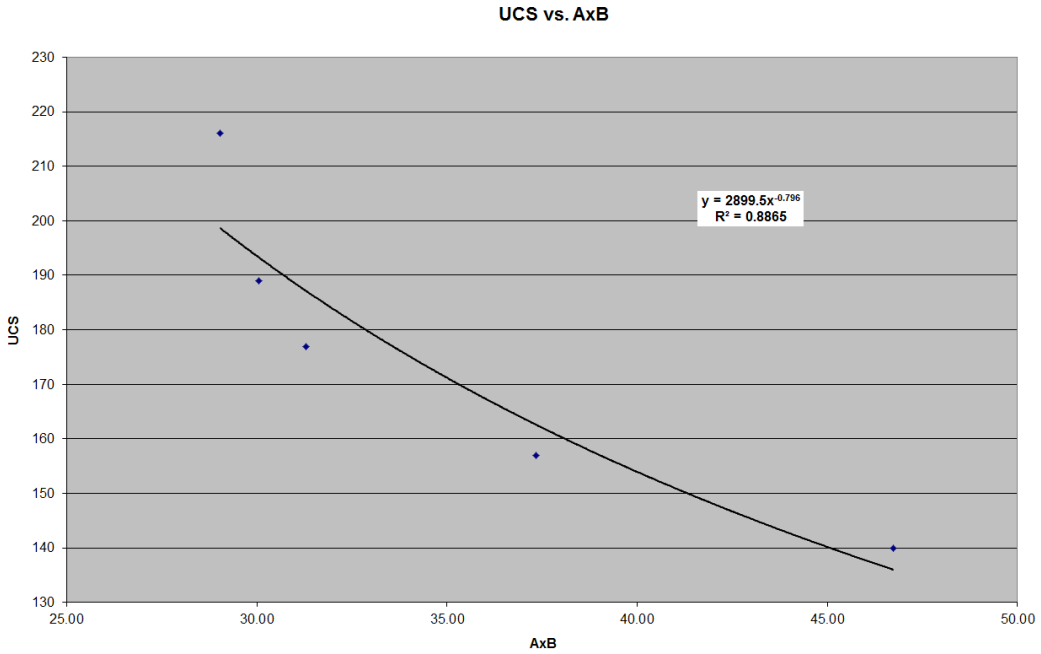


Figure 23: UCS vs. DWT (AxB) showing a good correlation (Bye, 2004).

The trend shows a good correlation, however, the small number in the sample test does not make this relationship conclusive. The large amount of UCS data, derived from PL testing, could be used for increased downstream applications if this relationship is confirmed. Each strength and hardness test has been described in the appendix (Appendix 3).

2.5 Drilling

Drilling, and rotary drilling specifically, involves the spinning of drill rods with an attached cutting tool (or bit) by means of a motor (Bourgoyne *et al.*, 1986). The system at Mogalakwena involves torque being transmitted through the drill rods (or drill string) by a top drive attached to a travelling block on a mast (Atals Copco, 2012). The top drive system is electric and screws directly into the top of the drill rod (Bar-Cohen & Zacny, 2009). The Pit Viper rotary drilling mechanism uses a high bit load coupled with a low rotation rate of the roller-cone bit to exploit the weakness in rock compressive strength. The Pit Viper can apply a maximum load of 53 tons of feed pressure.

Penetration rate is a function of the effective drilling time and the total depth drilled:

$$Penetration\ Rate(ROP) = \frac{Length\ of\ Hole\ (m)}{Time\ (hr)}$$

The penetration rate is a rudimentary value used to describe drilling performance and efficiency.

2.5.1 Machine variables affecting drilling performance

Regrinding is the effect of drilled cuttings being unable to escape the hole being drilled. It occurs when cuttings are not efficiently cleared with compressed air (bailing) or if the space between the rod and side of the hole (annular space) is insufficient to allow the passing of cuttings. Regrinding occurs between the wall and the bit itself. The effects increase bit wear and reduce drilling performance. Large cuttings of a denser rock are more prone to regrinding. Solutions range from increasing bailing velocity or decreasing the annular space (Atals Copco, 2012) .

Drilling performance is governed by many machine factors such as (Bourgoyne *et al*., 1986):

- Thrust
- Rotation speed
- Bit type
- Rod diameter
- Lubricants
- Air pressure and bailing rate

2.5.1.1 Drilling and Rock Breakage

Rock failure by drilling occurs as a result of 3 distinct mechanisms (Bourgoyne *et al*., 1986) (Heinz, 2009):

1) Crushing
2) Shearing
3) Abrading

The energy, weight on bit (WOB), required to drill rock is directly proportional to the rock's UCS (Bar-Cohen & Zacny, 2009). Rocks fail when applied load exceeds the compressive strength of the rock. A higher WOB or a lower UCS value for the rock will result in a higher penetration rate (Figure 24) (Bourgoyne *et al*., 1986).

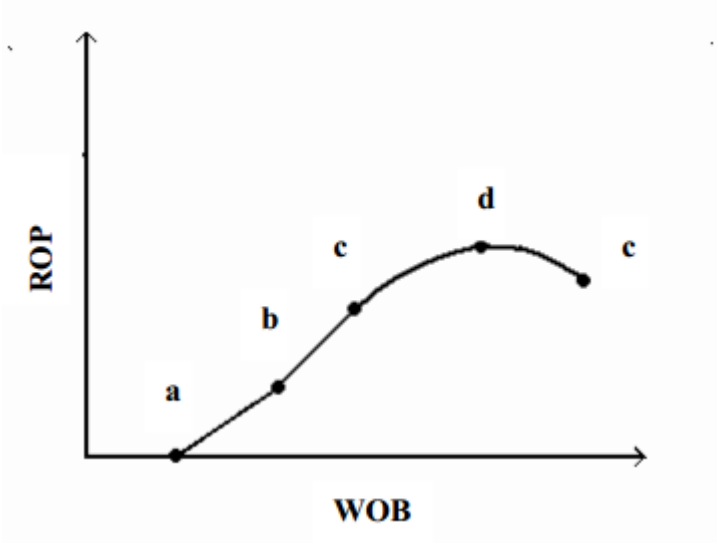


Figure 24: Typical ROP vs. WOB response plot (Source: Osgouei, 2007)

During drilling, rock breakage occurs when the weight on bit (WOB) is greater than rock strength (a) (Figure 24). ROP increases until maximum efficiency is reach (b to c). This relationship becomes less linear as cleaning efficiency decreases (c to d). A decrease in ROP is observed at higher WOB due to the decreasing efficiency of cleaning of cuttings and the complete burying of cutting elements in the rock mass (collectively termed bit floundering) (d to e) (Bourgoyne *et al*., 1986).

Jacques du Toit, Rock Engineer at Mogalakwena Mine, created a generalised penetration rate plan for North, Central and South Pit based on manually reported drilling time and depth (Figure 25). The model is useful for basic planning but inherently carries human errors in reporting.

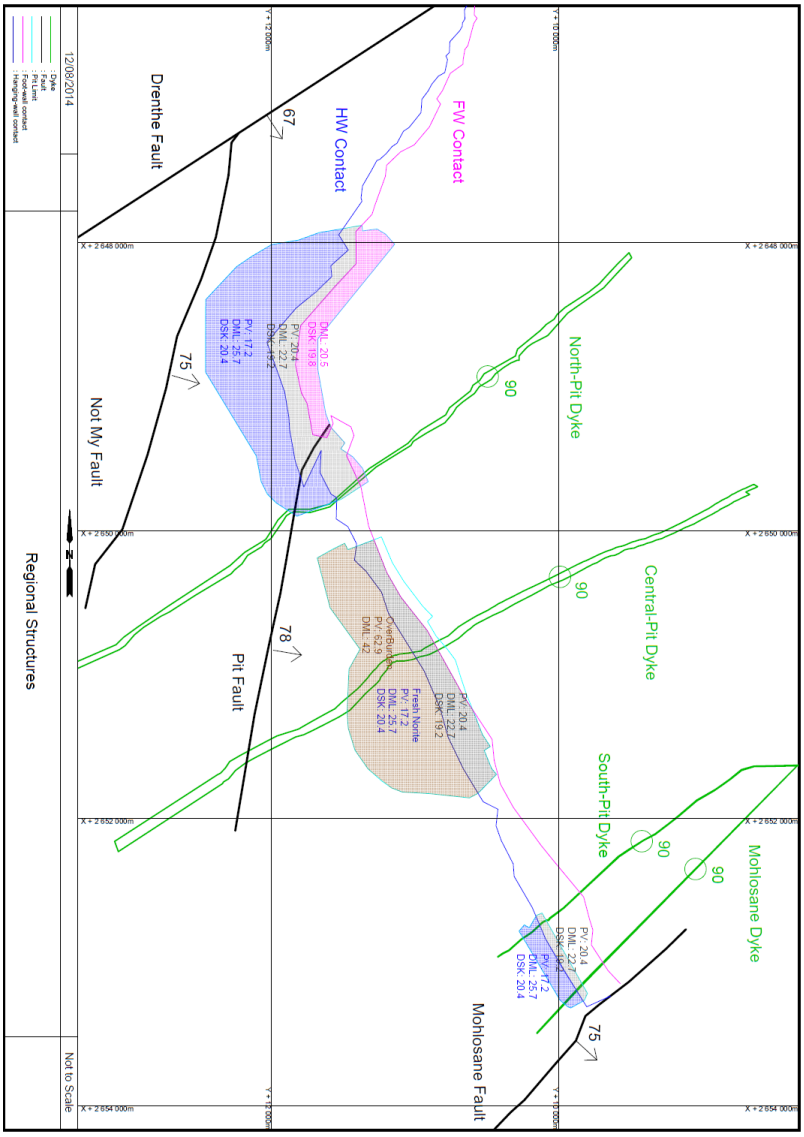


Figure 25: Mean drilling penetration rate for 3 drill rig types per stratigraphic unit (Source: Du Toit, 2014)

Drilling rigs are scheduled according to the number of holes required to be drilled. Penetration rates as a function of rock strength are not incorporated.

2.5.1.2 Measurement While Drilling

Sensory technology installed onto pre-existing or purpose built machinery which record a wealth of information are continually being developed. This is a highly technical area of expertise. Methods are being improved and developed at a fast rate. Sensory technology can be installed onto drilling rigs that will record and store drilling parameters for a drilled hole. Such technology is termed a measurement while drilling (MWD) system. Companies establish algorithms to convert the data into a drilling index for rock recognition based primarily on penetration rate and WOB. These algorithms need to be calibrated to site specific rocks. Representative rock samples must be collected and tested. The calibration itself needs to be continuously updated (A Bye 2014, pers. comm.).

MWD rock recognition systems work best when large differences in rock mass strength exist in the rock. Subtle changes in rock strength may be lost within the noise margin in uniform deposits. Any new equipment or operators must be fully incorporated, trained and calibrated for the information generated to be useful. Autonomous drilling will negate the human error component (A Bye 2014, pers. comm.; P Martensson 2014, pers. comm.). This technology can be installed on site and the data produced, if accurate, can be made useful for downstream mining processes including blasting and comminution (Figure 26).

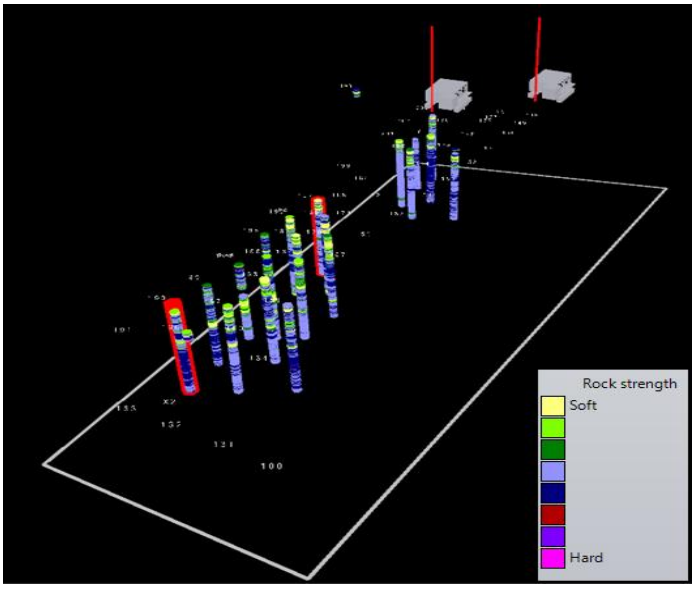


Figure 26: 326-085 being drilled and the reporting of relative rock strength by PV149

MWD systems represent vast potential *in situ,* fit for purpose characterisation of ore for downstream processes.

2.6 Summary

Pre-existing and relevant research was investigated in this chapter. The chapter highlighted areas in which drilling and processing performance can be optimised with a better understanding of geological characteristics. The next chapter discusses the methodology

CHAPTER 3: METHODOLOGY

3.1 Introduction

This chapter outlines the sequential aims of the project and the method in which the objectives are to be achieved. The steps are bulleted for clarity. The project has 5 main areas of investigation. Each area is dealt with sequentially and all investigations relate to the use of rock strength understanding on mining and processing applications.

3.2 Textural Distribution of Major Rock Types

The distribution of texture and grain size per major reef lithology type was achieved through the following steps:

1) Export Data

   UCS data was sourced from the exploration database stored on SABLE Warehouse. Data from the farm OY farm which is the property on which 80% of production is produced.

   Data exported was:

   - Hole position
   - Rock type
   - Stratigraphy
   - Texture
   - Grain size

2) Lithological Distribution Analysis

A distribution analysis of the reef rocks was conducted to identify the major rock types. The percentage of occurrence of each rock type in the database was calculated to determine the weighting of rock types in the entire database.

3) Reef Distribution

The distribution of rock types within the reef is investigated by sorting the data according to stratigraphy. The major reef rock types were identified.

4) Textural Distribution

The textural distribution for each of the major rock types was investigated using distributions of all textural identifications.

5) Grain size Distribution

The grain size distribution for each of the major rock types was investigated using distributions of all grain size identifications.

6) Field Check

A field check investigated the changes in lithology, texture and grain sizes in the pit.

3.3 Rock Strength and Textural Distribution

The compressive strength for the major reef rock types was investigated through the following steps:

1) Calculate mean UCS

   UCS results for the rock types were split according to texture and grain size.

2) Validate UCS results

   A sample set of exploration core underwent PL tests. The PLI results were converted to UCS.

3.4 Strength and Hardness Relationships

1) Strength and hardness test work comparison

   The relationship between UCS, BWI and DWT was investigated by comparing means from a limited database. Strong correlations will highlight relationships that may need to be investigated further.

3.5 Drilling Performance and Rock Strength

Pit Viper PV 149 was used to investigate drilling performance over different rock types.

1) Penetration rate data was exported after patterns were drilled.

An export function within the RockMa system was used to calculate ROP of blast holes.

2) Compare HW, Reef and FW performance

   The ROP in different stratigraphic units was investigated. The mean ROP for the different stratigraphic units was calculated within the OY farm boundary.

   Two values for UCS were used in the analysis, both of which were sourced from the exploration database. The first is the accepted UCS value for the rock which was derived from UCS test work. The second UCS value was sourced from this project using the PL derived UCS.

3) Quantify variability in drilling performance within a rock type

   The specific rock type of the blast hole was taken into account when comparing ROP. Variation in the rock type was quantified.

3.6 Strength Modelling

A 3D model was created to spatially quantify the *in situ* rock strength within OY. Voxler 3 modelling software was used to plot strength.

1) Apply mean UCS to all lithologies.

2) Compare grain size of sample to reported UCS result.

3) Apply grain size adjusted UCS to relevant lithologies.

4) Plot UCS in 3D model

3.7 Financial benefit Analysis

1) Apply benefit of ore strength domaining to South Plant comminution process.

3.8 Summary

This chapter outlines the steps in which the 5 investigation areas were carried out. The 5 areas represent 5 distinct but related investigations culminating in the creation of a 3D model to represent textually adjusted UCS. The next chapter discusses the results of the investigations.

CHAPTER 4: RESULTS AND INTERPRETATION

4.1 Introduction

The chapter that follows discusses the results of the investigations into texture, rock strength and applicable uses. The results are based largely on the exploration database and culminates with the creation of a 3D model of grain size adjusted UCS. The results are displayed in a catalogued manner in order to make this project easy reference material for future work.

4.2 Textural Distribution of Major Rock Types

The data export was done from the exploration SABLE database covering OY farm. Only boreholes from the Complete Branch were exported which constituted 754 boreholes. The Complete Branch in SABLE represents boreholes which have passed various validation tests and have been deemed acceptable to be used in the resource model. The exploration boreholes were plotted using Datamine Studio 3 (Figure 27). The exploration boreholes show a good spread across the farm boundary.

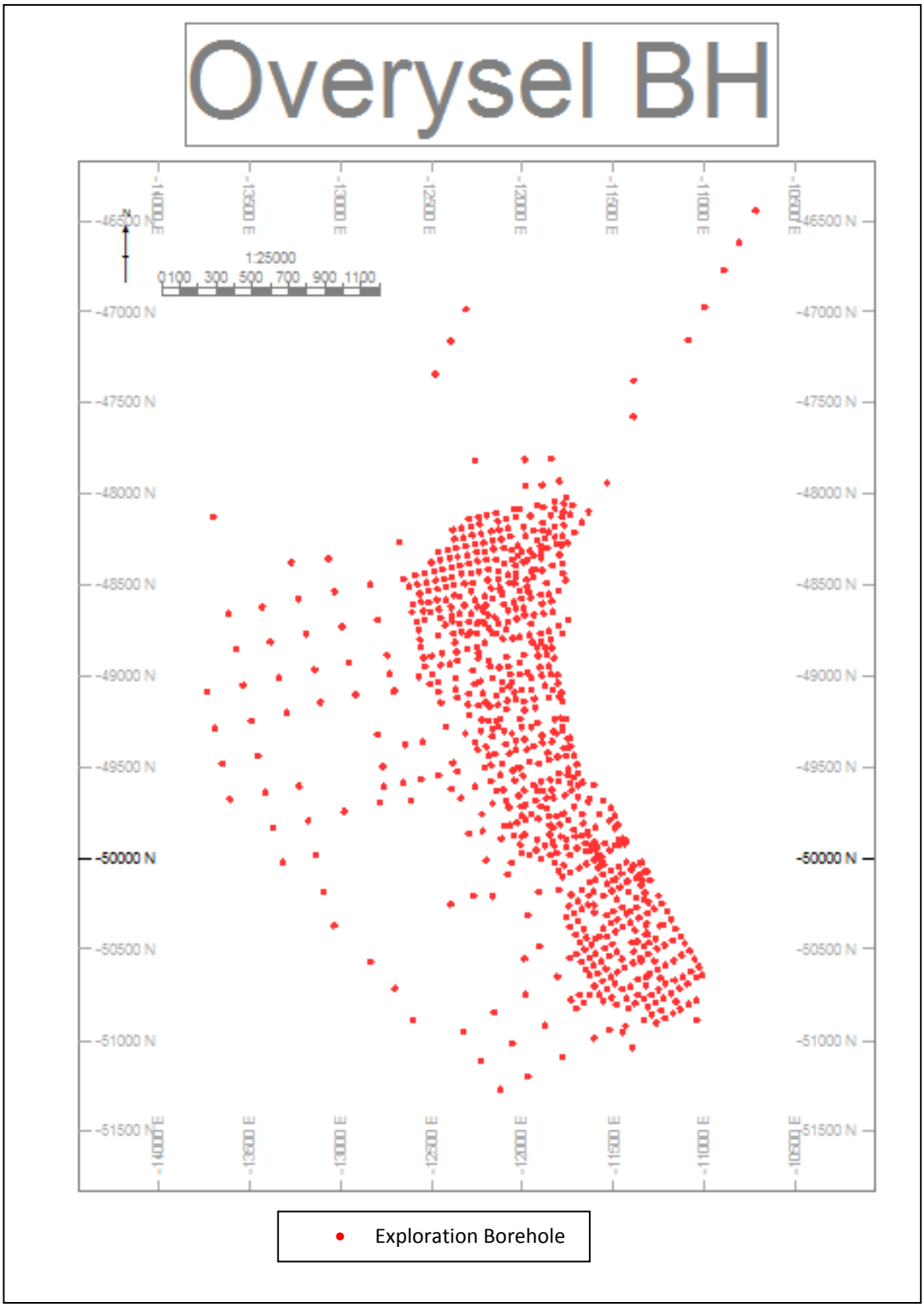


Figure 27: Distribution of 754 exploration holes located on Overysel farm used for hardness data.

4.2.1 Lithology Distribution Analysis

There were 97 rock types in the entire database covering 315 022.354m[1]. Rock distribution percentages from the total meters logged (Table 6). Common rocks consist of 92.99% of the database. 7.01% are minor rock types.

Table 6: Total percentage of rock types in the OY exploration database.

Stratigraphy	Rock Type	OY	Distribution in Stratigraphy	Percent per stratigraphy
HW	Norite	26.64%	47.75%	55.79%
	Leuco -	6.05%	10.85%	
	Mela -	0.71%	1.27%	
	Gabbronorite	7.06%	12.66%	
	Leuco -	2.46%	4.41%	
	Mela -	3.77%	6.75%	
	Variable Textured Anorthosite	5.47%	9.81%	
	Poikalitic Anorthosite	3.63%	6.50%	
Reef	Pyroxenite	4.04%	16.36%	24.72%
	Serpentinised Pyroxenite	1.97%	7.99%	
	Feldspathic Pyroxenite	14.02%	56.71%	
	Serpentinised Feldspathic Pyroxenite	0.98%	3.95%	
	Pegmatoidal Feldspathic Pyroxenite	0.91%	3.67%	
	Serpentinite	0.74%	3.01%	
	Calc-Silicate	0.39%	1.57%	
	Parapyroxenite	0.59%	2.37%	
	Serpentinised Parapyroxenite	1.01%	4.09%	
	Feldspathic Parapyroxenite	0.07%	0.28%	
FW	Granofels	7.63%	99.11%	7.70%
	Dolomite	0.07%	0.89%	
Vein	Granite (includes FW granites)	3.74%	78.15%	4.78%
	Quartz Feldspathic Vein	1.04%	21.85%	
	Total	92.99%		
	Minor rock types	7.01%		

[1] All core loss meters were removed from the dataset.

The distribution is shown graphically in Figure 28. Other rock types include a variety of minor rock types and intrusives. Dolomite, which makes up the footwall of Zwartfontein and Sandsloot properties is almost absent in North Pit. Quartz feldspathic vein occurs in the reef along faults, shear zones and discrete veins making up to 1% of total rock types. These rock types will be ignored for this study.

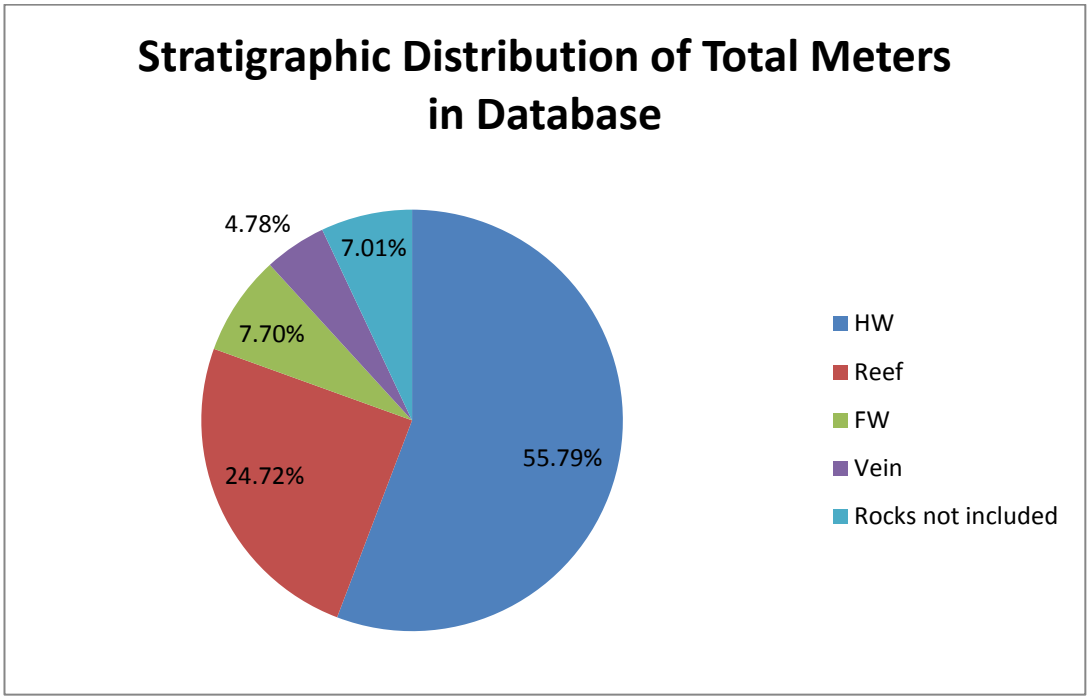


Figure 28: Stratigraphic distribution of OY exploration database.

The reef constitutes 24.72% of the rocks in the exploration database while the other rocks, excluding the minor rock, types constitute waste rocks (Table 6).

The stratigraphic distribution of rock types conforms well to the actual mining tons for 2011 to 2013 and the planned tons for 2014 (Table 7). This adds weight to the representative nature of the OY database.

Table 7: Waste and ore production per year.

	2011		2012		2013		2014 (Planned)	
Type	Tons	Percentage	Tons	Percentage	Tons	Percentage	Tons	Percentage
Ore	17786274	24.80%	14662646	22.77%	18488706	24.53%	18695070	21.85%
Waste	53933185	75.20%	49721279	77.23%	56882957	75.47%	66860620	78.15%
Total	71719459		64383925		75371663		85555690	

In summary, actual production of ore from 2011 to 2013 relative to waste conforms closely to database distribution (Table 8).

Table 8: Total reported waste and ore production from 2011 to 2013.

	Actual 2011 - 2013	
Type	Tons	Percentage
Ore	50937626	24.09%
Waste	160537421	75.91%
Total	211475047	

The representativity of the exploration database is acceptable to proxy the amount and types of rocks mined. Ore tons mined is 24.09% while reef in the exploration database is 24.72%.

4.2.2 Reef Distribution

Distribution of rock types within the reef package are graphically represented in Figure 29. Feldspathic pyroxenite constitutes the majority of the rock types.

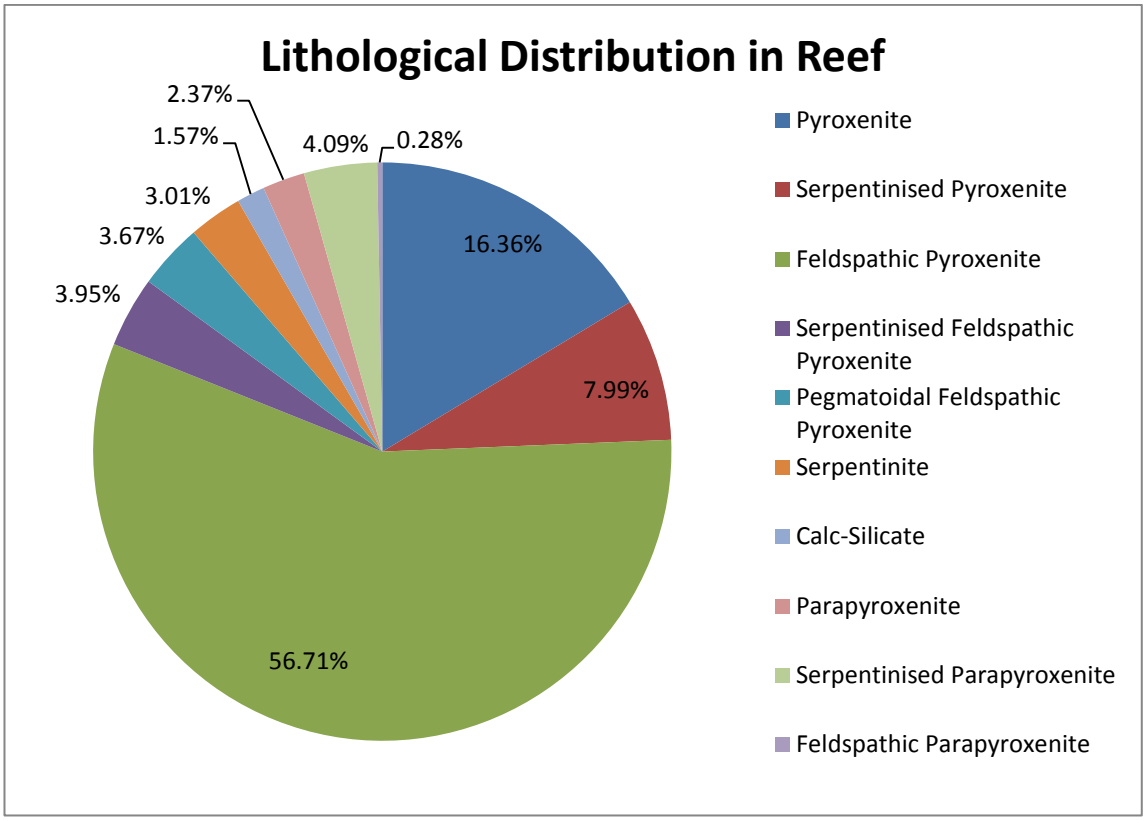


Figure 29: Lithological distribution in the reef package at OY.

4.2.3 Textural Distribution

Textual variability is high in the Platreef. There are 34 lookups for texture in the SABLE database as described while logging the core. The texture "Blank" is applied where no texture was recorded during core logging. Investigations were conducted on the mineralised reef and foot wall. The abbreviations for the textures used in the report can be found in Table 9. The full list of abbreviations for textural descriptions can be found in Appendix 2.

Table 9: Textural abbreviations and descriptions.

TEXTURE	Description
BND	Banding
BREC	Brecciated
CUMU	Cumulate
GRAPHIC	Graphic
HOM	Homogeneous
PEG	Pegmatoidal
POIK	Poikalitic
RECRY	Recrystallised
VARI	Varitextured (varied)

4.2.3.1 Reef

The distribution of textures in the reef is recorded in Table 10. The results are graphically represented in Figure 30. The results show a general trend of cumulus texture in altered rocks and the use of the term recrystallised for metamorphic and altered rocks. 42.43% of lithology entries in the database were not logged with textural information. The majority of reef rocks can be described by 4 textures, namely; cumulus (CUM), pegmatoidal (PEG), recrystallised (RECRY) and varied (VARI). Varied texture is used to when multiple grain sizes and textures occur within a small area.

4.2.3.2 Footwall

The footwall rock in OY is solely granofels (GF). Granofels exhibit a large variability in textures for a single rock type (Table 11). Results show that granofels are described using 5 textures, namely; banded (BND), brecciated (BREC), cumulus, recrystallised and varied (Figure 31). 50.26% of the granofels do not have a recorded texture in the database.

Table 10: Distribution of textures in the reef.

Texture	CALCSIL	FPYX	PARAFPYX	PARAPYX	PEGFPYX	PYX	SERP	SFPYX	SPARAPYX	SPYX	Total
CUMU	9.85%	42.48%	36.67%	14.02%	3.72%	63.08%	2.61%	56.33%	45.98%	59.98%	42.56%
PEG	0.05%	0.75%	0.67%	0.78%	86.24%	0.34%	0.32%	0.03%	0.00%	0.27%	4.29%
RECRY	53.06%	0.69%	59.23%	12.59%	0.22%	0.57%	12.20%	12.96%	36.29%	30.93%	6.69%
VARI	1.10%	3.85%	0.00%	0.00%	0.00%	0.13%	0.00%	0.20%	1.74%	0.41%	2.45%
Blank[2]	32.25%	51.22%	2.02%	69.26%	9.79%	34.30%	76.41%	29.74%	11.33%	6.94%	42.43%
Other											1.59%

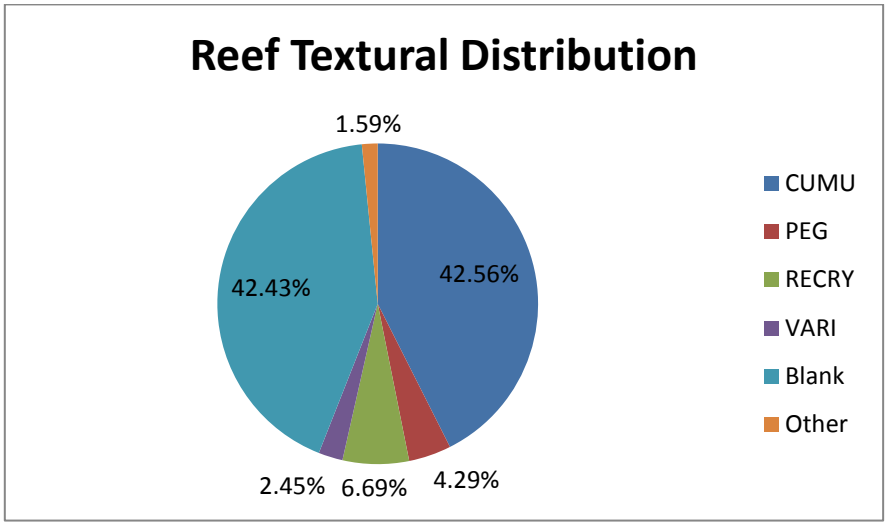


Figure 30: Textural distribution in the reef.

[2] The term Blank is used for entries without textural information.

Table 11: Textural distribution in the footwall granofels.

Texture	GF	Total
BND	3.58%	3.58%
BREC	1.07%	1.07%
CUMU	5.00%	5.00%
RECRY	19.33%	19.33%
VARI	3.97%	3.97%
Blank	50.26%	50.26%
Other		16.78%

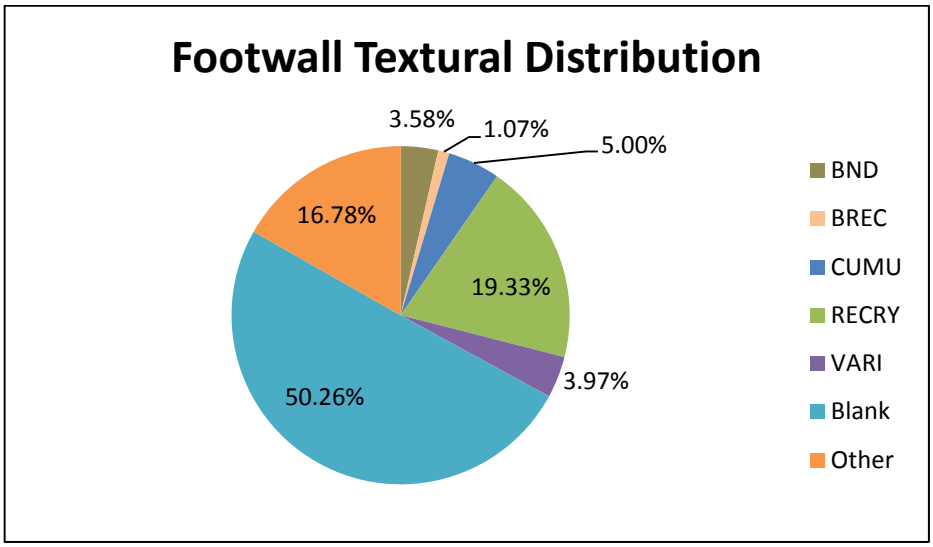


Figure 31: Textural distribution in the footwall.

4.2.4 Grain Size Distribution

There are 17 grain size categories used in SABLE (Appendix 2). Categories allow for the identification of a bimodal or a host rock showing multiple grain sizes i.e. F-C (fine – coarse). The exploration core is logged visually and grain size is described using a hand held ruler based on ISRM recommendations for grain size descriptive categories.

Grain sizes for the major textural descriptions for each rock are analysed. This will produce a textual description which will describe 90% of that particular rock type. The grain size abbreviations and descriptions are shown in Table 12.

Table 12: Grain size abbreviations and descriptions used in the report.

GRAIN SIZE	Description
VF	Very fine
F	Fine
F-M	Fine to medium
F-C	Fine to coarse
F-PEG	Fine to pegmatoidal
M-F	Medium to fine
M	Medium
M-C	Medium to coarse
M-VC	Medium to very coarse
M-PEG	Medium to pegmatoidal
C-M	Coarse to medium
C	Coarse
C-VC	Coarse to very coarse
C-PEG	Coarse to pegmatoidal
VC	Very coarse
VC-PEG	Very coarse to pegmatoidal
PEG	Pegmatoidal

4.2.4.1 Reef

Rock types occurring in the reef are analysed below. The following properties for each rock type are described:

- Total meters in the exploration database that are listed as the rock type.
- The meters that are described using the major textures.
- The total representativity of the rock using the major textures.

4.2.4.1.1 Feldspathic Pyroxenite

The distribution of textures describing feldspathic pyroxenite in the OY database is summarised (Figure 32):

Total feldspathic pyroxenite meters:	23354.996m
Covered by cumulus, varied and blank:	20415.311m
Other textures:	2939.685m
Representativity of textures:	87.4%

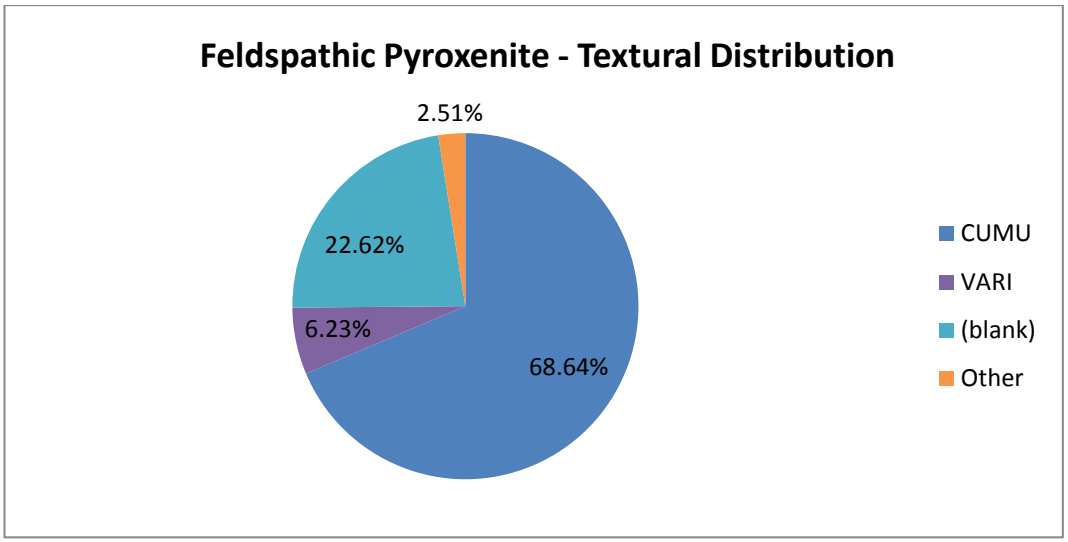


Figure 32: Feldspathic pyroxenite - Textural distribution of feldspathic pyroxenite.

Grain size distribution analysis results show the following (Table 13 and Figure 33):

- Dominant texture is cumulus.
- Blank texture is mirroring both cumulus and vari results.
- Dominant grain sizes are F to M-PEG (highlighted in green).
- Selected grain sizes and textures account for 21549.816m.

Representativity of feldspathic pyroxenite using the identified textures (including the blank texture) and grain sizes is **92.27%.**

Table 13: Feldspathic pyroxenite - Grain sizes per texture and their occurrence in the exploration database in meters. Dominant grain sizes are highlighted in green.

Grain Size	CUMU (m)	VARI (m)	Blank (m)	Total (m)
VF	10.18		12.86	23.04
F	625.93	44.58	406.44	1076.95
F-M	2002.78	316.86	699.71	3019.35
F-C	834.69	129.83	65.88	1030.39
F-PEG	256.24	116.44		372.68
M-F	1822.9		365.33	2188.23
M	6826.31	485.35	2249.815	9561.48
M-C	2719.13	209.83	959.735	3888.69
M-VC	50.47		6.95	57.42
M-PEG	566.27	151.46	66.99	784.72
C-M	40.89			40.89
C	122.48		24.62	147.1
C-VC	87.92		95.52	183.44
C-PEG	7.69		99.96	107.65
VC	39.63		8.75	48.38
VC-PEG			5.97	5.97
PEG	0.08			0.08
Blank	17.03		214.68	231.71
Total	**16030.616**	**1454.35**	**5283.21**	**22768.176**

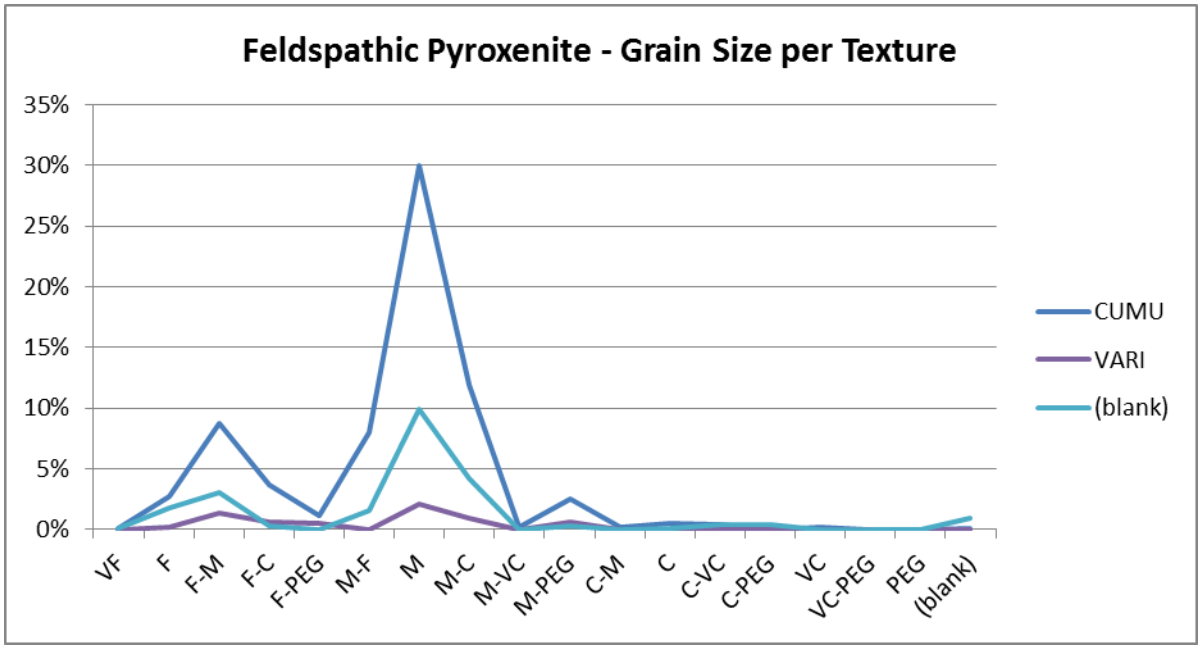


Figure 33: Feldspathic pyroxenite - Grain size distribution for each textural description.

4.2.4.1.2 Pyroxenite

The distribution of textures describing pyroxenite in the OY database is summarised (Figure 34):

Total pyroxenite meters:	6380.77m
Described by cumulus and blank:	6208.02m
Other textures:	172.75m
Representativity of chosen textures:	97.29%

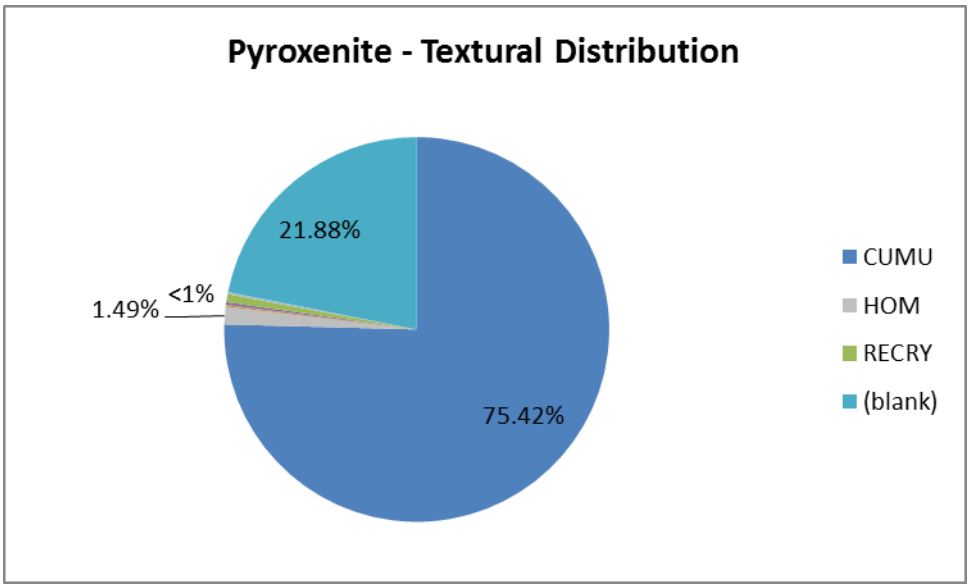


Figure 34: Pyroxenite - Textural distribution of pyroxenite.

Grain size distribution analysis results show the following (Table 14 and Figure 35):

- Dominant texture is cumulus.
- Blank is mirroring cumulus results and can be assumed to be cumulus texture.
- Dominant grain sizes are F till M-PEG
- Selected grain sizes and textures account for 5717.84m

Representativity of feldspathic pyroxenite using the identified textures (including the blank texture) and grain sizes is **89.61%**.

Table 14: Pyroxenite - Grain sizes per texture and their occurrence in the exploration database in meters. Dominant grain sizes are highlighted in green.

Grain Size	CUMU (m)	Blank (m)	Total (m)
VF	82.22	8.86	91.08
F	1568.83	290.82	1859.64
F-M	716.38	143.85	860.23
F-C	113.53		113.53
F-PEG	6.9		6.9
M-F	593.63	63.31	656.94
M	1265.59	327.7	1593.29
M-C	295.7	292.49	588.19
M-VC	27.76		27.76
M-PEG	22.07		22.07
C-M	13.51		13.51
C	20.47	69.14	89.61
C-VC	69.94		69.94
VC	2.25		2.25
Blank	13.29	199.79	213.08
Total	**4812.065**	**1395.955**	**6208.02**

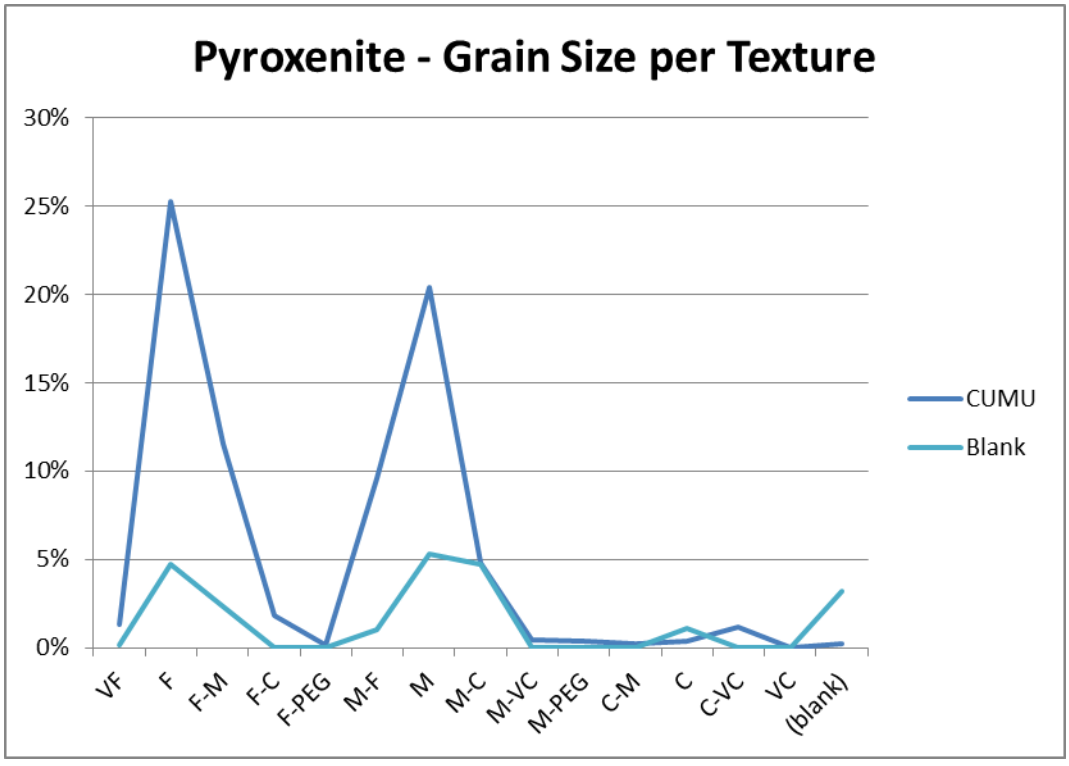


Figure 35: Pyroxenite - Grain size distribution for each textural description.

4.2.4.1.3 Serpentinite

The distribution of textures describing serpentinite in the OY database is summarised (Figure 36):

Total serpentinite meters:	2336m
Described by cumulus, homogenous, recrystallised and blank:	2256m
Other textures:	80m
Representativity of chosen textures:	96.58%

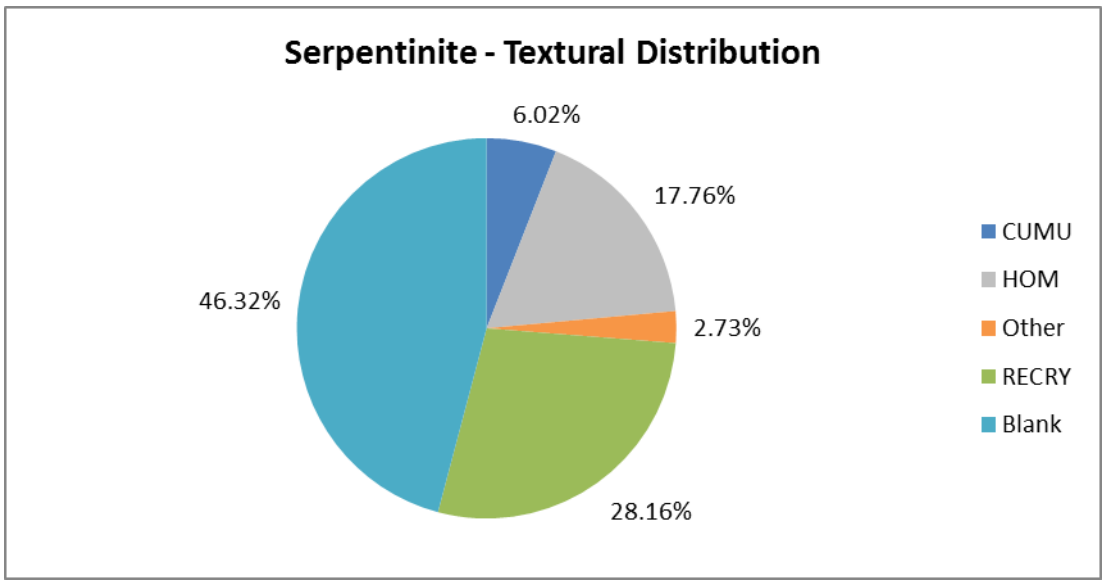


Figure 36: Serpentinite - Textural distribution of serpentinite.

Grain size distribution analysis results show the following (Table 15 and Figure 37):

- Dominant textures are cumulus, homogenous and recrystallised.
- All textures mirror each other except cumulate which consists of VF grain sizes.
- Dominant grain sizes are VF, F and M.
- Selected grain sizes and textures account for 2101m

Representativity of serpentinite using the identified textures (including the blank texture) and grain sizes is **89.94%.**

Table 15: Serpentinite - Grain sizes per texture and their occurrence in the exploration database in meters. Dominant grain sizes are highlighted in green.

Grain Size	CUMU (m)	HOM (m)	RECRY (m)	Blank (m)	Total (m)
VF	74		26	10	110
F	69	571	770	421	1831
F-M	9	5	3	8	25
F-C	1	3	1		5
M-F	4	3	5	1	13
M	47	3	86	24	160
M-C	1		21	2	24
C		1	4	3	8
Blank	1			79	80
Total	**206**	**586**	**916**	**548**	**2256**

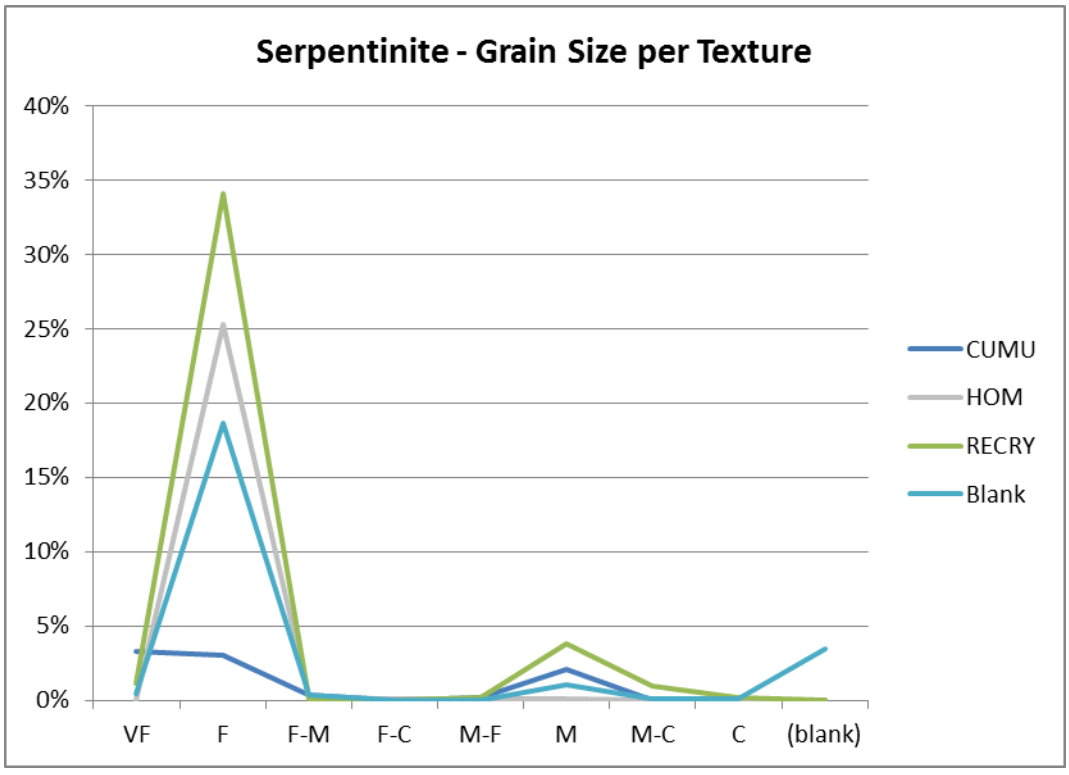


Figure 37: Serpentinite - Grain size distribution for each textural description.

4.2.4.1.4 Serpentinised Pyroxenite

The distribution of textures describing serpentinised pyroxenite in the OY database is summarised (Figure 38):

Total serpentinised pyroxenite meters:	1434m
Described as cumulus, recrystallised and blank:	1387m
Other textures:	47m
Representativity of chosen textures:	96.72%

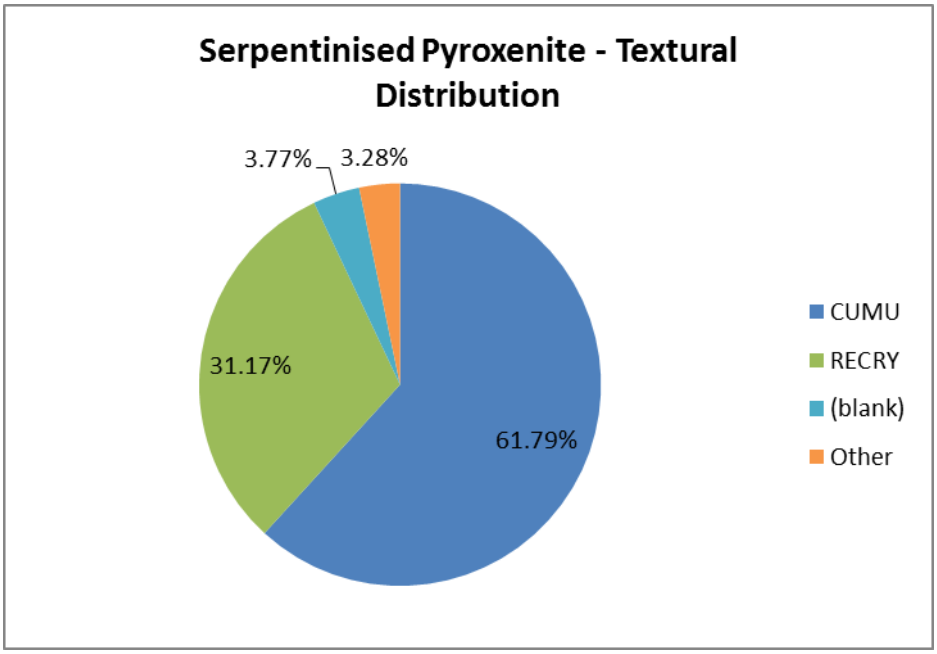


Figure 38: Serpentinised pyroxenite - Textural distribution of serpentinised pyroxenite.

Grain size distribution analysis results show the following (Table 16 and Figure 39):

- Dominant textures are cumulus and recrystallised.
- Textures show mirroring in grain size distribution.
- Dominant grain sizes are F, F-M, M-F, M and M-C.
- Selected grain sizes and textures account for 1387m

Representativity of feldspathic pyroxenite using the identified textures (including the blank texture) and grain sizes is **91.84%.**

Table 16: Serpentinised pyroxenite - Grain sizes per texture and their occurrence in the exploration database in meters. Dominant grain sizes are highlighted in green.

Grain Size	CUMU (m)	RECRY (m)	Blank (m)	Total (m)
VF		2	1	3
F	116	125	24	265
F-M	225	50	1	276
F-C	11	22		33
M-F	69	46		115
M	309	152	18	479
M-C	142	38	2	182
M-VC	1			1
M-PEG	3	1		4
C-M		7		7
C	7	2	2	11
C-VC	1	1		2
VC	1			1
Blank	1	1	6	8
Total	**886**	**447**	**54**	**1387**

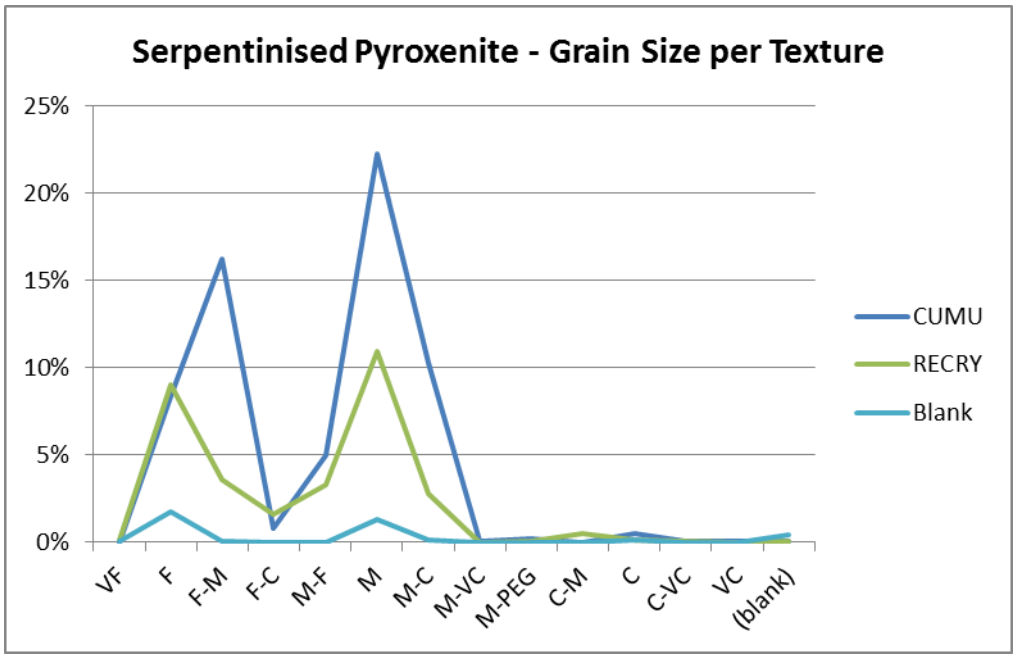


Figure 39: Serpentinised pyroxenite - Grain size distribution for each textural description.

4.2.4.1.5 Serpentinised Feldspathic Pyroxenite

The distribution of textures describing serpentinised feldspathic pyroxenite in the OY database is summarised (Figure 40):

Total serpentinised feldspathic pyroxenite meters:	971m
Described as cumulus, recrystallised and blank:	950m
Other textures:	21m
Representativity of chosen textures:	97.84%

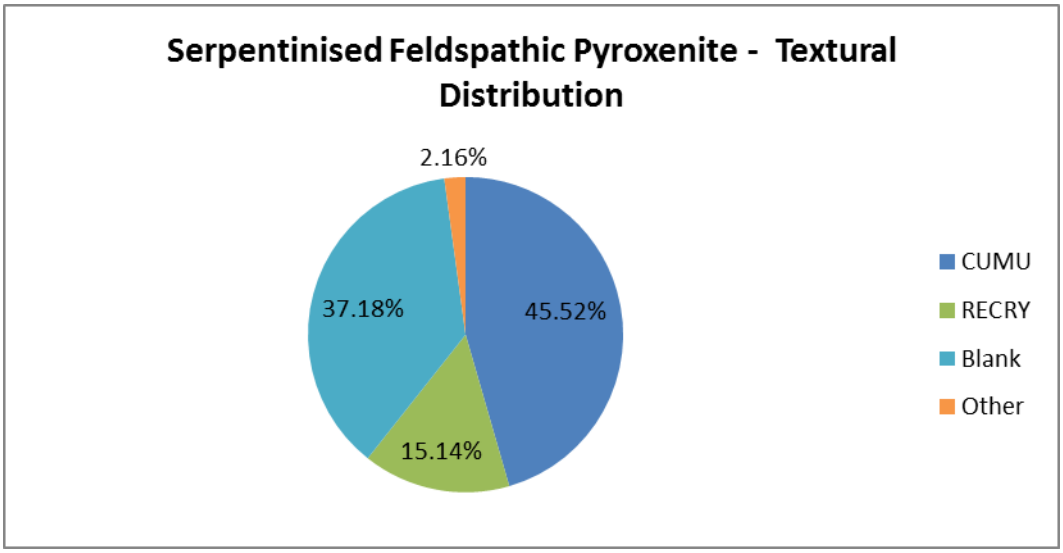


Figure 40: Serpentinised feldspathic pyroxenite - Textural distribution of serpentinised feldspathic pyroxenite.

Grain size distribution analysis results show the following (Table 17 and Figure 41):

- Dominant textures are cumulus, recrystallised and blank.
- Dominant grain sizes are F, F-M, M-F, M and M-C.
- This rock type is very similar to serpentinised pyroxenite in textural distribution.
- Selected grain sizes and textures account for 884m

Representativity of serpentinised feldspathic pyroxenite using the identified textures (including the blank texture) and grain sizes is **91.04%.**

Table 17: Serpentinised feldspathic pyroxenite - Grain sizes per texture and their occurrence in the exploration database in meters. Dominant grain sizes are highlighted in green.

Grain Size	CUMU (m)	RECRY (m)	Blank (m)	Total (m)
VF	3			3
F	33	13	12	58
F-M	43	6	3	52
F-C	12	22		34
F-PEG		1		1
M-F	25	18		43
M	215	54	324	593
M-C	101	28	9	138
M-PEG	3		3	6
C-M	1	5		6
C	4		1	5
VC	1			1
VC-PEG	1			1
Blank			9	9
Total	**442**	**147**	**361**	**950**

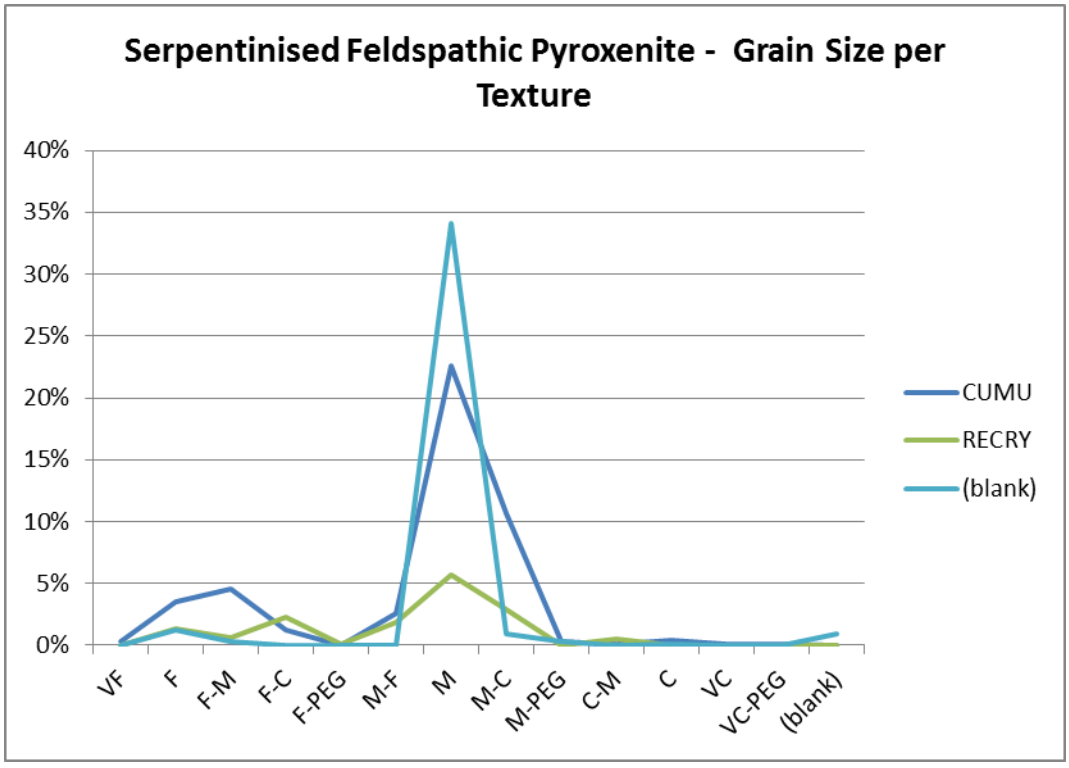


Figure 41: Serpentinised feldspathic pyroxenite - Grain size distribution for each textural description.

4.2.4.1.6 Pegmatoidal Feldspathic Pyroxenite

The distribution of textures describing pegmatoidal feldspathic pyroxenite in the OY database is summarised (Figure 42):

Total pegmatoidal feldspathic pyroxenite meters:	591m
Described as pegmatoidal:	562m
Other textures:	29m
Representativity of chosen textures:	95.09%

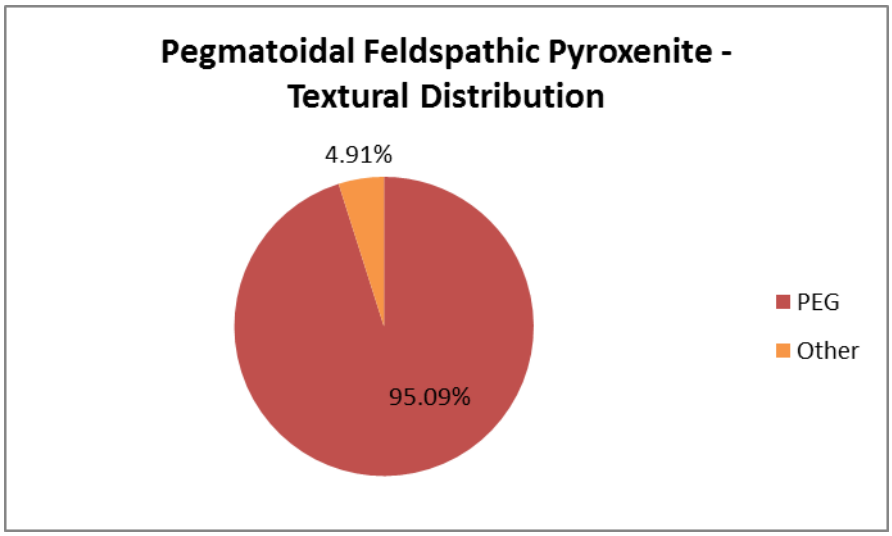


Figure 42: Pegmatoidal feldspathic pyroxenite - Textural distribution of pegmatoidal feldspathic pyroxenite.

Grain size distribution analysis results show the following (Table 18 and Figure 43):

- Dominant texture is pegmatoidal.
- Dominant grain sizes are M, M-C, M-PEG, C, C-VC, C-PEG, PEG.
- Pegmatoids described as medium grained assumed to represent rock recrystallised in close proximity to coarse grained pegmatoids.
- Selected grain sizes and textures account for 550m

Representativity of pegmatoidal feldspathic pyroxenite using the identified textures (including the blank texture) and grain sizes is **93.06%.**

Table 18: Pegmatoidal feldspathic pyroxenite - Grain sizes per texture and their occurrence in the exploration database in meters. Dominant grain sizes are highlighted in green.

Grain Size	PEG (m)	Total (m)
F-M	2	2
M-F	5	5
M	93	93
M-C	61	61
M-VC	2	2
M-PEG	114	114
C	35	35
C-VC	18	18
C-PEG	42	42
VC	2	2
VC-PEG	1	1
PEG	187	187
Grand Total	**562**	**562**

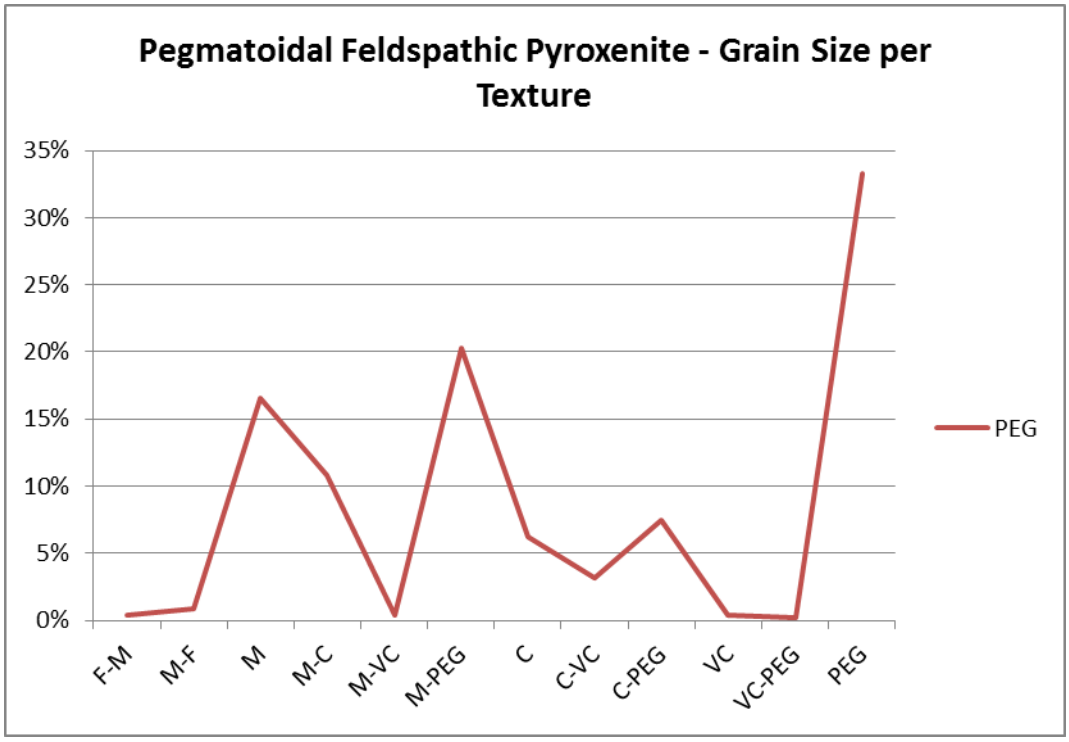


Figure 43: Pegmatoidal feldspathic pyroxenite - Grain size distribution for each textural description.

4.2.4.1.7 Parapyroxenite

The distribution of textures describing Parapyroxenite in the OY database is summarised (Figure 44):

Total parapyroxenite meters:	646m
Described as cumulus, recrystallised and blank:	637m
Other textures:	9m
Representativity of chosen textures:	98.61%

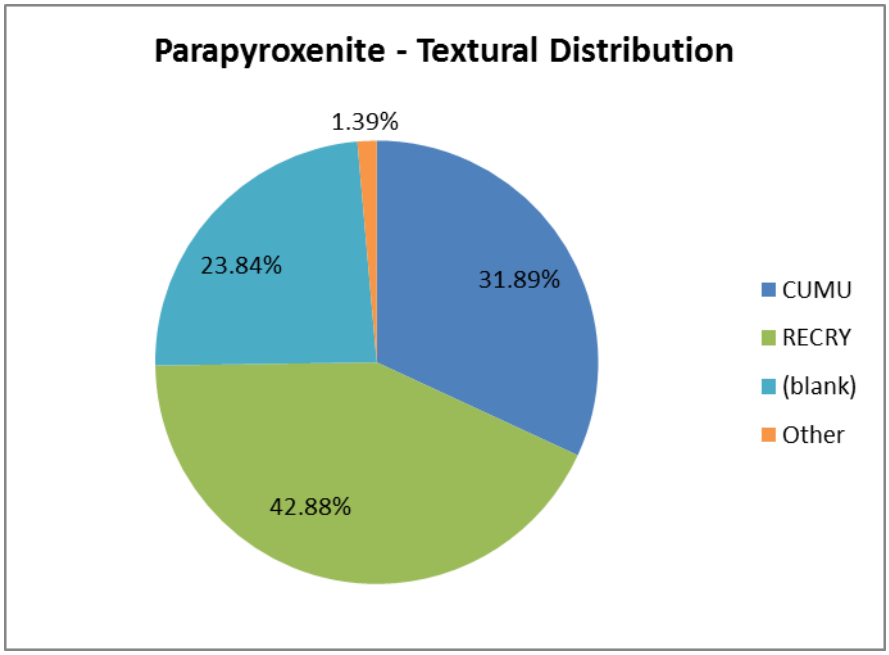


Figure 44: Parapyroxenite - Textural distribution of parapyroxenite.

Grain size distribution analysis results show the following (Table 19 and Figure 45):

- Dominant textures are cumulus and recrystallised.
- Dominant grain sizes are F,F-M,M-F,M,M-C
- Selected grain sizes and textures account for 585m

Representativity of parapyroxenite using the identified textures (including the blank texture) and grain sizes is **90.56%.**

Table 19: Parapyroxenite - Grain sizes per texture and their occurrence in the exploration database in meters. Dominant grain sizes are highlighted in green.

Grain Size	CUMU (m)	RECRY (m)	Blank (m)	Total (m)
VF	2	3		5
F	23	122	48	193
F-M	63	13	23	99
F-C	1	3		4
M-F	15	12		27
M	41	113	45	199
M-C	59	3	5	67
M-PEG		2		2
C-M		2		2
C			3	3
Blank	2	4	30	36
Total	**206**	**277**	**154**	**637**

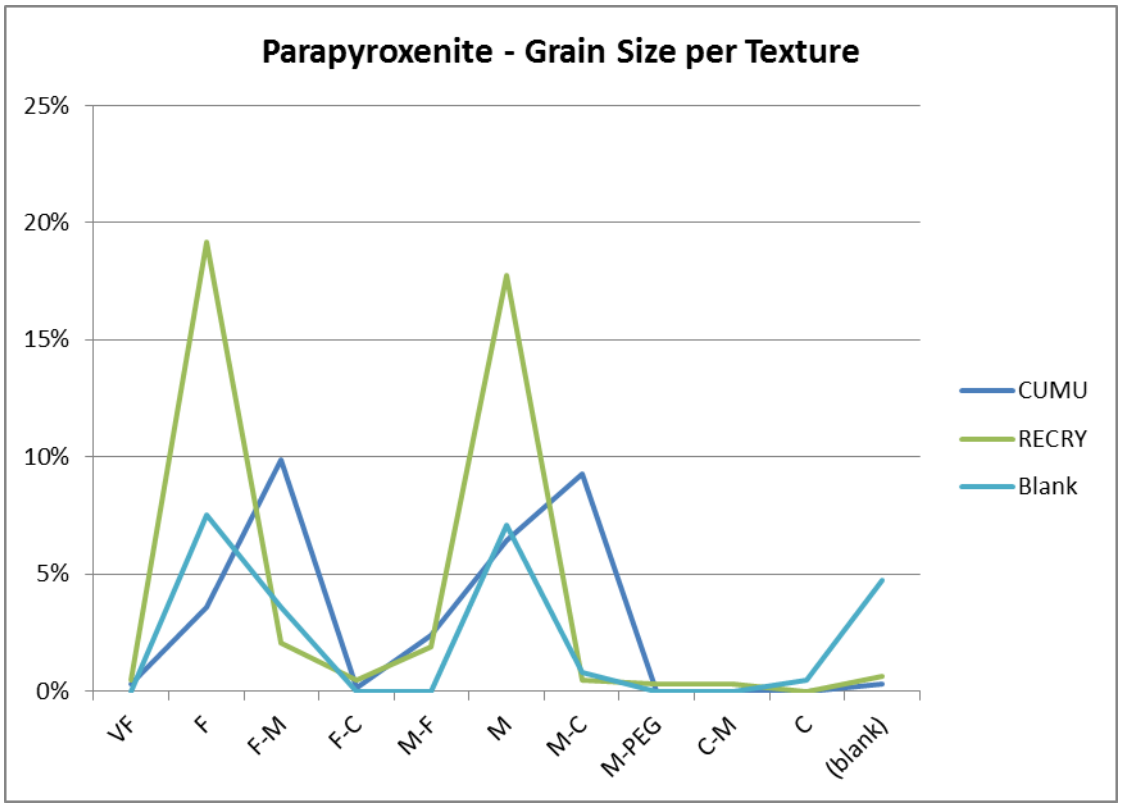


Figure 45: Parapyroxenite - Grain size distribution for each textural description.

4.2.4.1.8 Serpentinised Parapyroxenite

The distribution of textures describing serpentinised parapyroxenite in the OY database is summarised (Figure 46):

Total serpentinised parapyroxenite meters:	913m
Described as cumulus, recrystallised and blank:	869m
Other textures:	44m
Representativity of chosen textures:	95.18%

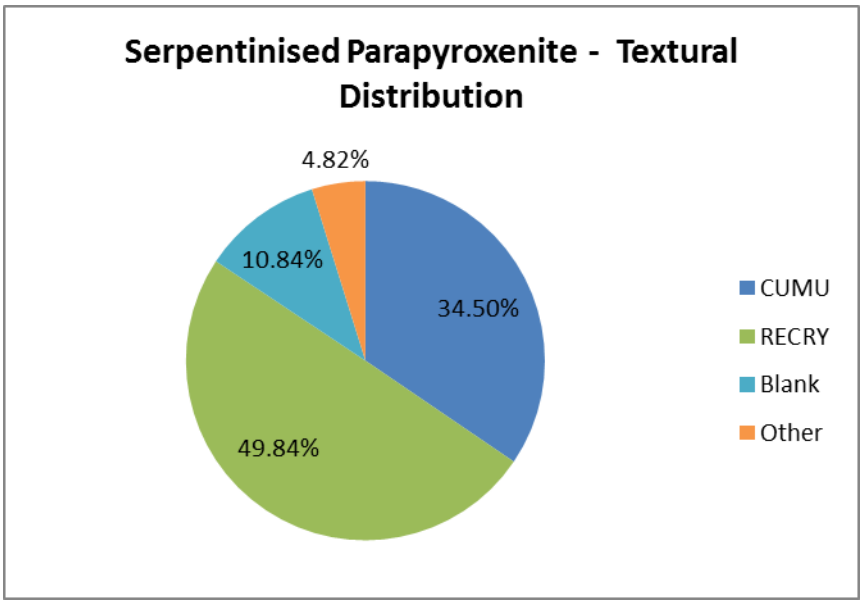


Figure 46: Serpentinised parapyroxenite - Textural distribution of serpentinised parapyroxenite.

Grain size distribution analysis results show the following (Table 20 and Figure 47):

- Dominant textures are cumulus and recrystallised.
- Dominant grain sizes are F, F-M, M-F, M, M-C.
- Grain size distribution similar to parapyroxenite.
- Selected grain sizes and textures account for 829m

Representativity of serpentinised parapyroxenite using the identified textures (including the blank texture) and grain sizes is **90.80%.**

Table 20: Serpentinised parapyroxenite - Grain sizes per texture and their occurrence in the exploration database in meters. Dominant grain sizes are highlighted in green.

Grain Size	CUMU (m)	RECRY (m)	Blank (m)	Total (m)
VF	2	3		5
F	28	228	19	275
F-M	51	34	2	87
F-C	6	7		13
M-F	35	47		82
M	79	124	61	264
M-C	114	5	2	121
C-M		5		5
Blank		2	15	17
Total	**315**	**455**	**99**	**869**

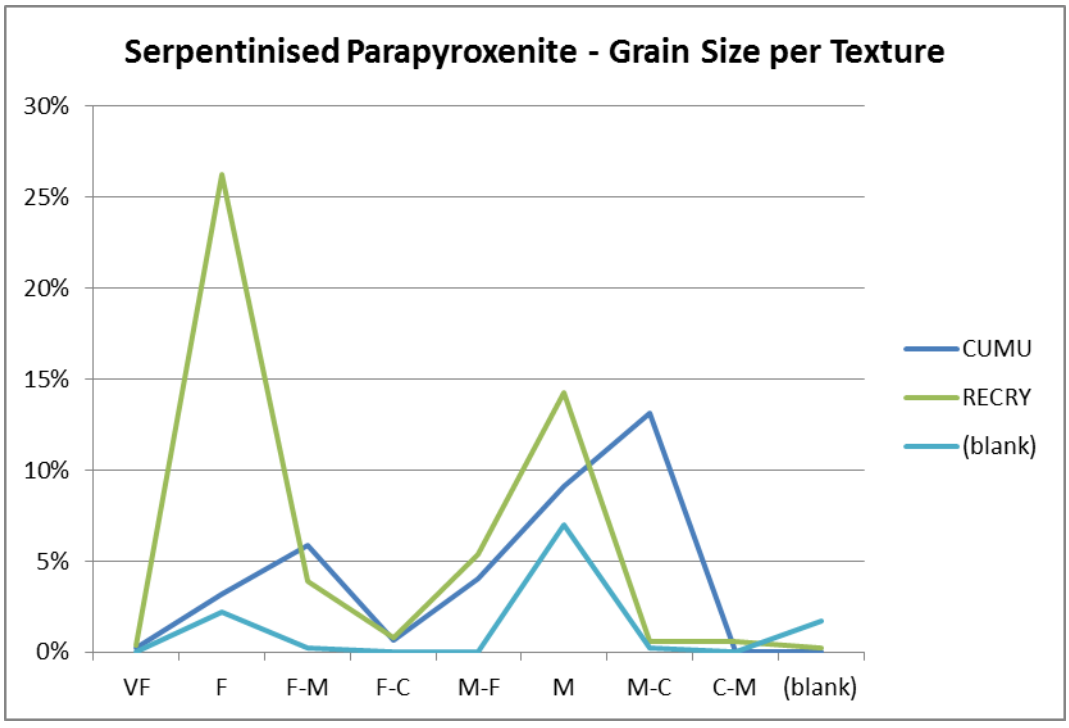


Figure 47: Serpentinised parapyroxenite - Grain size distribution for each textural description.

4.2.4.1.9 Feldspathic Parapyroxenite – Minor Rock Tpye

The distribution of textures describing feldspathic parapyroxenite in the OY database is summarised (Figure 48):

Total feldspathic parapyroxenite meters:	200m
Described as cumulus, recrystallised and blank:	195m
Other textures:	5m
Representativity of chosen textures:	97.5%

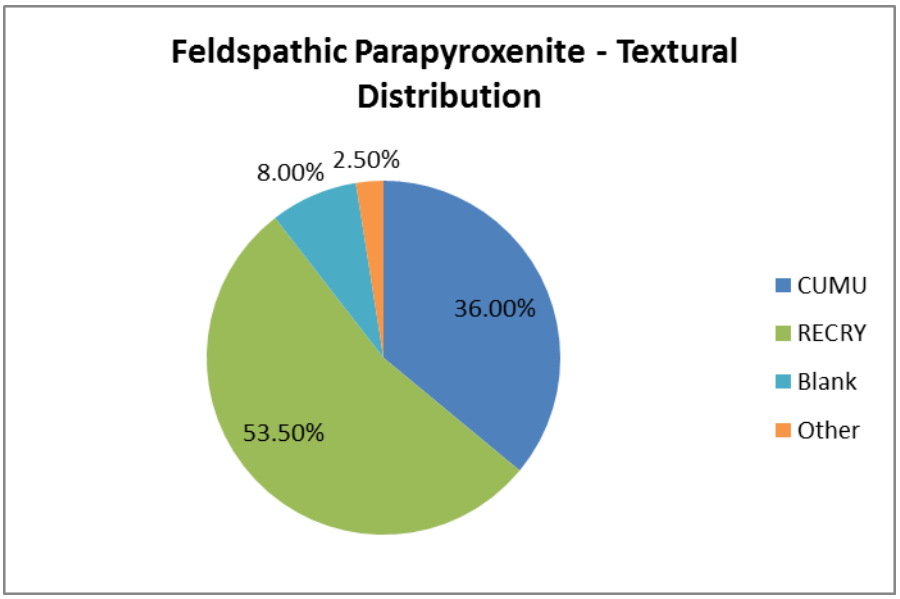


Figure 48: Feldspathic parapyroxenite - Textural distribution of feldspathic parapyroxenite.

Grain size distribution analysis results show the following (Table 21 and Figure 49):

- Dominant textures are cumulus and recrystallised.
- Dominant grain sizes are F,M,M-C
- Grain size distribution similar to parapyroxenite.
- Selected grain sizes and textures account for 170m

Representativity of serpentinised parapyroxenite using the identified textures (including the blank texture) and grain sizes is **85%.**

Table 21: Feldspathic parapyroxenite - Grain sizes per texture and their occurrence in the exploration database in meters. Dominant grain sizes are highlighted in green.

Grain Size	CUMU (m)	RECRY (m)	Blank (m)	Total (m)
VF	1			1
F	5	11	14	30
F-M	8	1		9
F-C		4		4
M-F	1	8		9
M	30	73	1	104
M-C	27	9		36
C-M		1		1
Blank			1	1
Total	**72**	**107**	**16**	**195**

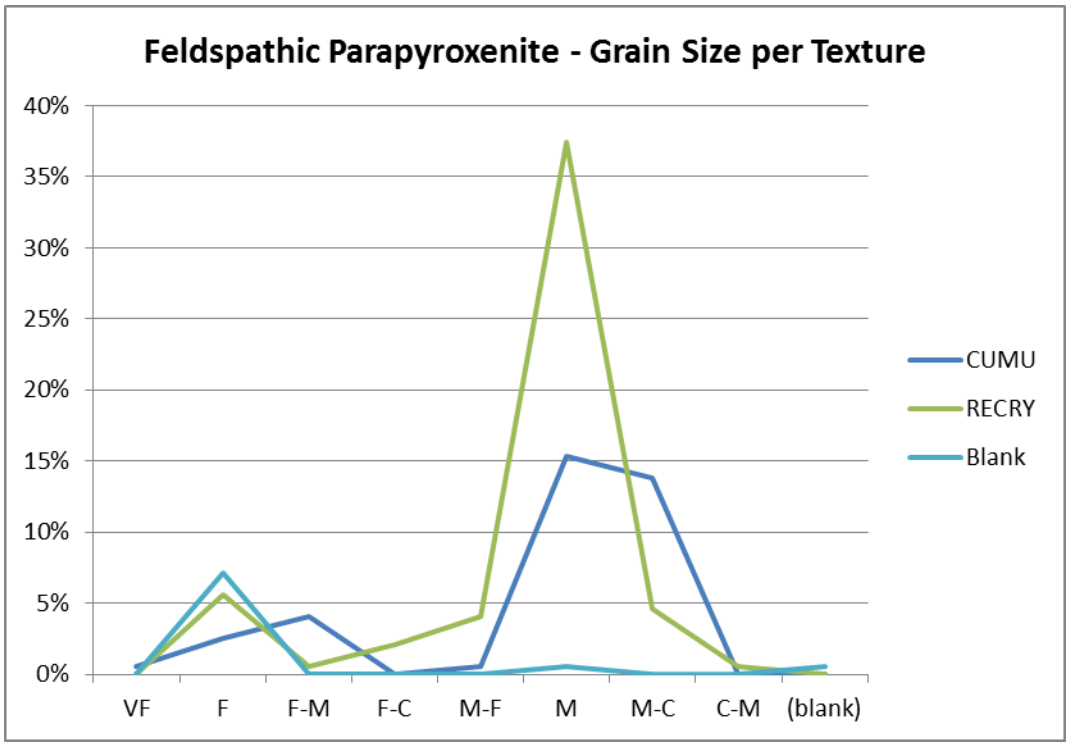


Figure 49: Feldspathic parapyroxenite - Grain size distribution for each textural description.

4.2.4.1.10 Calc-Silicate

The distribution of textures describing calc-silicate in the OY database is summarised (Figure 50):

Total calc-silicate meters:	523m
Described as cumulus, recrystallised and blank:	480m
Other textures:	43m
Representativity of chosen textures:	91.78%

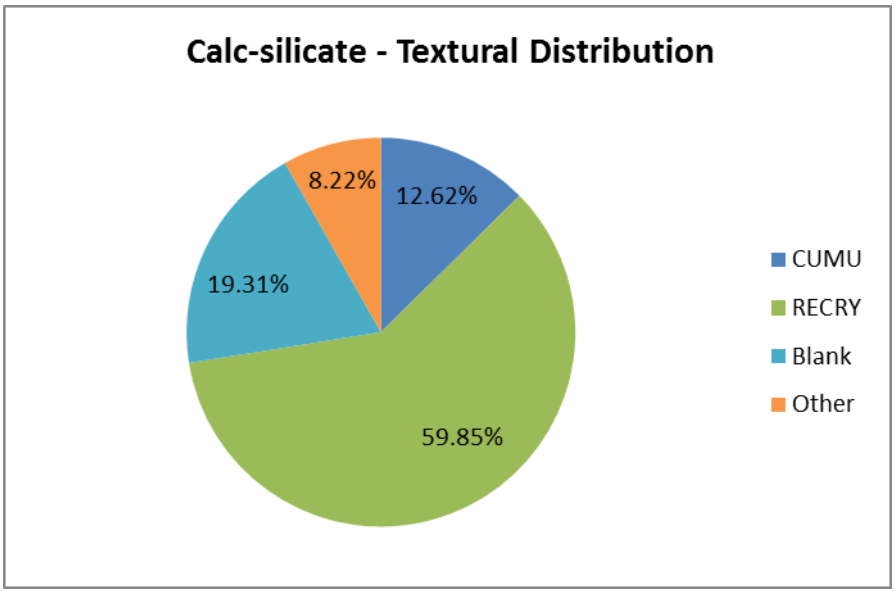


Figure 50: Calc-silicate - Textural distribution of calc-silicate.

Grain size distribution analysis results show the following (Table 22 and Figure 51):

- Dominant textures are cumulus and recrystallised.
- Dominant grain sizes are F,F-M, M-F,C
- Selected grain sizes and textures account for 392m

Representativity of serpentinised parapyroxenite using the identified textures (including the blank texture) and grain sizes is **74.95%.**

Table 22: Calc-silicate - Grain sizes per texture and their occurrence in the exploration database in meters. Dominant grain sizes are highlighted in green.

Gain Size	CUMU (m)	RECRY (m)	Blank (m)	Total (m)
VF		2		2
F	10	75	56	141
F-M	18	33	3	54
F-C	1	2	2	5
M-F	19	31		50
M	18	96	33	147
M-C		71		71
M-VC		1		1
C-M		1		1
C			1	1
Blank		1	6	7
Total	**66**	**313**	**101**	**480**

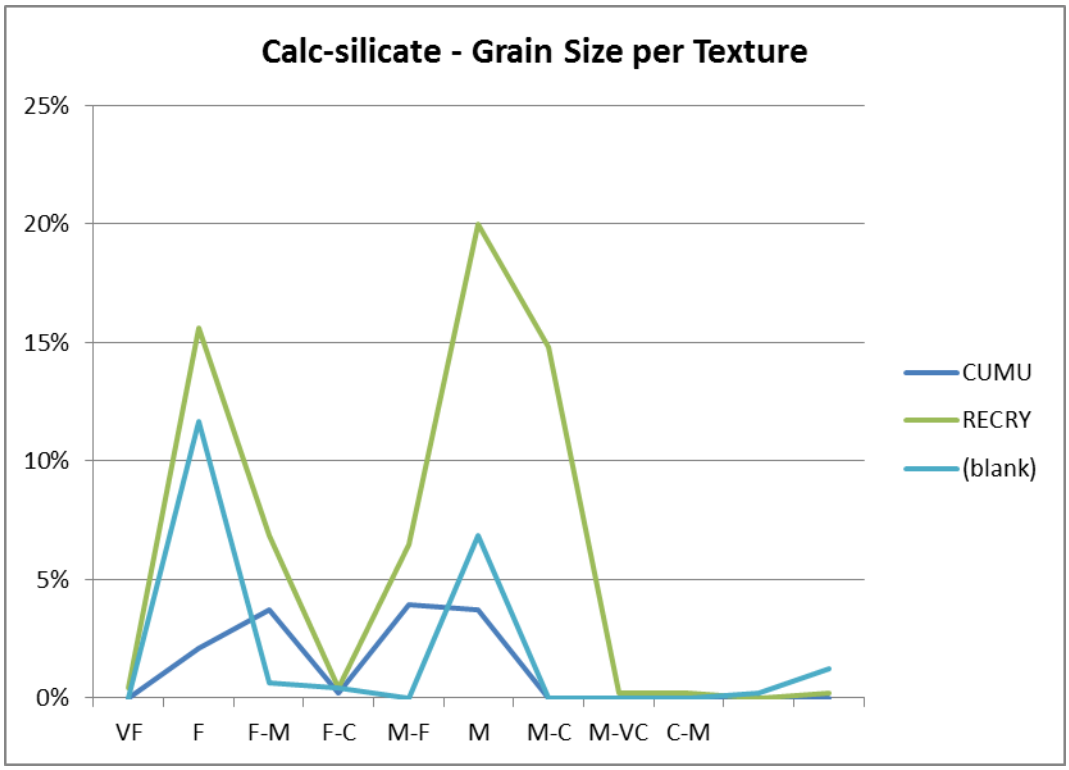


Figure 51: Calc-silicate - Grain size distribution for each textural description.

4.2.4.2 Footwall

4.2.4.2.1 Granofels

The distribution of textures describing granofels in the OY database is summarised (Figure 54):

Total granofels meters:	21041.397m
Described as banded, brecciated, cumulus, graphic, recrystallised, varied and blank:	20868.167m
Other textures:	173.23m
Representativity of chosen textures:	99.18%

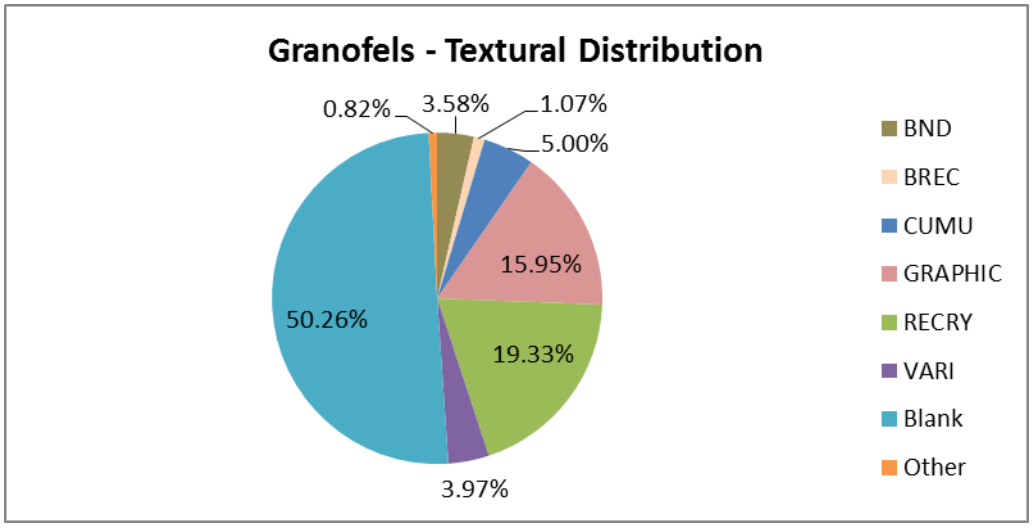


Figure 52: Granofels - Textural distribution of granofels.

Grain size distribution analysis results show the following (Table 23 and Figure 53):

- Dominant textures are cumulus and recrystallised.
- Dominant grain sizes are VF,F, F-M,F-C,M,M-C
- Selected grain sizes and textures account for 19172.887m

Representativity of granofels using the identified textures (including the blank texture) and grain sizes is **91.92%.**

Table 23: Granofels - Grain sizes per texture and their occurrence in the exploration database in meters. Dominant grain sizes are highlighted in green.

Grain size	BND (m)	BREC (m)	CUMU (m)	GRAPHIC (m)	RECRY (m)	VARI (m)	Blank(m)	Total (m)
VF	642.73				76.86		1162.81	1882.4
F	86.79	64.855	75.28	1760.77	1939.681		4632.941	8560.317
F-M	24.19	57.695	162.66	3.31	103.925		1272.38	1624.16
F-C		22.465		494.46	429.33		216.37	1162.625
F-PEG				370.72				370.72
M-F			32.6	35.08	192.56		164.29	424.53
M		10.59	753.24	84.48	867.06		2366.145	4081.515
M-C		25.62	28.05	456.96	293.73	836.01	221.5	1861.87
M-PEG				151.21	50.47			201.68
M-VC		7.71						7.71
PEG					0.18			0.18
C-M		2.89			6.04			8.93
C			0.32		0.34	0.35	24.53	25.54
C-PEG					79.67		10.8	90.47
Blank		32.61			28.33		504.58	565.52
Total	**753.71**	**224.435**	**1052.15**	**3356.99**	**4068.176**	**836.36**	**10576.346**	**20868.167**

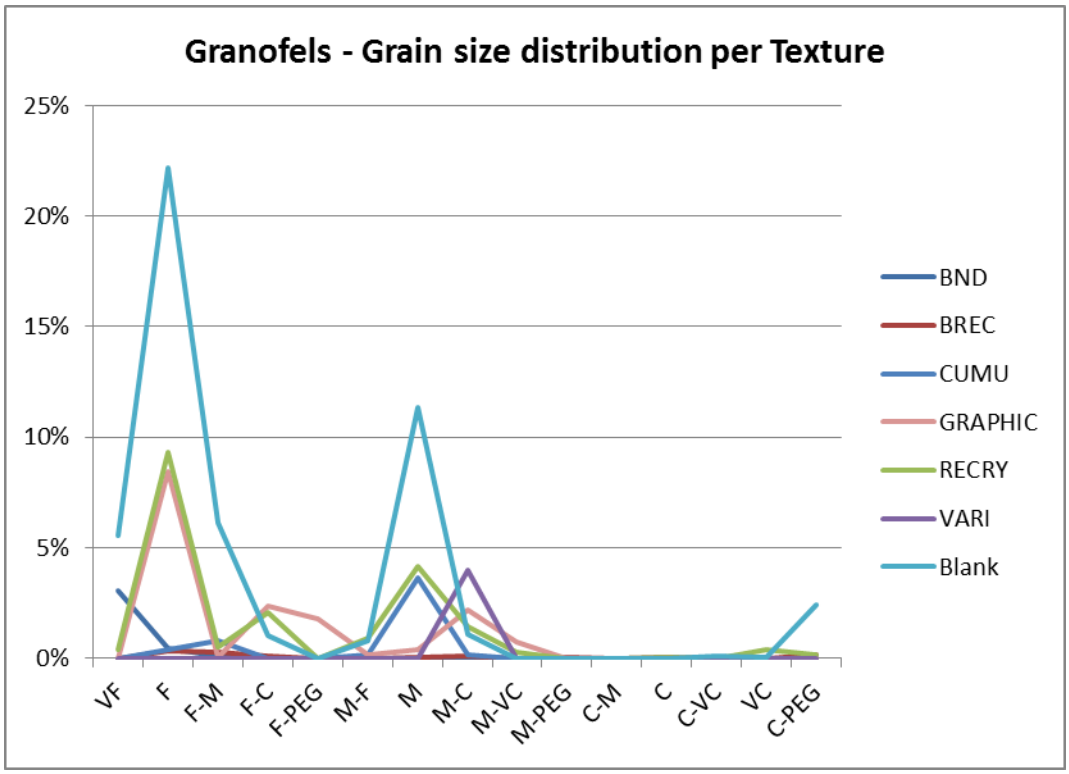


Figure 53: Granofels - Grain size distribution for each textural description.

4.2.5 Field Checks

A brief investigation into establishing the change in lithology, texture and grain size in reef rocks was carried out. An ore pattern (326/063) and an ore stockpile (S7) were chosen and photographic evidence was captured.

The hanging wall contact with the reef can be sharp and irregular. The change in composition from a gabbronorite to a feldspathic pyroxenite is clear due to the darker colour of the latter (Figure 54).



Figure 54: Isolated area of mineralised Cr-rich feldspathic pyroxenite lying within barren hanging wall gabbronorite.

The ore is located within the hanging wall as can be seen in the plan (Figure 55 and Figure 56).

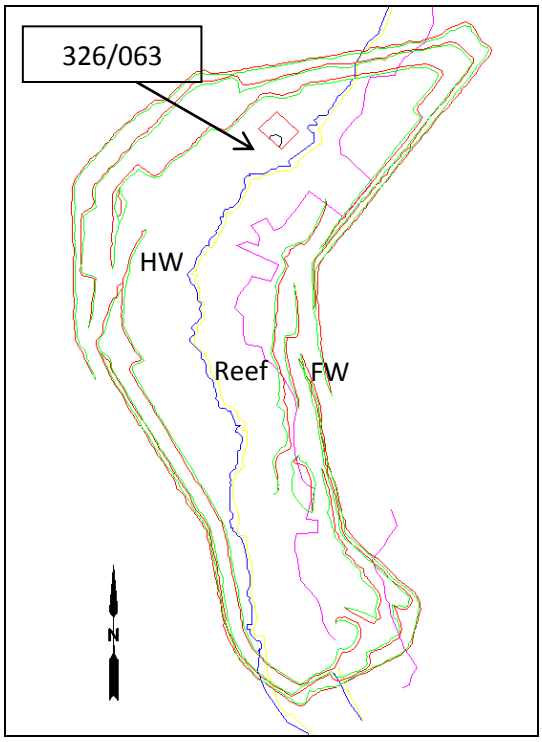


Figure 55: North Pit with bench outlines. The ore line is running N-S with the blue line showing the hanging wall contact. 326/063 is falling in the hanging wall.

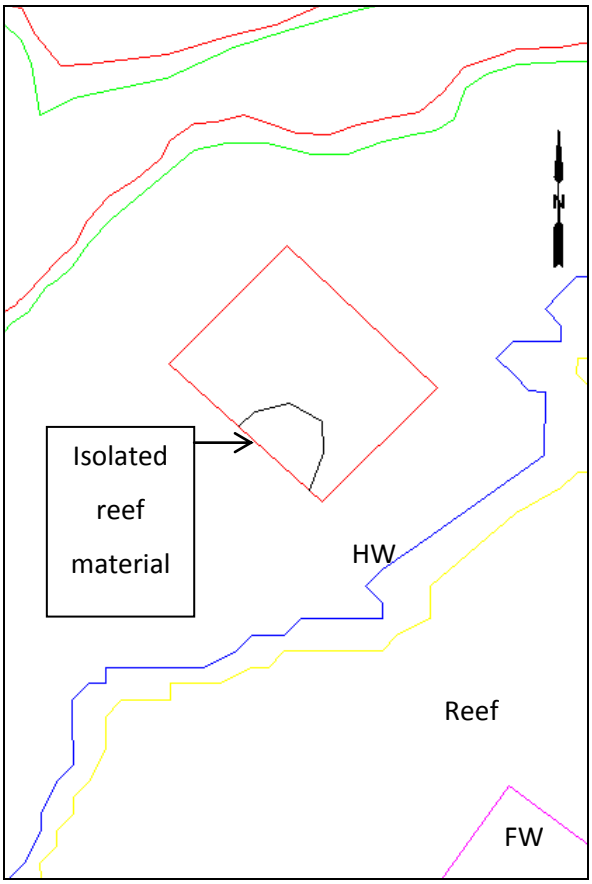


Figure 56: 326/063 is within the expected hanging wall waste. The black line represents the presence of discordant reef material rich in Cr and PGEs.

The field checks confirm the high variability in textures within the same rock type. Additionally, contacts between rock types vary from sharp to gradational. Sharp contacts persist at the HW- Reef boundary and the FW - Reef boundary. Similar textural differences are evident in exploration core.

Sharp contacts within the reef are also evident between rock types. Chromite rich rock types occur sporadically as lenses or seams (Figure 57 and Figure 58). Compositional variability occurs in a small range.

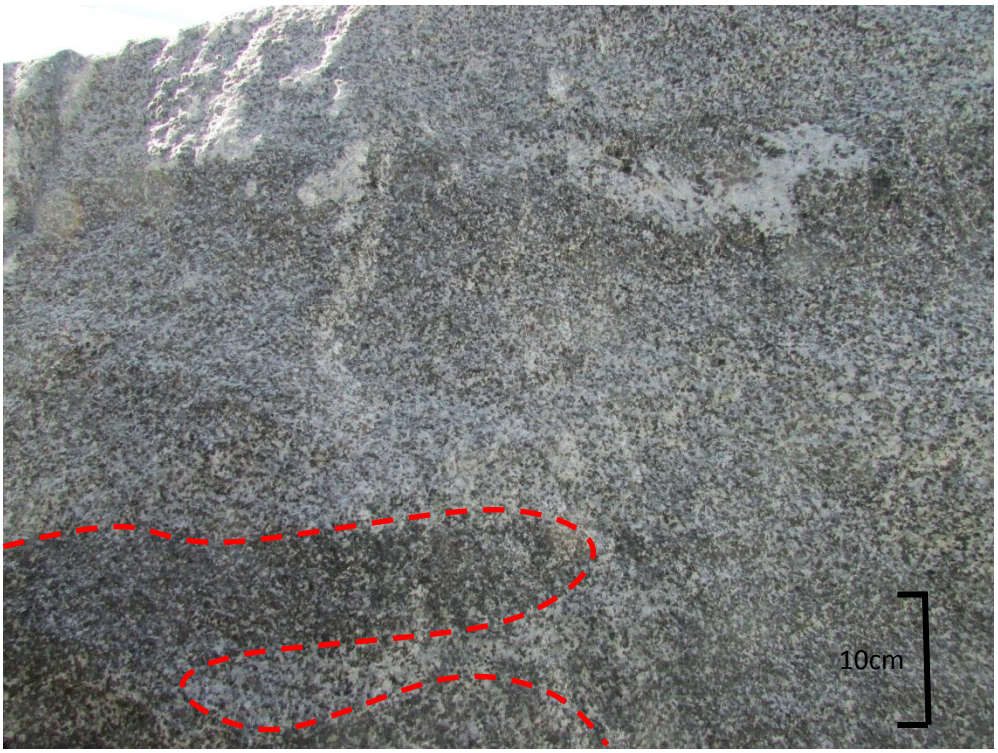


Figure 57: Sharp contact between barren gabbronorite and feldspathic pyroxenite from 326/063.



Figure 58: Sharp contact between fine grained Cr-rich feldspathic pyroxenite and a medium grained feldspathic pyroxenite from 326/063. The Cr-rich component is higher in PGE content with a direct relationship with more mafic minerals.

Areas of alteration (serpentinisation and chloritisation) with associated recrystallisation and change in grain size also show sharp contacts (Figure 59). Gradational contacts due to percolation of hydrothermal fluids also exist.

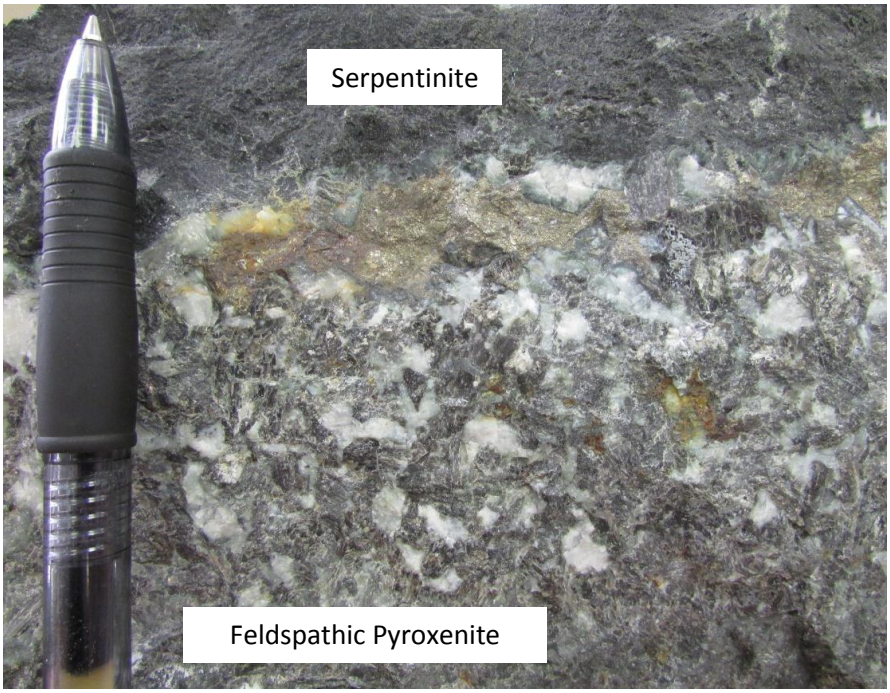


Figure 59: A fine-grained serpentinite has a sharp contact with a coarse grained feldspathic pyroxenite. The feldspathic pyroxenite then becomes finer towards the bottom of the photograph.

A single rock type can exhibit changes in grain size over short distances. Figure 60 shows a change from coarse to fine grained feldspathic pyroxenite over a distance of 150mm.



Figure 60: A feldspathic pyroxenite which grades from medium to fine-medium grain size. A sharp contact with a fine grained chromitite seam is seen on the right.

4.3 Rock Strength and Textural Relationship

The exploration database contains the laboratory test results. The following rock tests have been conducted on ore at Mogalakwena Mine from 1996 to 2006 by various institutions (Table 24):

Table 24: Rock tests from 1996 to 2006 (Source: Little, 2006)

Test Type	Sandsloot	Zwartfontein	Overysel	Tweefontein	Total
UCS	97	105	137	0	329
PL	2422	5772	1898	2360	14499
BWI	36	23	19	0	78
DWT	11	21	16	0	48

Point load testing commenced in 2005 on every exploration borehole. 10 samples of each rock type undergo a Point Load Test (PL). During testing, rock breakage occurs along planes of weakness, joints, bedding and other points of weakness (Napier-Munn *et al.*, 1999). Samples for PL testing must be chosen according to their lack of identifiable weaknesses which will affect test results (ISRM, 1985). The PLI results must be representative of solid *in situ* rock.

UCS results calculated from PLI tests at the Mogalakwena Mine exploration coreyard were plotted against 5 rock types. The 1497 data points originated from OY farm (Table 25). This is the initial database used for the study.

Table 25: UCS data per rock type

Rock Type	Full description	Results
PYX	Pyroxenite	334
FPYX	Feldspathic Pyroxenite	455
SPYX	Serpentinised Pyroxenite	275
Calcsil	Calc-Silicate	21
GF	Granofels	412
	Total	1497

The results show serpentinised pyroxenite, feldspathic pyroxenite and granofels give similar UCS results (Figure 61). Pyroxenite has a lower UCS range and this discreet characteristic may potentially be reflected in penetration rates. The 21 calc-silicate results are insufficient for an accurate comparison and are rare in the North Pit. The results from the exploration dataset show a range of 180-220 MPa for the other rock types (serpentinised pyroxenite, calc-silicate, feldspathic pyroxenite and granofels).

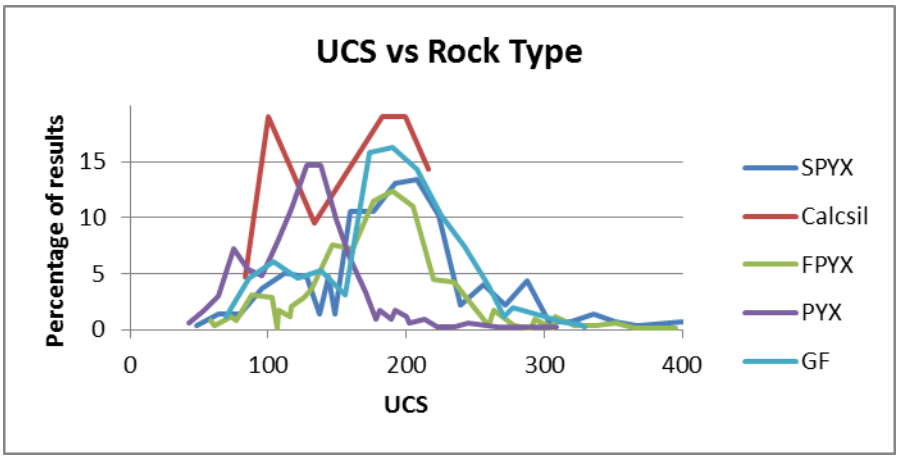


Figure 61: UCS data per rock type - initial study.

The database used above investigated average values for a geotechnical unit length which simplified rock types into the categories seen. A more detailed study of textural and grain size parameters for actual test samples is necessary.

4.3.1 Strength, Texture and Grain Size

An export of the SABLE Database sourced 21 445 UCS values for the OY database. The UCS values were converted from PLI results. The UCS data from the exploration boreholes was categorised according to lithology and subdivided according to the texture and grain sizes identified in the previous chapter.

A mean UCS for the particular grain size for all relevant textures was applied and plotted. The term Blank for textural description is allocated to core intersections which do not have an entry for texture. This category was included in the combined UCS vs. grain size due to the amount of entries with no textural description. The standard deviation (Std Dev) for each rock type subcategory, which includes texture and grain size, was calculated.

4.3.1.1 Reef

4.3.1.1.1 Feldspathic Pyroxenite

The following textures and grain sizes were used when comparing grain size and UCS for feldspathic pyroxenite (Table 26):

- Cumulus
- Varied
- Blank

Table 26: Grain size and UCS relationship for feldspathic pyroxenite

		UCS			
Grain Size	**PL Tests**	**Min**	**Max**	**Mean**	**Std Dev**
F	91	73.22	351.80	211.35	58.47
F-M	415	46.88	424.64	215.10	56.67
F-C	97	58.56	351.43	213.92	55.03
M-F	286	58.56	395.34	197.16	67.18
M	1005	37.51	395.34	199.15	58.57
M-C	477	37.51	439.27	192.91	63.00
M-PEG	72	87.85	367.11	202.39	58.07
Total	**2443**	**37.51**	**439.27**	**201.55**	**60.49**

The results were plotted and show a fair trend of decreasing rock strength with increasing grain size (Figure 62).

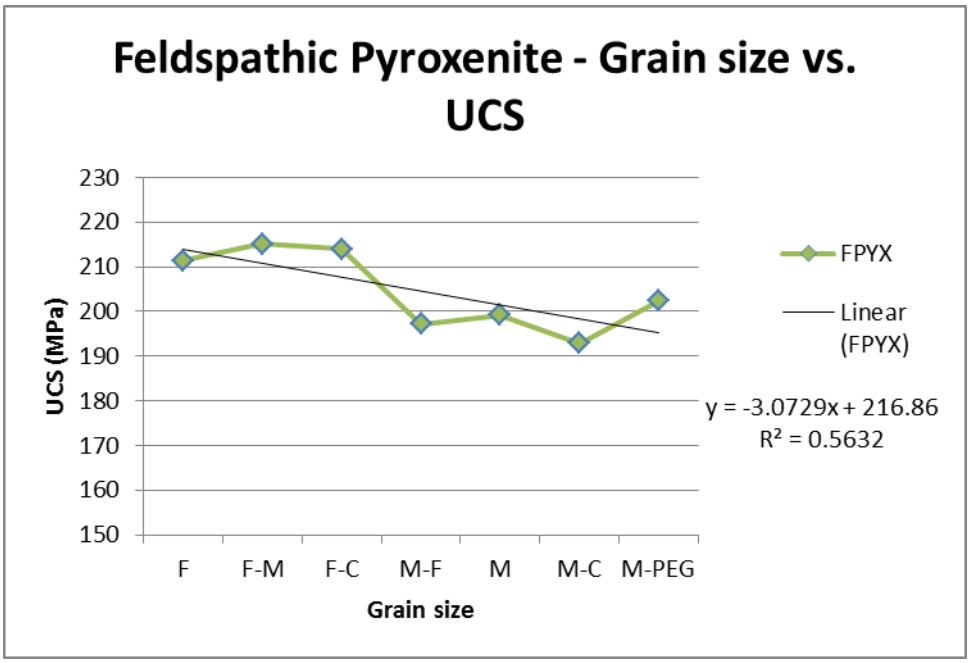


Figure 62: Grain size and UCS for feldspathic pyroxenite using cumulus, varied and blank textures.

The values for M-PEG were removed because PL accuracy at large grain sizes is affected (ISRM, 1985). The results for feldspathic pyroxenite with the M-PEG grain size removed show a good correlation (Figure 63).

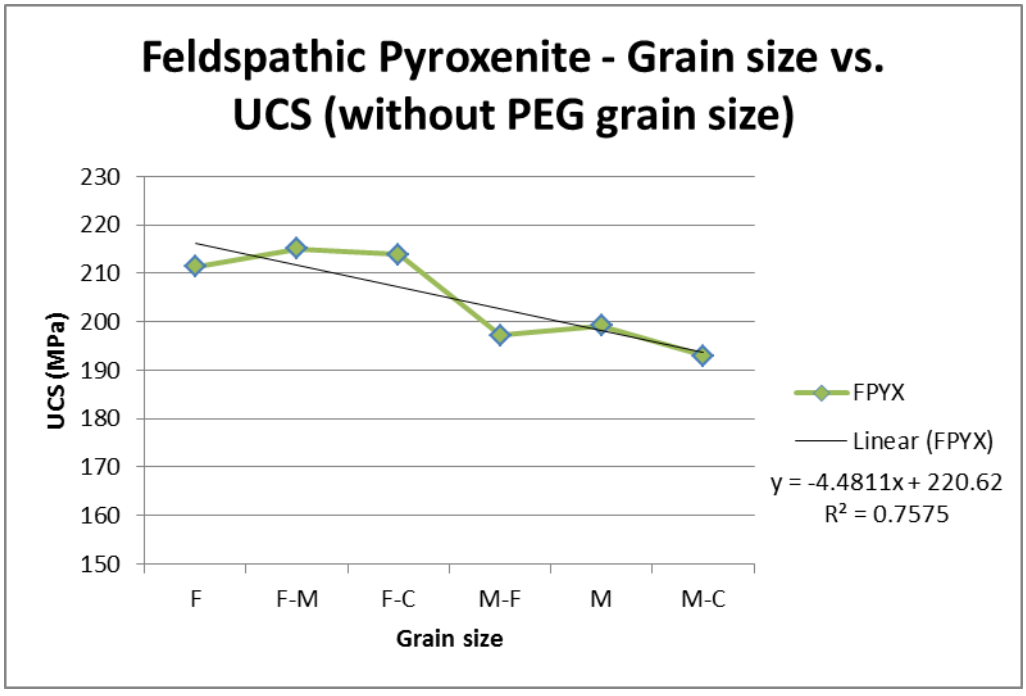


Figure 63: Grain size and UCS for feldspathic pyroxenite using cumulus, varied and blank textures (M-PEG grain size removed).

4.3.1.1.2 Pyroxenite

The following textures and grain sizes were used when comparing grain size and UCS for pyroxenite (Table 27):

- Cumulus
- Blank

Table 27: Grain size and UCS relationship for pyroxenite.

		UCS			
Grain Size	**PL Tests**	**Min**	**Max**	**Mean**	**Std Dev**
F	363	33.38	287.52	155.11	52.56
F-M	132	63.89	276.88	149.68	46.11
M-F	148	44.50	234.29	139.80	50.29
M	219	42.59	255.58	137.23	45.51
M-C	34	31.95	189.12	119.04	37.13
Total	**896**	**31.95**	**287.52**	**146.04**	**49.88**

There were no PL results for C and VC grained pyroxenite. The data was plotted on Figure 64 which shows very good correlation between decreasing rock strength and increasing grain size.

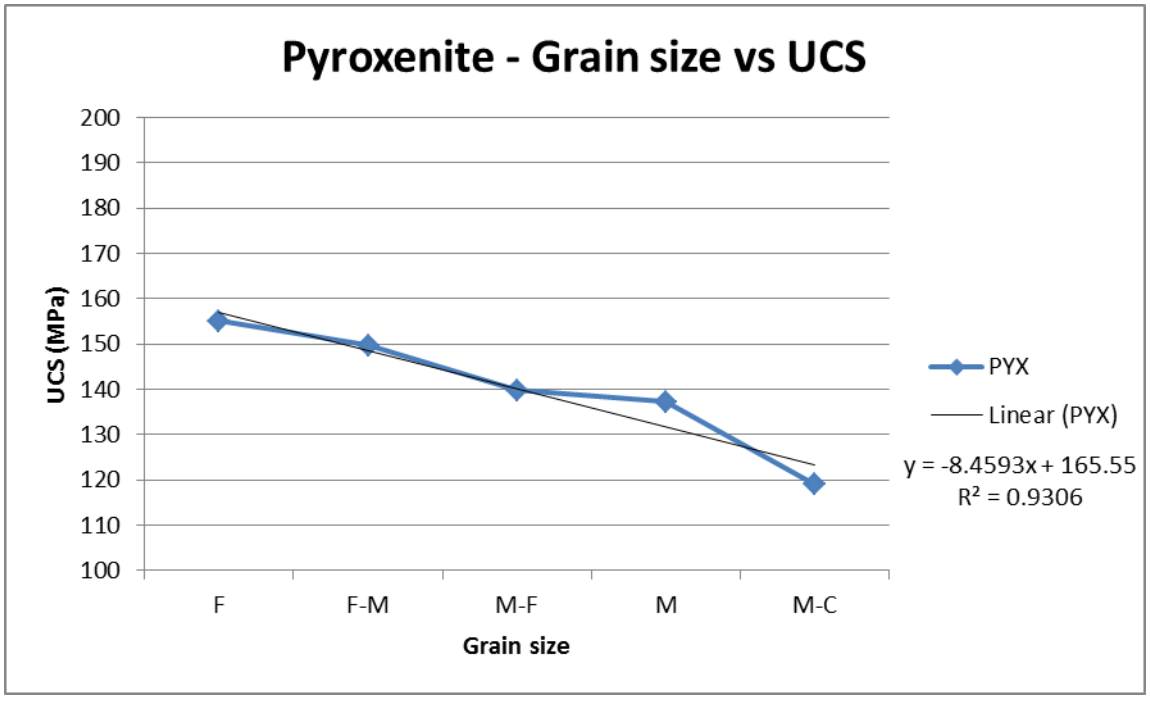


Figure 64: Grain size and UCS for pyroxenite using cumulus and blank textures.

4.3.1.1.3 Serpentinite

The following textures and grain sizes were used when comparing grain size and UCS for serpentinite (Table 28):

- Cumulus
- Homogeneous
- Recrystallised
- Blank

Table 28: Grain size and UCS relationship for serpentinite.

		UCS			
Grain Size	**PL Tests**	**Min**	**Max**	**Mean**	**Std Dev**
F	100	30.60	234.28	109.31	40.55
M	4	58.56	205.00	109.82	69.20
Total	**104**	**30.60**	**234.28**	**109.33**	**41.47**

There were no results for VF grained samples. There were no values for cumulus Serpentinite. The resulting data was plotted in Figure 65. There is no change in Serpentinite strength with grain size. There is low confidence for the medium grained samples due to the small population of tests.

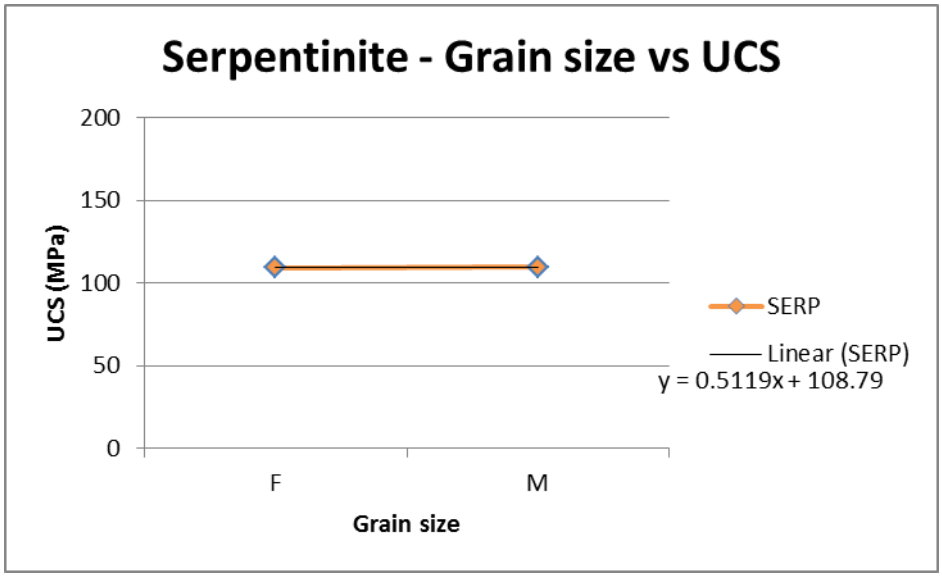


Figure 65: Grain size and UCS for serpentinite using cumulus, homogeneous, recrystallised and blank textures.

4.3.1.1.4 Serpentinised Pyroxenite

The following textures and grain sizes were used when comparing grain size and UCS for serpentinised pyroxenite (Table 29):

- Cumulus
- Recrystallised
- Blank

Table 29: Grain size and UCS relationship for serpentinised pyroxenite.

		UCS			
Grain Size	**PL Tests**	**Min**	**Max**	**Mean**	**Std Dev**
F	58	66.74	303.50	167.59	65.78
F-M	159	63.89	333.74	171.68	59.52
M-F	105	31.94	351.43	157.60	65.37
M	82	63.89	423.82	164.26	68.61
M-C	109	47.93	351.43	157.47	60.50
Total	**513.00**	**31.94**	**423.82**	**164.13**	**63.22**

The results plotted show that the partly altered serpentinised pyroxenite has a good correlation (Figure 66). The fully altered Serpentinite had a poor correlation.

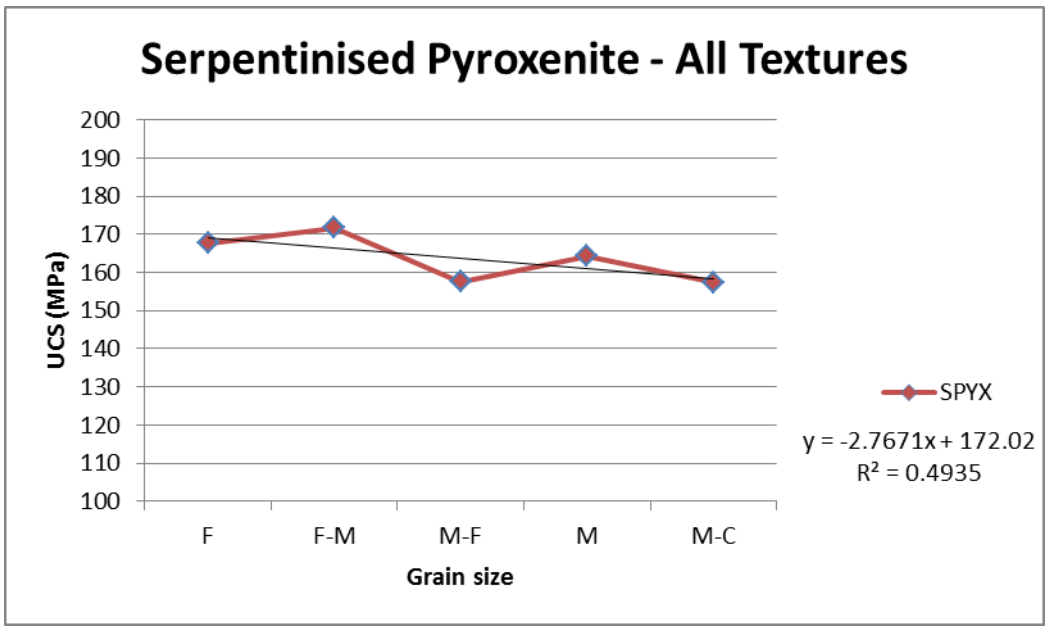


Figure 66: Grain size and UCS for serpentinised pyroxenite using cumulus, recrystallised and blank textures.

4.3.1.1.5 Serpentinised Feldspathic Pyroxenite

The following textures and grain sizes were used when comparing grain size and UCS for serpentinised feldspathic pyroxenite (Table 30):

- Cumulus
- Recrystallised
- Blank

Table 30: Grain size and UCS relationship for serpentinised feldspathic pyroxenite.

		UCS			
Grain Size	**PL Tests**	**Min**	**Max**	**Mean**	**Std Dev**
F	35	95.83	333.74	197.10	58.70
F-M	36	83.42	287.52	183.10	52.55
M-F	44	63.89	367.39	193.78	67.22
M	216	50.06	319.46	158.06	56.04
M-C	83	63.89	383.78	162.34	73.88
Total	**414.00**	**50.06**	**383.78**	**168.19**	**62.67**

The results are plotted on Figure 67 which shows a good correlation.

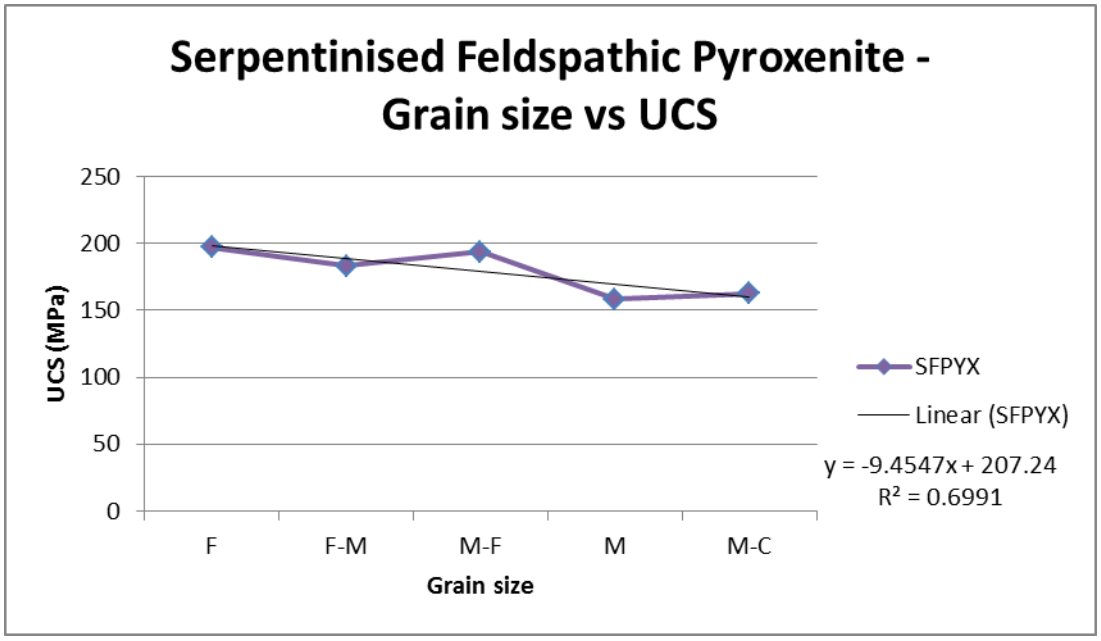


Figure 67: Grain size and UCS for serpentinised feldspathic pyroxenite using cumulus, recrystallised and blank textures.

4.3.1.1.6 Pegmatoidal Feldspathic Pyroxenite

The following texture and grain sizes were used when comparing grain size and UCS for pegmatoidal feldspathic pyroxenite (Table 30):

- Pegmatoidal

Table 31: Grain size and UCS relationship for pegmatoidal feldspathic pyroxenite.

		UCS			
Grain Size	**PL Tests**	**Min**	**Max**	**Mean**	**Std Dev**
M	20	111.82	319.46	200.47	60.32
M-C	12	127.80	367.10	287.75	72.22
M-PEG	60	79.87	351.43	219.11	65.64
C-PEG	29	79.87	287.52	179.57	55.93
PEG	48	79.87	283.68	170.66	51.55
Grand Total	**169**	**79.87**	**367.10**	**201.23**	**67.29**

There is a good correlation from grain size M-C to PEG (Figure 68). The rock type should not have a grain size of M as this is not strictly a pegmatoidal feldspathic pyroxenite.

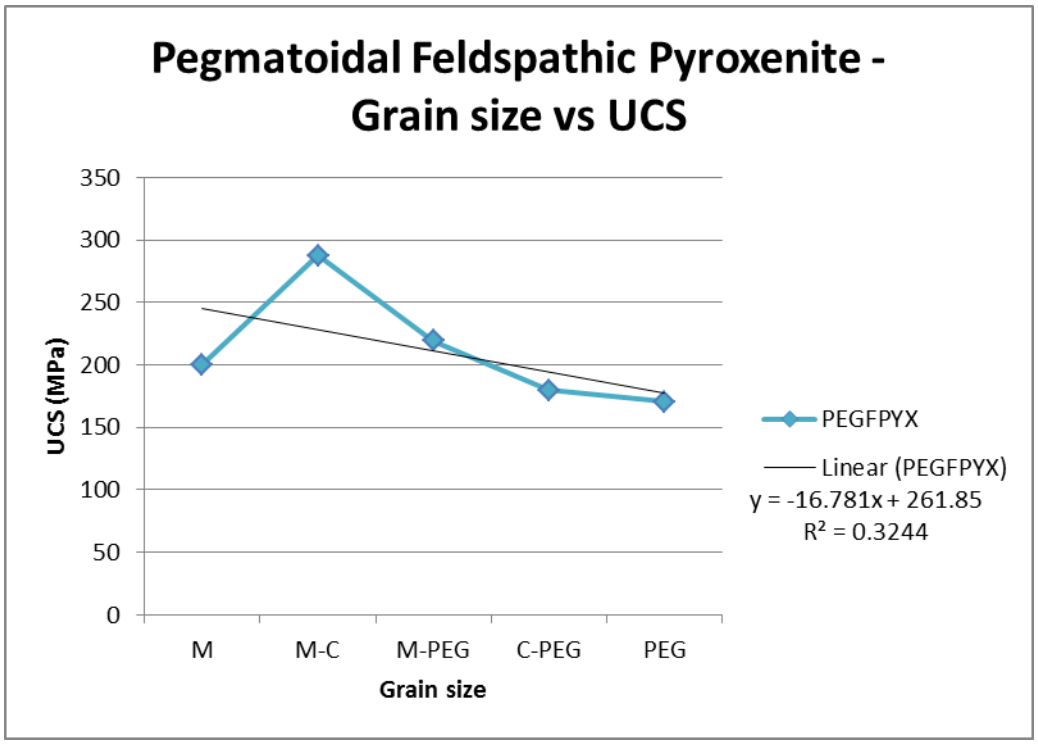


Figure 68: Grain size and UCS for pegmatoidal feldspathic pyroxenite using pegmatoidal texture.

The M grain size was removed and a very good correlation exists (Figure 69). The M grain size mean UCS value for pegmatoidal feldspathic pyroxenite is 200.47MPA. This is very close to the M grain size for feldspathic pyroxenite (199.15MPa) and is not surprising given their similar composition.

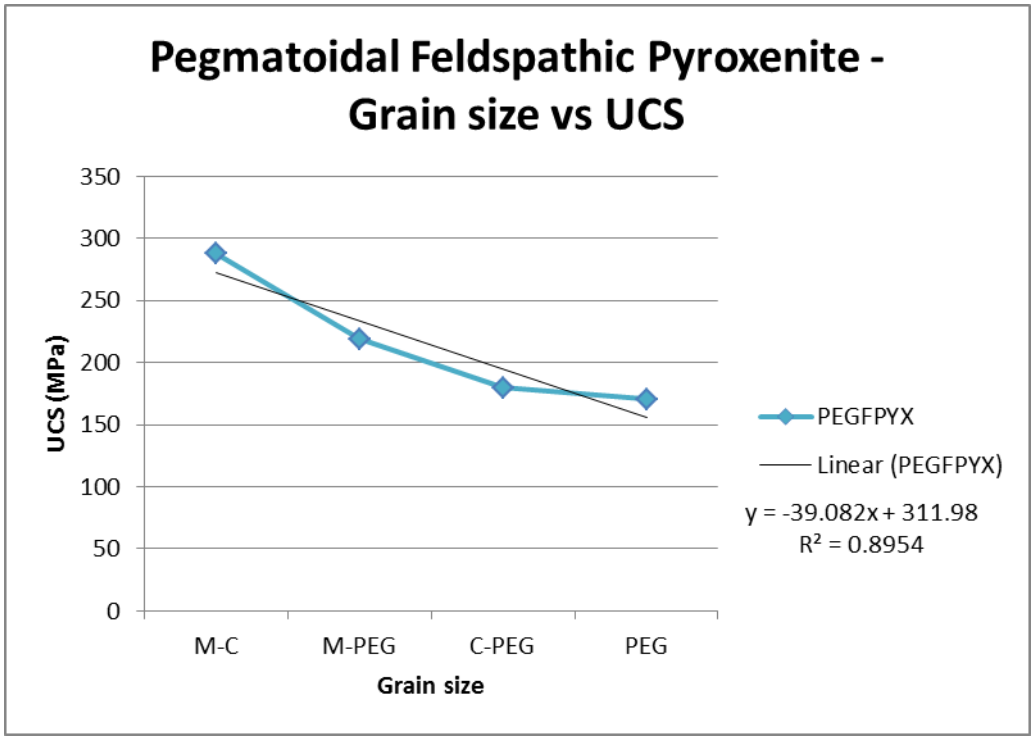


Figure 69: Grain size and UCS for pegmatoidal feldspathic pyroxenite using pegmatoidal texture. M grain size category has been removed.

4.3.1.1.7 Parapyroxenite

The following textures and grain sizes were used when comparing grain size and UCS for parapyroxenite (Table 32):

- Cumulus
- Recrystallised
- Blank

Table 32: Grain size and UCS relationship for parapyroxenite.

		UCS			
Grain Size	**PL Tests**	**Min**	**Max**	**Mean**	**Std Dev**
F	11	111.80	354.09	216.85	76.51
F-M	42	136.28	484.54	298.68	93.62
M-F	15	111.80	391.36	235.37	69.64
M	4	116.82	410.00	224.18	130.18
Total	**72.00**	**111.80**	**484.54**	**268.85**	**94.09**

There are no M-C PL results for parapyroxenite. The results were plotted on Figure 70 and show a very poor correlation. This is a highly altered rock similar to Serpentinite and discrepancies in descriptions are assumed to be more subjective.

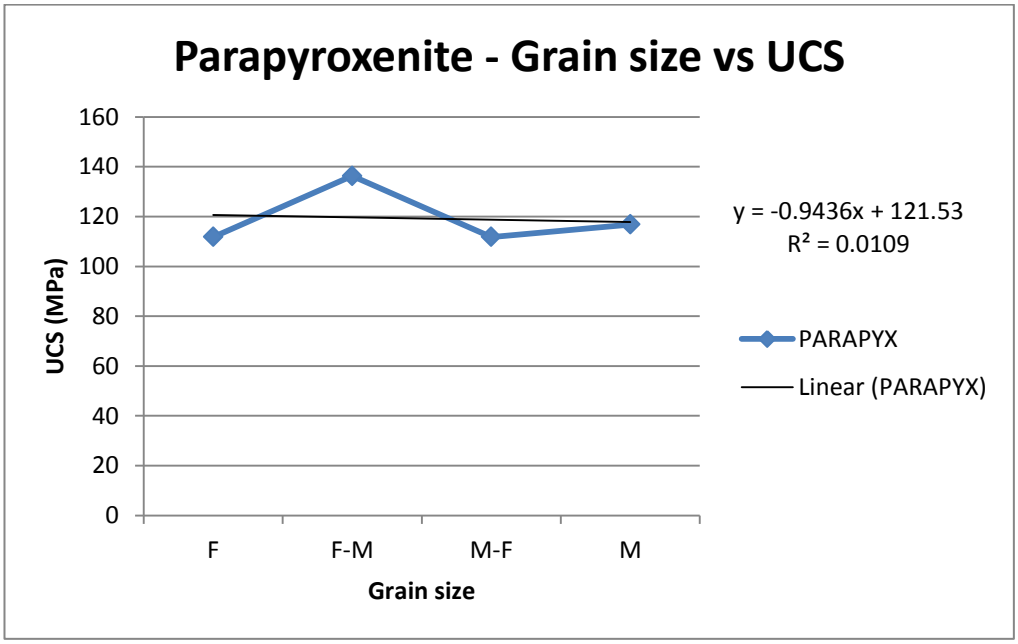


Figure 70: Grain size and UCS for parapyroxenite using cumulus, recrystallised and blank textures.

4.3.1.1.8 *Serpentinised Parapyroxenite*

The following textures and grain sizes were used when comparing grain size and UCS for serpentinised parapyroxenite (Table 33):

- Cumulus
- Recrystallised
- Blank

Table 33: Grain size vs. UCS relationship for serpentinised parapyroxenite.

		UCS			
Grain Size	**PL Tests**	**Min**	**Max**	**Mean**	**Std Dev**
F	111	63.89	303.50	163.47	57.87
F-M	113	66.74	319.46	161.52	55.41
M-F	86	50.06	505.27	179.19	72.87
M	155	66.74	335.45	171.03	59.58
M-C	110	79.87	300.36	176.03	59.77
Total	**575**	**50.06**	**505.27**	**169.88**	**60.83**

The results were plotted and the findings show the opposite relationship between UCS and grain size that is observed with unaltered rocks (Figure 71). The correlation is fair (R^2=0.5).

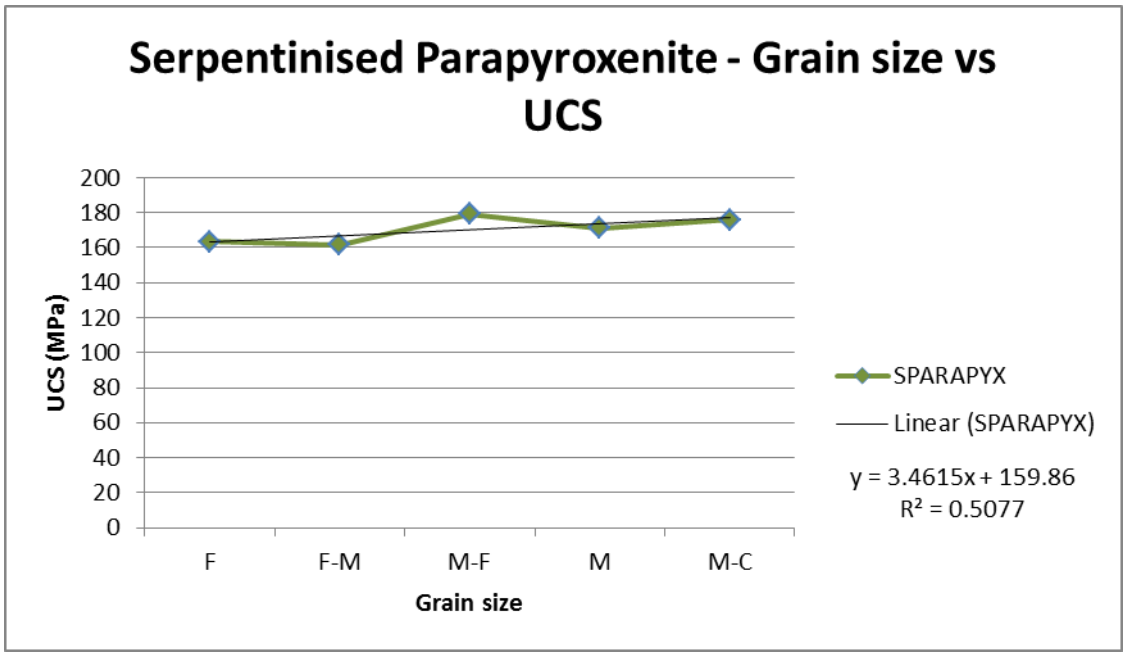


Figure 71: Grain size and UCS for parapyroxenite using cumulus, recrystallised and blank textures.

4.3.1.1.9 *Feldspathic Parapyroxenite*

The following textures and grain sizes were used when comparing grain size and UCS for feldspathic parapyroxenite (Table 34):

- Cumulus
- Recrystallised
- Blank

Table 34: Grain size vs. UCS relationship for feldspathic pyroxenite.

		UCS			
Grain Size	**PL Tests**	**Min**	**Max**	**Mean**	**Std Dev**
F	10	95.83	239.62	169.32	48.34
M	23	95.83	351.43	224.32	77.13
Total	**33.00**	**95.83**	**351.43**	**207.66**	**73.53**

There were no values for blank textures. The results show a wide range in UCS values between F and M grained rocks (Figure 72). The results have low confidence due to the small population group of tests.

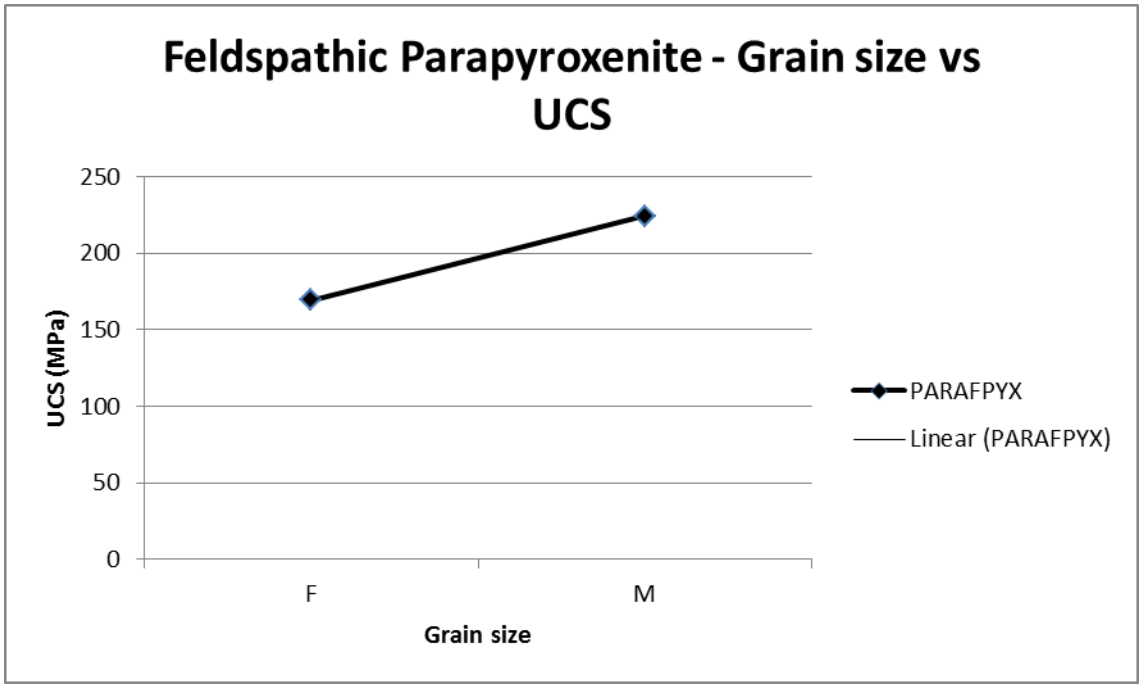


Figure 72: Grain size and UCS for serpentinised parapyroxenite using cumulus, recrystallised and blank textures.

4.3.1.1.10 Calc-silicate

The following textures and grain sizes were used when comparing grain size and UCS for calc-silicate (Table 35):

- Cumulus
- Recrystallised
- Blank

Table 35: Grain size vs. UCS for calc-silicate.

		UCS			
Grain Size	**PL Tests**	**Min**	**Max**	**Mean**	**Std Dev**
F	60	66.55	299.5	150.55625	53.198
F-M	40	83.2	399.35	182.6175	75.59
M-F	28	66.55	449.25	180.6535714	104.42
M	88	33.275	349.425	156.4107955	69.89
Grand Total	**216**	**33.275**	**449.25**	**162.78**	**73.03**

The results are plotted on Figure 73 and show a wide range of UCS values. There is no clear correlation between grain size and UCS.

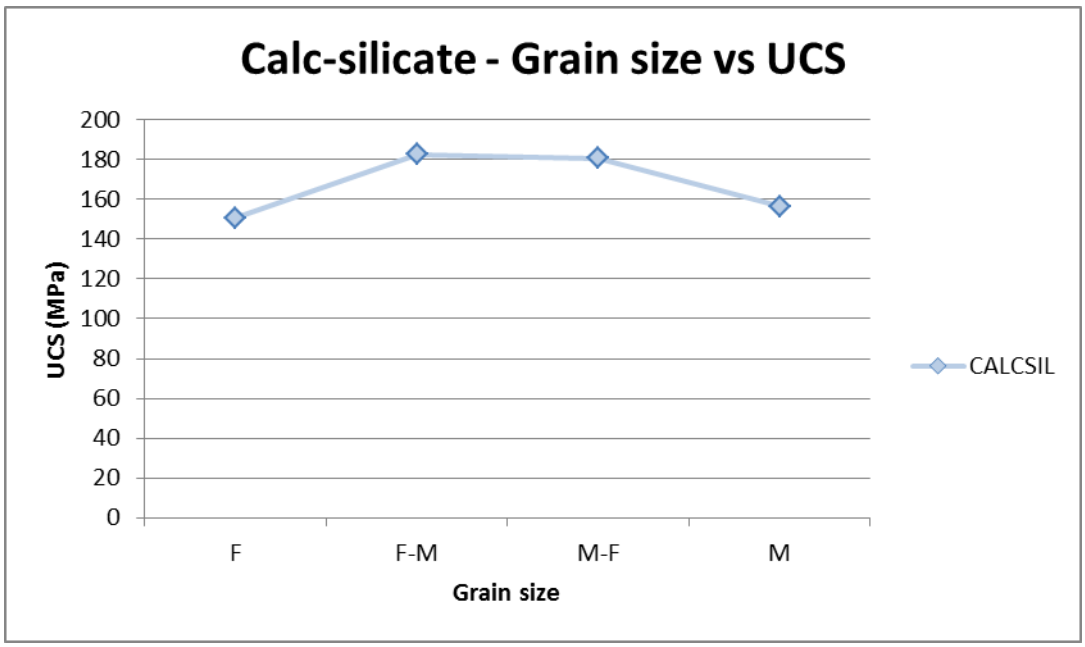


Figure 73: Grain size and UCS for calc-silicate using cumulus, recrystallised and blank textures.

4.3.1.2 Footwall

4.3.1.2.1 Granofels

The following textures and grain sizes were used when comparing grain size and UCS for granofels (Table 36):

- Brecciated
- Cumulus
- Graphic
- Recrystallised
- Varied
- Blank

Table 36: Grain size vs. UCS relationship for granofels.

		UCS			
Grain Size	**PL Tests**	**Min**	**Max**	**Mean**	**Std Dev**
VF	27	103.82	311.48	214.71	54.35
F	917	54.11	553.75	234.74	75.23
F-M	122	86.53	415.77	226.33	77.93
F-C	144	22.15	363.40	199.39	64.52
M	462	22.15	484.54	215.19	67.13
M-C	312	72.31	467.22	241.35	72.98
Total	**1984**	**22.15**	**553.75**	**227.87**	**73.19**

There were no results for blank textured granofels. The results show a bimodal distribution (Figure 74). This is indicative of the 2 main components of granofels (fine grained mafic and medium grained felsic). Additionally, granofels fall predominantly above 200Mpa except on two occasions; Blank texture at grain size F-C and brecciated texture at grain size M-C. Granofels is a complex rock type and caution must be used when making conclusions.

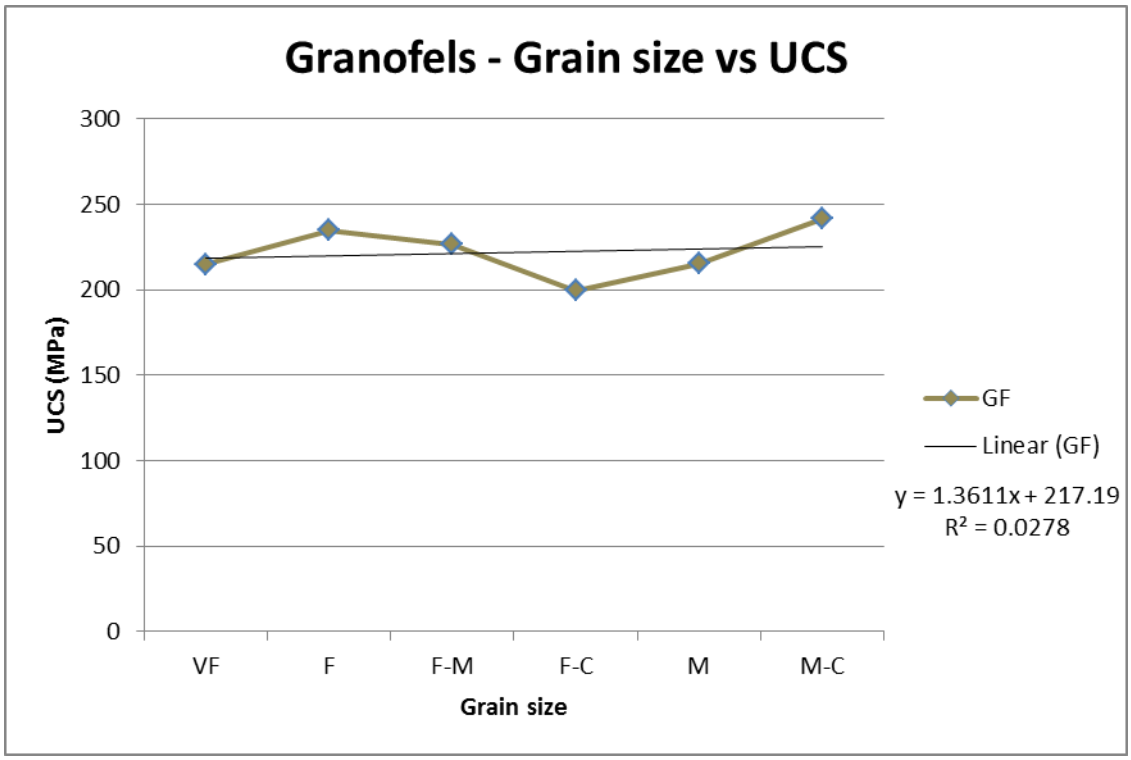


Figure 74: Grain size and UCS f\or feldspathic pyroxenite using cumulus, varied and blank textures. 1984 samples

4.3.2 Field Tests -Validation Dataset

A PL instrument was used on 100 samples of BQ exploration core (Figure 75). The method was diametral and operated by the able Mr Teffo. Samples were cut to 100mm and were 36mm diameter. This created a L:D (length : diameter) ratio of 2.78 which is suitable for diametral testing. Samples with grain sizes that were larger than 30% of the core diameter were discarded (ISRM, 1985). Relatively large grain sizes (pegmatoidal) impact the tests in that the test will be affected more by grain boundary cohesion which distorts overall rock strength results.



Figure 75: The 100 samples from 4 BHs. Samples were measured to 10cm and cut with a diamond core cutter.

The PL machine was operated by the competent and safety conscious Mr Teffo (Figure 76).



Figure 76: Mr Lesibama Klimboy Teffo operating the Point Load equipment during the testing of the 100 samples.

Three type specimens of feldspathic pyroxenite are shown in Figure 77– Figure 82. These photographs of the test samples illustrate the visually distinct grain size variation within a single rock type.



Figure 77: Sample 25 from ZN981D0 exhibiting a fine-medium grained assemblage of euhedral clinopyroxene and orthopyrothene crystals with intercumulus anorthite.

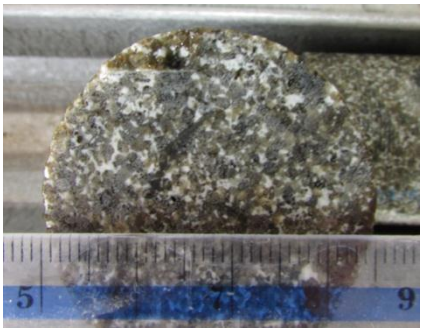


Figure 78: Sample 25.

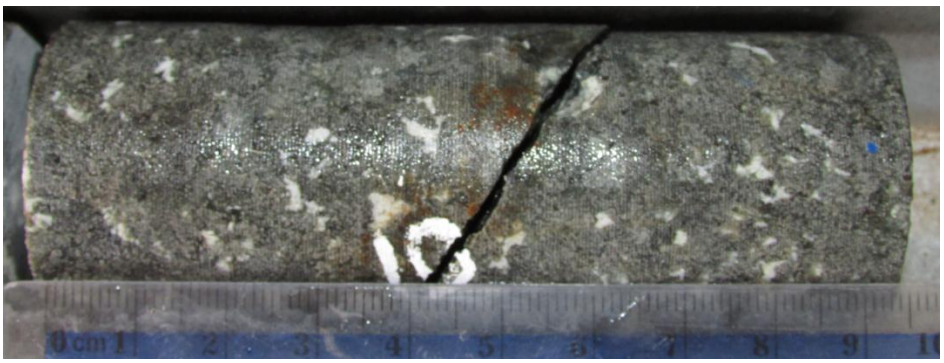


Figure 79: Sample 10 from ZN890D0. Sample was marked and cut before undergoing PL test.



Figure 80: Sample 10 from ZN890.

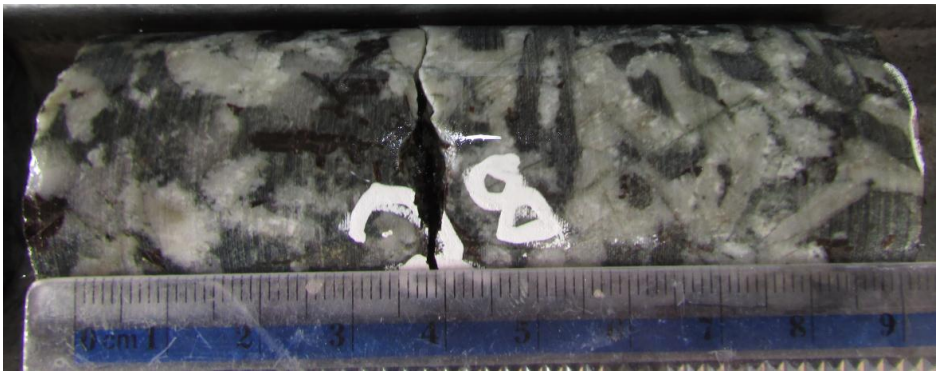


Figure 81: Sample 28 from ZN891D0 showing a pegmatitic texture.

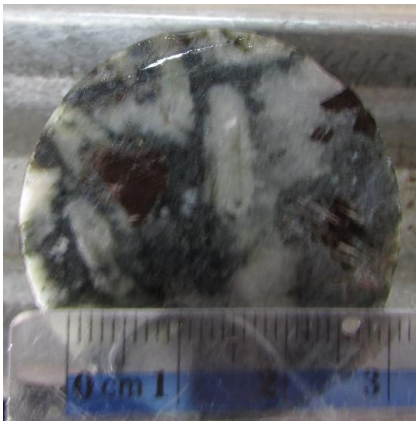


Figure 82: Sample 28 with mica minerals.

The test gives a load (kN) amount at failure which is read off a dial. This result is used as the input to convert the test to MPa taking into account the size of the core. The test method follows international best practice (ISRM, 1985):

First the uncorrected point load strength (I_s) in MPa is calculated:

$$I_s = P/D_e^2$$

Where:

P is the load in kN

D_e is the equivalent core diameter (D = D_e for diametral testing on core)

Secondly, the uncorrected point load strength (I_s) is changed to a standardised reference diameter of 50mm ($I_s(50)$):

$$I_s(50) = F \times I_s$$

Where:

$$F = (D_e/50)^{0.45}$$

Lastly, the $I_s(50)$ is converted to UCS by using a conversion factor (Hayes & Piper, 2003).

The PL tests on the 41 feldspathic pyroxenite samples converted to UCS is summarised below (Table 37):

Table 37: Results for feldspathic pyroxenite from the validation PLI test dataset.

	UCS			
Grain Size	Max	Min	Mean	Samples
F-M	417.3132	380.7068	401.2064	5
M	453.9197	256.245	352.3368	24
M-C	395.3494	204.996	317.7438	5
C	453.9197	212.3173	342.8802	6
VC	248.9237	248.9237	248.9237	1

The uncalibrated results show the same trends of decreasing strength with increasing grain size (Figure 83). The results are used to validate the trend but unfortunately cannot be used to validate the actual strength associated with varying grain sizes.

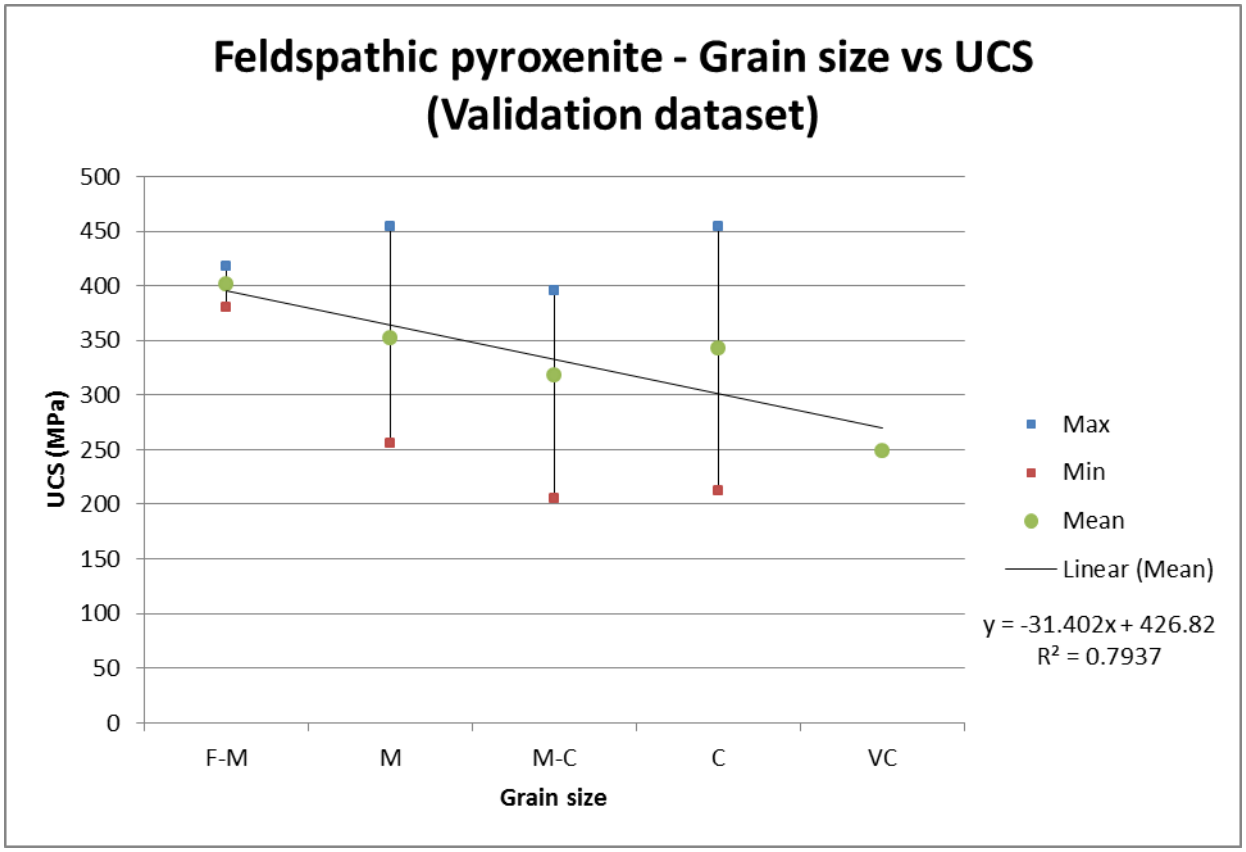


Figure 83: Grain size vs. UCS for feldspathic pyroxenite (validation dataset).

The results for the 2 components of granofels were tabled (Table 38) and plotted (Figure 86).

Table 38: UCS results for 2 components of granofels from the validation PLI test dataset.

	UCS			
Grain Size	Max	Min	Mean	Samples
M (Mafic)	545.1029	432.6214	497.5146	6
F (Felsic)	363.402	337.4447	348.9812	3

The results show 2 distinct UCS ranges (Figure 84). This validates the findings that granofels is a holistically complex rock type with a high degree of variability. However, a simple division into a fine grained mafic component and a medium grained felsic component allowed a more accurate description of PL responses.

The findings show that the fine grained mafic component is stronger than the medium grained felsic component.

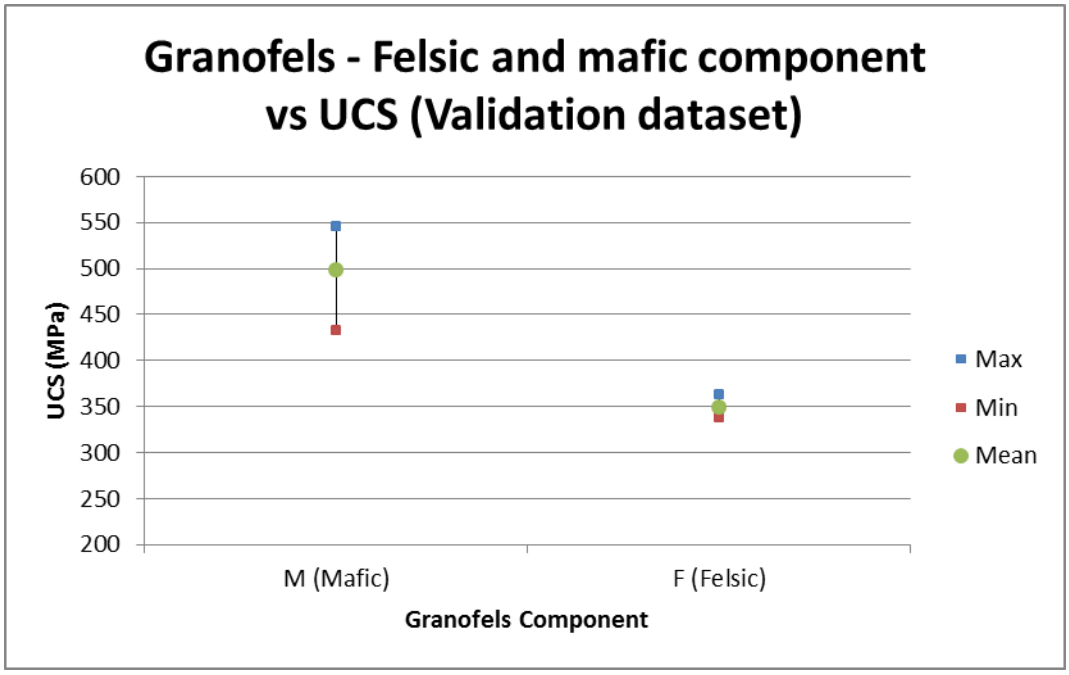


Figure 84: Two distinct population groups defined by grain size and composition in granofels

4.3.3 Summary of Grain Size Adjusted UCS

The summary of the investigation between UCS and grain size is shown in Table 39.

Table 39: Summary of grain size and UCS (MPa) relationship for all mineralised rock types.

Rock Type	Grain size	UCS	Mean UCS
FPYX	F	211	202
	F-M	215	
	F-C	214	
	M-F	197	
	M	199	
	M-C	193	
	M-PEG	202	
PYX	F	155	146
	F-M	150	
	M-F	140	
	M	137	
	M-C	119	
SPYX SPYX	F	168	164
	F-M	172	
	M-F	158	
	M	164	
	M-C	157	
SFPYX	F	197	168
	F-M	183	
	M-F	194	
	M	158	
	M-C	162	
SERP	F	109	109
	M	110	
PARAPYX	F	217	269
	F-M	299	
	M-F	235	
	M	224	
SPARAPYX	F	163	170
	F-M	162	
	M-F	179	
	M	171	
	M-C	176	

FPARAPYX	F	169	208
	M	224	
CALC	VF	215	228
	F	235	
	F-M	226	
	F-C	199	
	M	215	
	M-C	241	
GF	VF	215	228
	F	235	
	F-M	226	
	F-C	199	
	M	215	
	M-C	241	

4.3.3.1 Comparison to mean UCS currently used for rock types

The mean UCS for rock types currently used at Mogalakwena Mine are based on tests as described by Little (2006) (Table 40).

Table 40: Mean UCS values used at Mogalakwena Mine based on these tests (Little, 2006).

Rock type	Farm	PLI – UCS (MPa)			UCS Conversion factor
		Tests	Ave	Std Dev	
Norite	Overysel	345	178	62.8	23
	Sandsloot	128	199	72.3	
	Tweefontein	50	205	61.8	
	Zwartfontein	97	205	47.4	
Feldspathic pyroxenite	Overysel	930	178	49.6	22
	Sandsloot	34	197	81	
	Tweefontein	50	188	59.4	
	Zwartfontein	521	198	48.3	
Pyroxenite	Overysel	103	127	63	16
	Sandsloot	47	132	65.3	
	Tweefontein	20	139	47.7	
	Zwartfontein	33	111	36.8	
Parapyroxenite	Overysel	57	172	86.1	28
	Sandsloot	93	184	105	
	Tweefontein	10	344	194.5	
	Zwartfontein	142	211	60.2	
Serpentinite	Overysel	150	129	45.2	28
	Sandsloot	14	109	32	
	Zwartfontein	72	146	58.3	
Granofels	Overysel	470	212	68.1	26
	Sandsloot	20	230	80.1	
	Zwartfontein	273	208	49	
Calc-silicate	Overysel	22	121	59.9	25
	Sandsloot	64	116	63.8	
	Tweefontein	10	224	147.7	
	Zwartfontein	68	148	59.5	

These UCS mean values are added to the UCS evaluated field in the Geotechnical log in SABLE for geotechnical units that match the major rock types. The PL test data mean for rock types is listed under PLI UCS mean field.

The results for pyroxenite from Little (2006) range from 11-139MPa. The results from this investigation reveal a mean of 146MPa for pyroxenite. The average UCS value in SABLE is 90MPa. There is a large discrepancy between PLI derived UCS, the UCS values as reported by Little (2006) and the average used in SABLE. This is shown in Figure 85 for Norite where the PLI UCS average is 164MPa while the UCS evaluated result is 179MPa.

From	To	Unit Id	Mat Recov (m)	% Mat Recov	Intact	Intact rock >	% RQD	RQD Calc Method	Rock Type	Zone Name	IRS	UCS av	PLI UCS average	UCS evaluat	Weathering	Alteration
0.000	13.490	1	13.490	100		0.000	0	Intact > 10cm	N	HW	R3				W3	N
13.490	74.890	2	60.180	98		50.560	82.3	Intact > 10cm	N	HW	R5		164	179	W1	N
74.890	83.480	3	6.500	75.7		0.430	5	Intact > 10cm	N	HW	R4		164	179	W1	N
83.480	93.230	4	9.740	99.9		0.490	5	Intact > 10cm	N	HW	R5		164	179	W1	N
93.230	99.750	5	6.030	92.5		0.800	12.3	Intact > 10cm	SHRZONE	SZON	R3				W1	N
99.750	118.500	6	17.090	91.1		15.430	82.3	Intact > 10cm	BREC	REEF	R2				W1	N
118.500	152.710	7	29.900	87.4		15.450	45.2	Intact > 10cm	PARAFPYX	REEF	R4		145		W1	N
152.710	164.890	8	12.120	99.5		9.450	77.6	Intact > 10cm	GRAN	FW	R5		127		W1	N

Figure 85: OY1023 showing measured UCS (as calculated from PLI) and mean UCS for the rock type.

The large discrepancy in MPa of pyroxenite in particular needs to be investigated on site. There is a need to standardise the use of MPa values on site and amalgamate the datasets.

4.4 Strength and Hardness Relationships

There is a distinct correlation between rock material strength, as measured by UCS, and rock hardness (Heinz, 2009). This relationship was investigated using mean values for BWI and UCS by Little (2006). The descriptions of the strength and hardness tests can be found in Appendix 3. Results for DWT vs. UCS showed little correlation. Additional graphs of strength vs. hardness tests can be found in Appendix 3.

4.4.1 BWI vs. UCS

The mean results for BWI and UCS from test work done at OY are plotted (Figure 86).

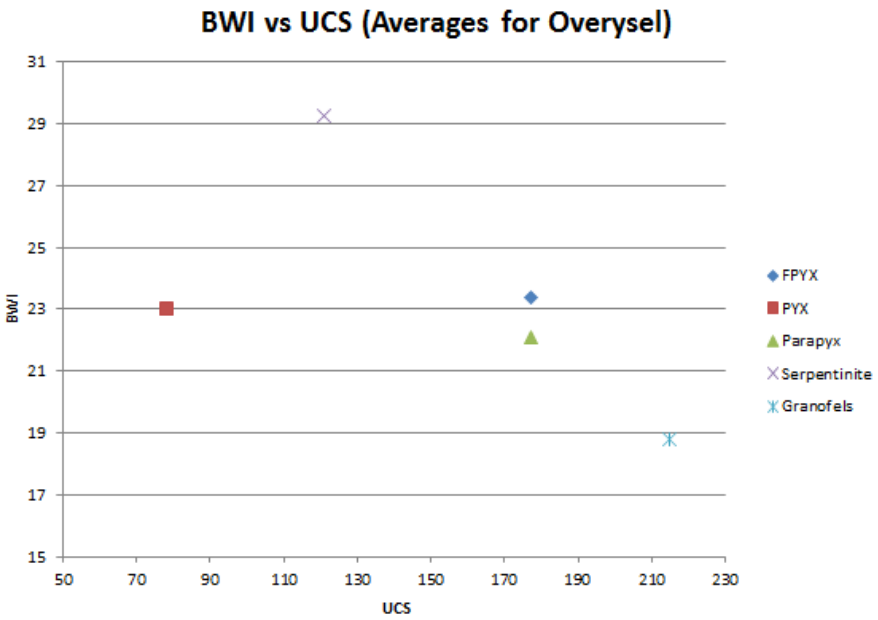


Figure 86: BWI vs. UCS for means for OY

Pyroxenite (PYX) shows a large discrepancy from the other rock types analysed. The same results are plotted without pyroxenite present (Figure 87). The R^2 value is 0.98 which is a very good correlation.

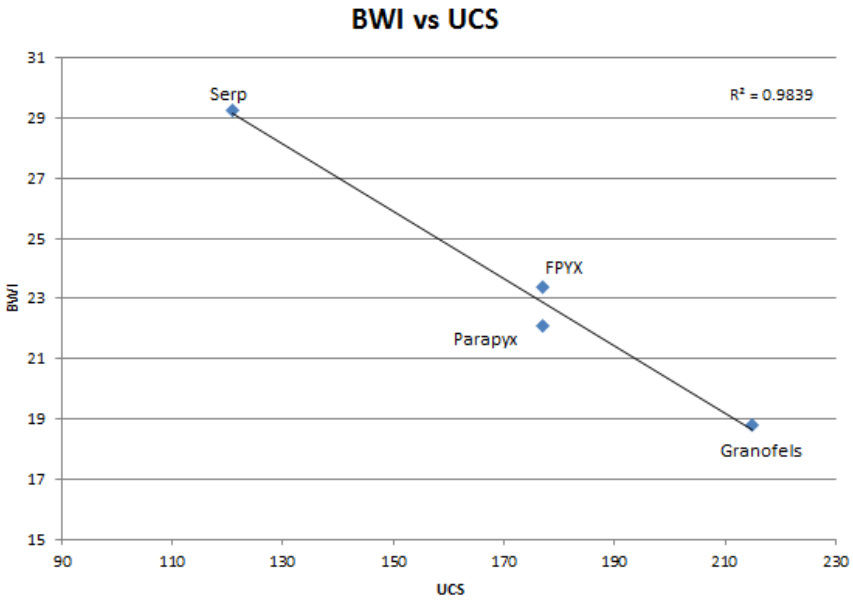


Figure 87: BWI vs. UCS OY means excluding pyroxenite.

The results for BWI vs. UCS at Zwartfontein were plotted (Figure 88) and shows a similar correlation ($R^2 = 0.89$)

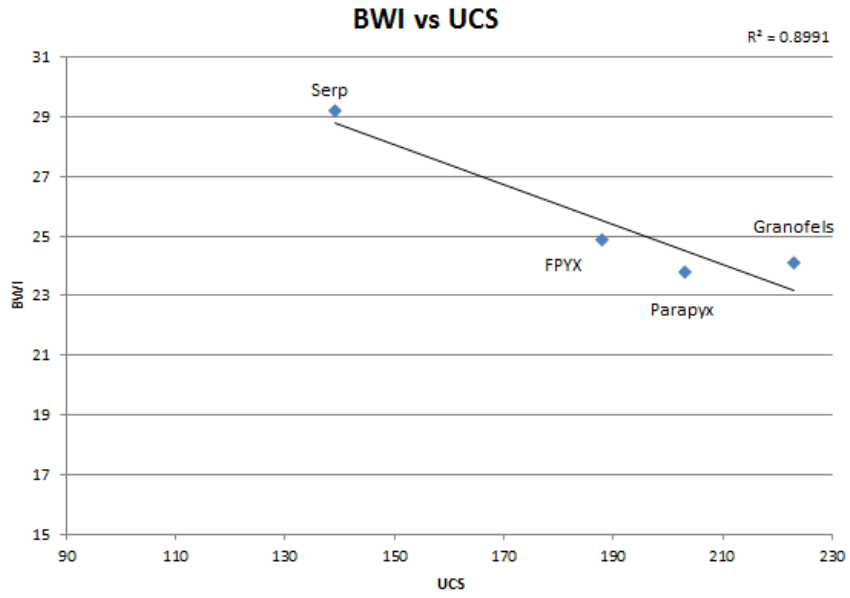


Figure 88: BWI vs. UCS from Zwartfontein means excluding pyroxenite.

The results show promise at Mogalakwena Mine, rock strength may be correlated to grinding hardness. Caution must be exercised due to the reported poor correlation between BWI and UCS at other mines. Further investigation is needed with a larger data set.

4.5 Drilling Performance and Rock Strength

4.5.1 Penetration Rates and Rock Types

The initial study into the relationship between penetration rate and rock type use manually recorded drilling times and drill depths. These records completed by drill operators proved inaccurate for use in this study. The manually recorded data showed a 15% discrepancy in recorded drilling time under controlled observation. Due to the small difference in rock type and hardness response, a 15% difference in drilling time will undoubtedly cover identifiable traits of specific rock types.

The installation of RockMa allows for automated reporting based on drilling actuals. PV149 was fully fitted and was used for investigation into penetration rates and rock types. 8 patterns that were drilled by PV149 were identified and the penetration data from the blast holes were sourced. The patterns are on the hanging wall, reef and footwall. Examples of these patterns are shown in Figure 89, Figure 90 and Figure 91. The grain size adjusted UCS was not used for the graphs to follow. Grain size descriptions do not exist for chip logging as yet.

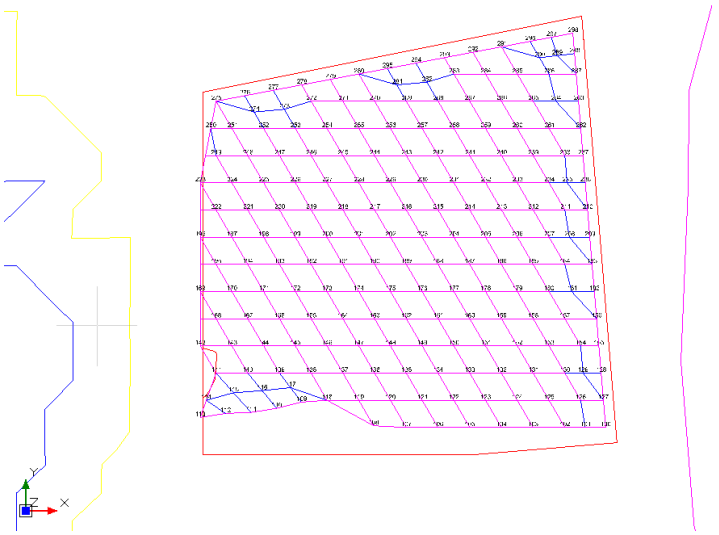


Figure 89: 326/050 with drilling grid falls within the reef package.

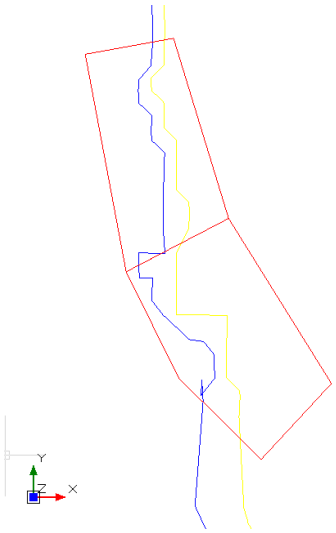


Figure 90: Pattern 323/036 and 326/037 lying across the HW and Reef contact. Ore line lies on toe elevation.

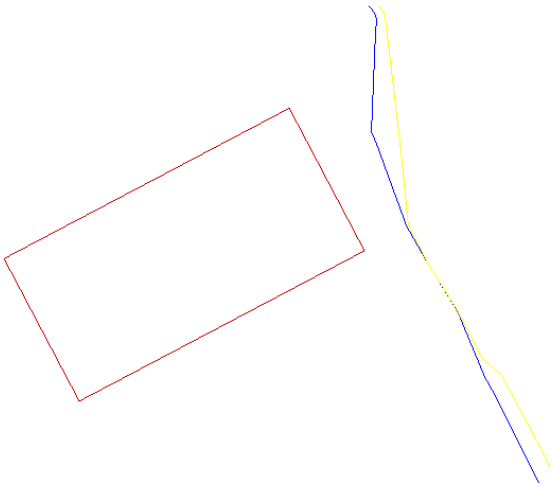


Figure 91: 411-076 falls within the estimated HW stratigraphy.

4.5.1.1 Penetration Rate and Stratigraphic Unit

In the exploration database, a mean UCS value is supplied. This value is used in Table 41 to compare to penetration rates. The reef UCS was calculated using an 8:2 split (derived from the exploration lithological distribution) between feldspathic pyroxenite (FPYX) and pyroxenite (PYX) (Table 6). The FW UCS was based on a mean value from the database. The Calculated UCS is the mean UCS for the rock type as calculated in this report (Table 41). This analysis does not include any grain size adjusted UCS results.

Table 41: Penetration rate per stratigraphic unit from PV149.

		Penetration Rate				
Rock Type	Holes	Max	Min	Mean	Mean UCS[3]	Calculated UCS[4]
HW	139	94.93	8.57	25.13	179	179
C-Reef	7	44.71	27.64	36.28	174	215
Reef	173	101	15	39	157.2[5]	190
FW	39	74.79	12.64	20.59	228	228

The results from Table 41 are displayed in Figure 92. There is a good correlation between penetration rate and exploration UCS (R^2 value of 0.75). The 2 points using the calculated mean UCS from this investigation show a good trend but do not fall on the same trend line. Both the mean UCS from the exploration database and the Calculated UCS (from this study) show a similar trend.

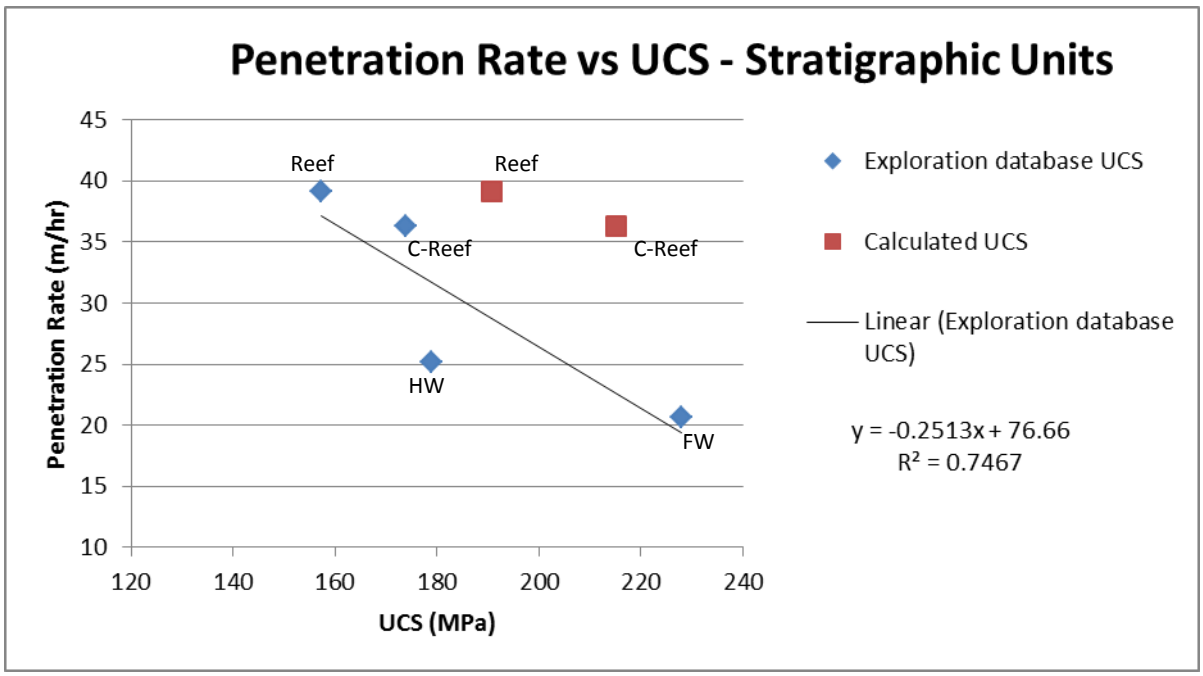


Figure 92: Penetration rates vs. UCS results from exploration defaults and those calculated for entire stratigraphic units

[3] Little (2006).
[4] UCS defaults in exploration database.
[5] 80:20 proportion between FPYX and PYX to determine average reef UCS value.

4.5.1.2. Penetration Rate and Specific Rock Type

Specific rock types from blast hole chip logging are compared to penetration rate in Table 41. Due to the recent application of the RockMa system, the available database is relatively small. Hybrid norite (H) is a term used for the description of recrystallised norite in direct contact with the reef.

Table 42: Penetration rate per rock type from PV149.

		Penetration Rate				
Rock Type	Holes	Max	Min	Mean	Mean UCS	Calculated UCS
H	6	25.67	19.26	22.19	176	176
FPYX	3	37.40	32.43	34.88	174	202
PYX	9	76.78	27.85	52.67	90	146
GF	48	83.56	12.65	28.86	228	228

The penetration rate is compared to the mean exploration UCS in Figure 93. The results show a fair correlation with an R^2 value of 0.68.

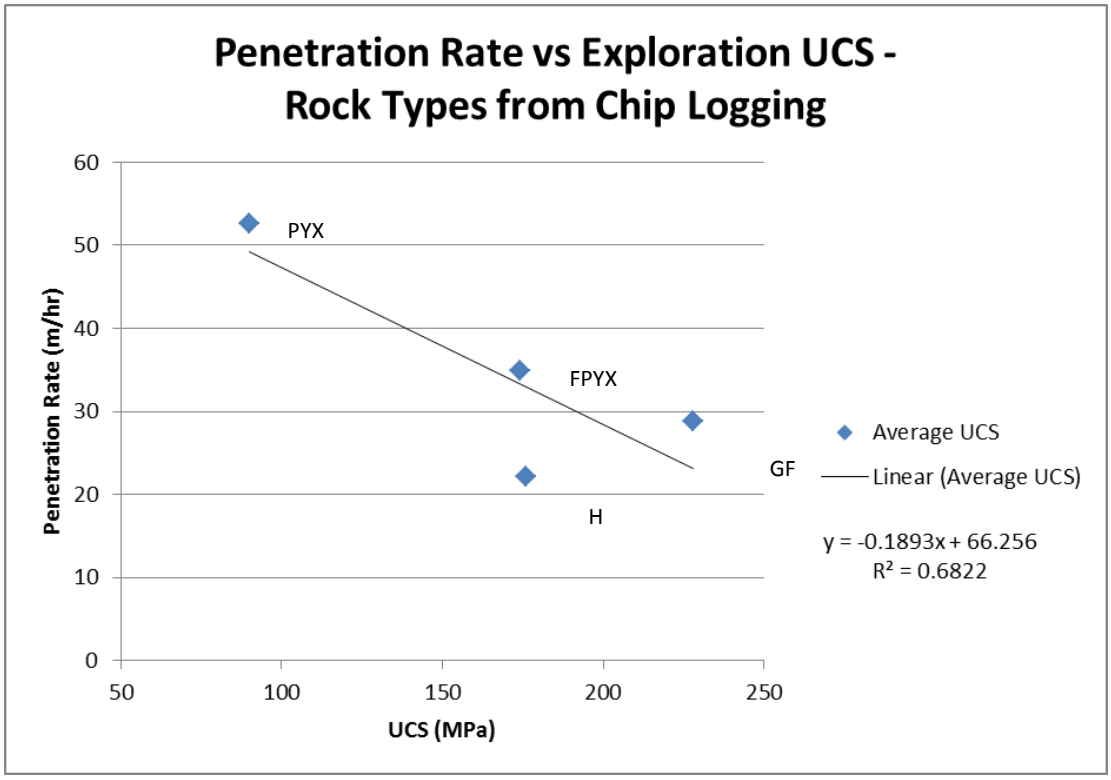


Figure 93: Penetration rates vs. UCS from the exploration database using rock types (Average UCS).

The rock types were plotted against the calculated UCS. The results show a poor correlation with a R^2 value of 0.37 (Figure 94).

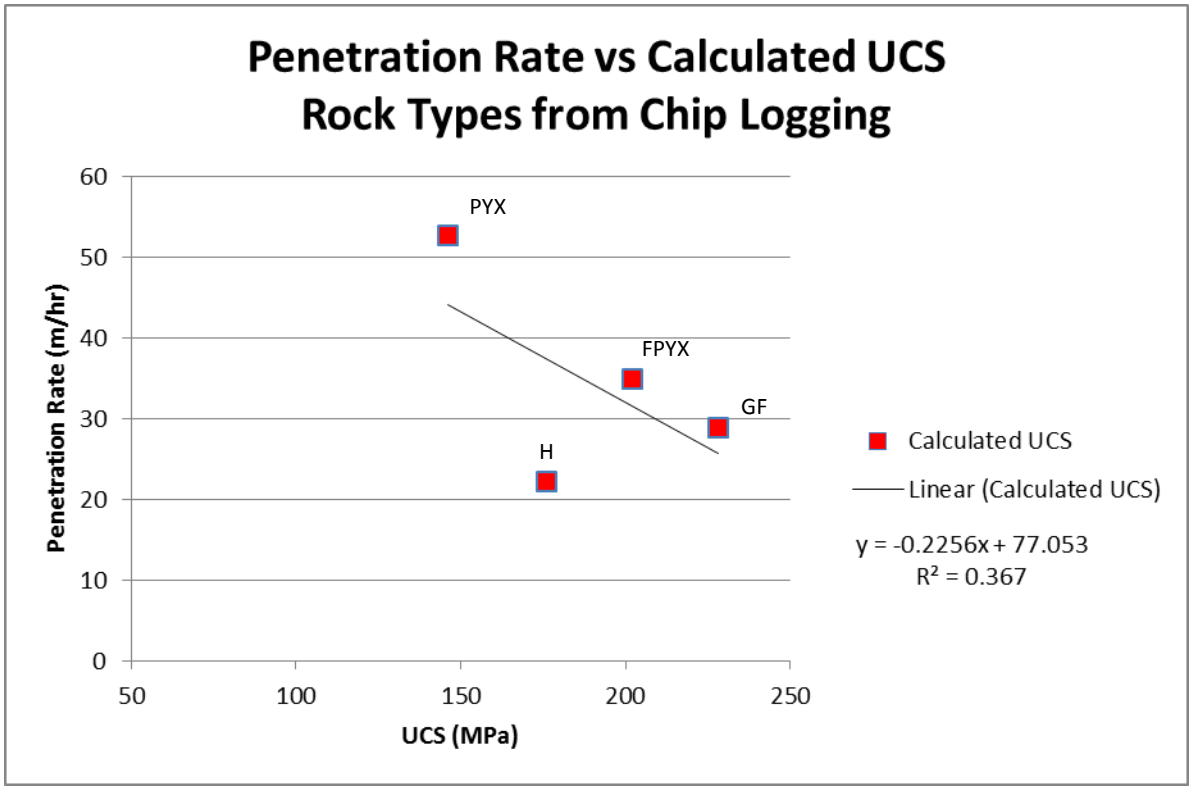


Figure 94: Penetration rates vs. UCS from exploration using rock types.

The results show the discrepancy between UCS used in exploration database and UCS as calculated from the PLI. The UCS values in the exploration database show a higher correlation with ROP.

4.5.2 RockMa MWD Initiative

The RockMa system has been successfully installed on PV149. The rig is recording relative rock strength through algorithms making use of digitally recorded drill data. This algorithm is not available for scrutiny. These algorithms are based generally on similar research as explained by Bourgoyne *et al.* (1986). The rock strength information being generated does rely on penetration rate data.

The rock strength data being generated by PV149 is illustrated in Figure 95.

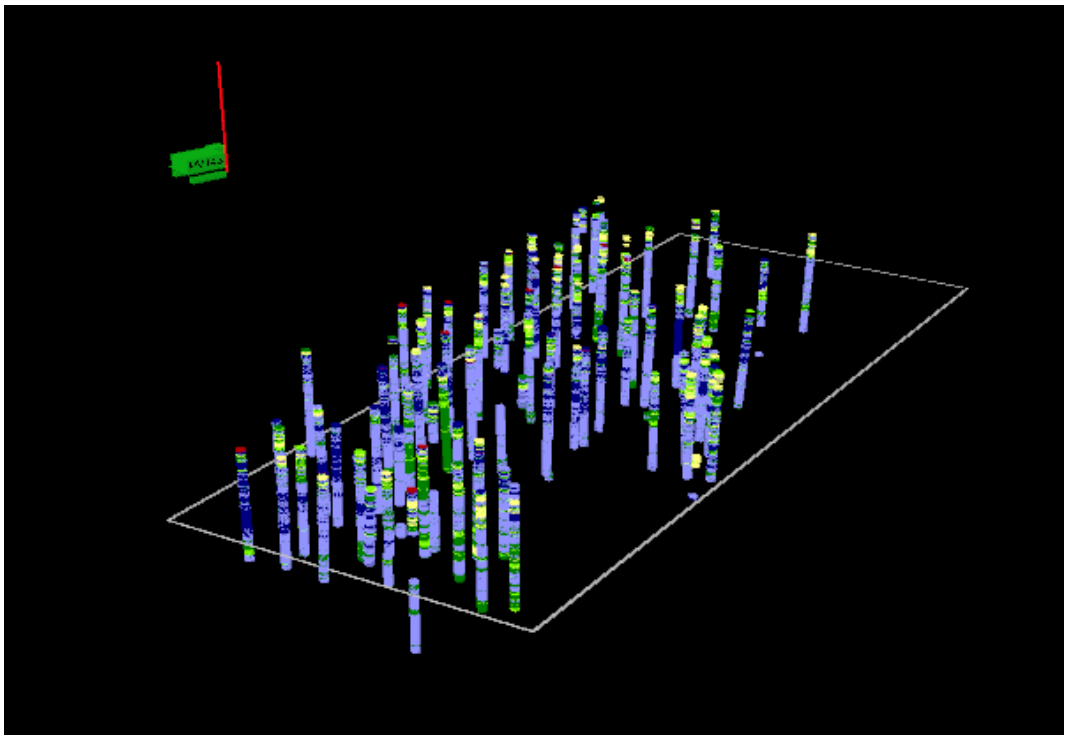


Figure 95: Pattern 326/141in HW drilled by PV149.

The strength display uses the legend in Figure 96.



Figure 96: Legend for rock strength in the RockMa system.

Cut 8 is the expansion project for North Pit. The top benches lie within a weathered zone. Weathered ore is not fed to the plant and must be separated from fresh ore. The relative rock strength information from Cut 8 shows a good use of the information in identifying the weathered horizon.

Figure 97 shows the rock strength of bench 8 at Cut 8. Notice the stronger rock on the left of the image.

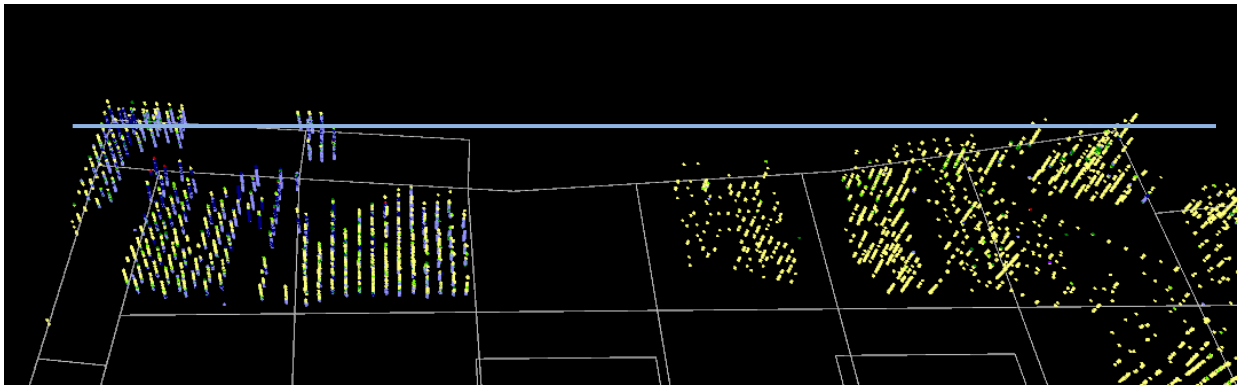


Figure 97: View looking East at Cut 8 on bench 8. Rock strength is greater in the North and decreases towards the South. Blue line is the length of the photograph

In field validation confirms that the strength information being generated from PV149 can be used to isolate weathered material from fresh beneath the surface (Figure 98).

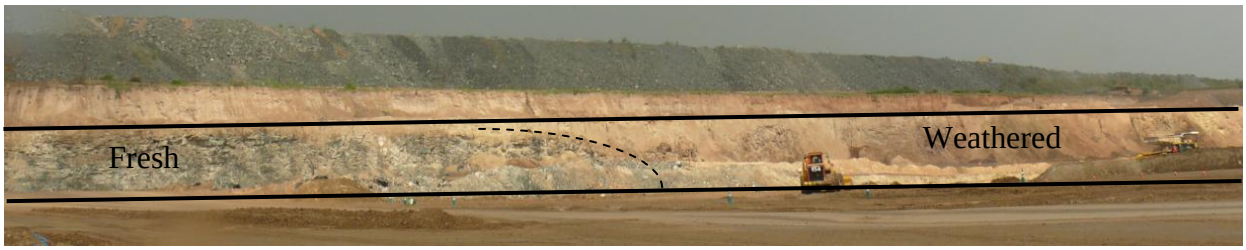


Figure 98: A view of the section marked in Figure 99; Fresh FW Granofels is seen on the left of the picture and becomes oxidised moving towards the right (South) (contact shown at the position of the dashed line). Bench 8 crest and toe indicated between two black lines.

Figure 99 shows the entire Cut 8 project. The RockMa strength data has shown that fresh material is being intersected in the footwall and hanging wall. The reef portion shows a higher degree of weathering which can be expected due to the higher mafic content.

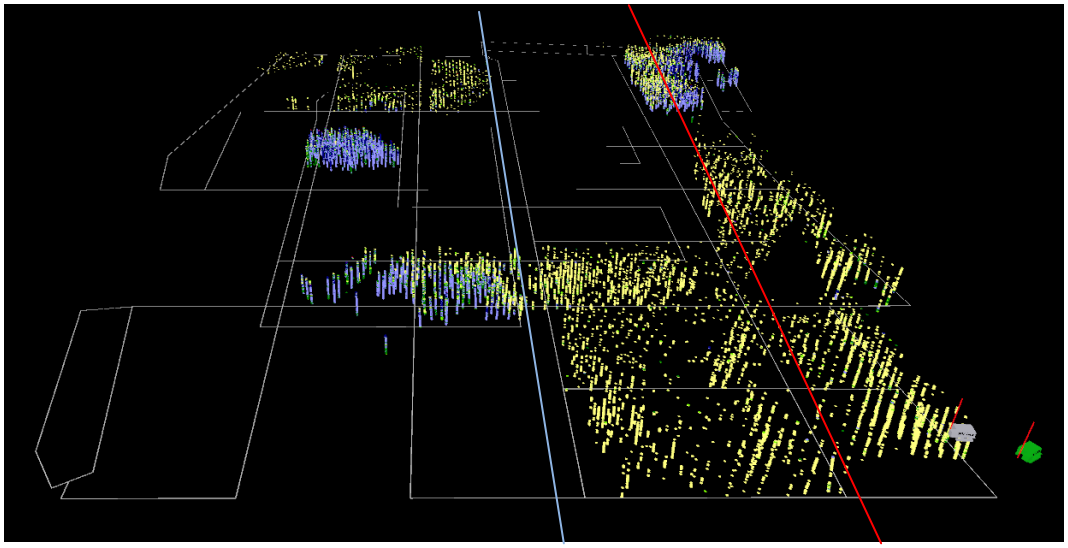


Figure 99: View of all Cut 8 drilling patterns. Colours represent relative rock strength data reported by PV149. Patterns with no rock strength data were not drilled by PV149. Lines represent estimated reef zone (HW contact is blue and FW is red).

Patterns bordering reef and footwall show the degree in difference between rock strengths. The trend from East to West at this border shows decreasing rock strength as the rig nears the reef. The system records changes in rock strength in a single hole. Figure 100 correctly shows that these trends are replicating the westerly dip of the orebody (red line).

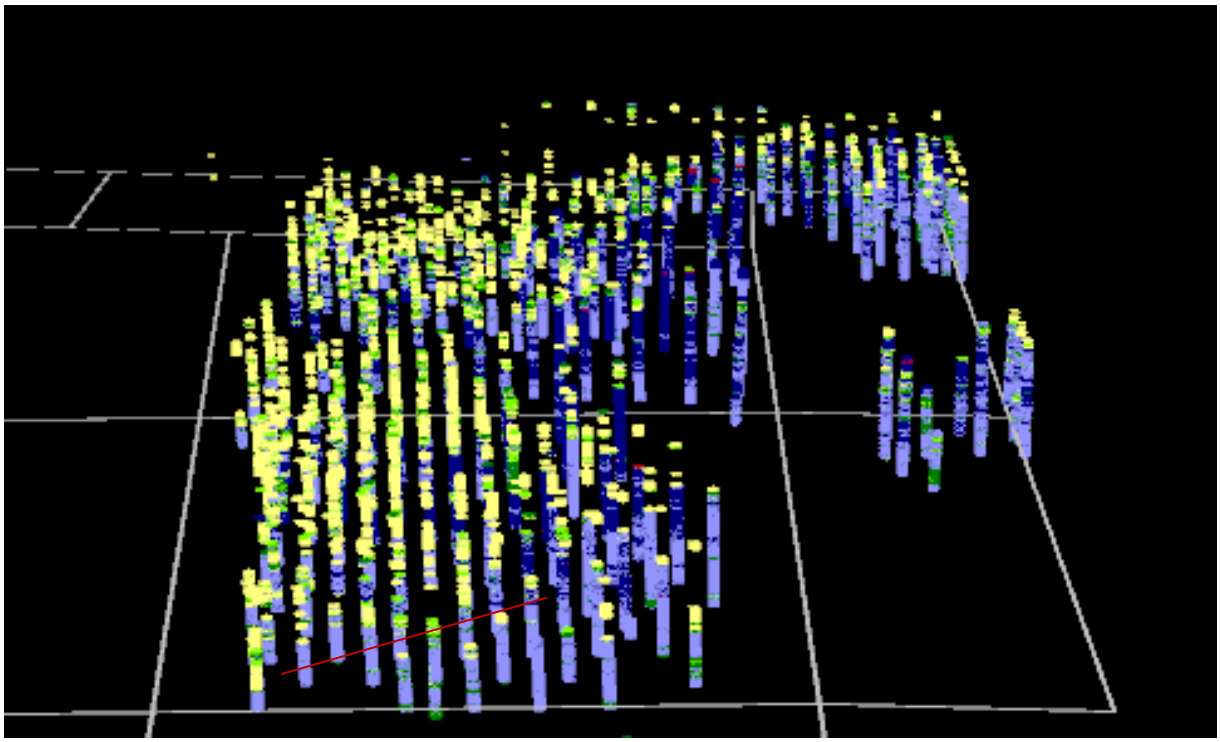


Figure 100: An oblique view of relative rock strength data for patterns in Cut 8. The red line shows the uneven dip of reef revealed through drilling through the FW contact.

The separation of weathered material from fresh would require greater selectivity from mining equipment. A standard ROP for all PVs is currently used in the scheduling of drilling rigs. The most noticeable issue occurs at Cut 8 where markedly higher ROPs are recorded and the planned drilling schedule for the month is thus out of sync with reality (Figure 101).

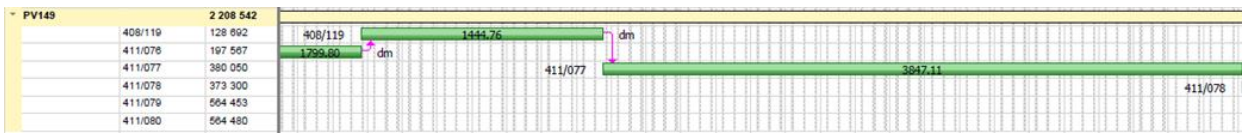


Figure 101: PV149 planned drilling for February. Drilling time for 408/119 and 411/077 is proportional yet bench 408 is oxidised with a significantly higher ROP.

It is reported that penetration rates are significantly higher for the weathered horizon. Using a standard ROP for scheduling drilling rigs is thus faulty as it assumes rock strength does not materially impact drilling penetration performance. The results from Table 41 and Table 42 can be applied to the scheduling of drill rigs for greater accuracy.

4.6 Rock Strength Modelling

The mean UCS results for hanging wall, reef and footwall rocks were applied to the OY lithology entries from the exploration database. Grain size adjusted UCS values were applied to all lithological entries which included a grain size description.

Voxler 3 was used as the modelling package. This software package is simple to use and can handle large amounts of data.

Grain size adjusted UCS values applied to boreholes in exploration database were plotted (Figure 105 and Figure 106). The darker blue areas of the boreholes are indicative of the footwall granofels which have the highest mean UCS. The light green indicates <200MPa and is seen in the reef horizon. The hanging wall is generally dark green indicating 200-220MPa.

Figure 102 shows the relative rock strength legend used in the model.



Figure 102: Rock strength legend: 138 - 300MPa

A 3D rendered block was created using the adjusted UCS values from the boreholes. The 3D model has been cut roughly through the centre of North Pit. The reef package is visible between footwall contact (red line) and hanging wall contact (blue line) (Figure 103).

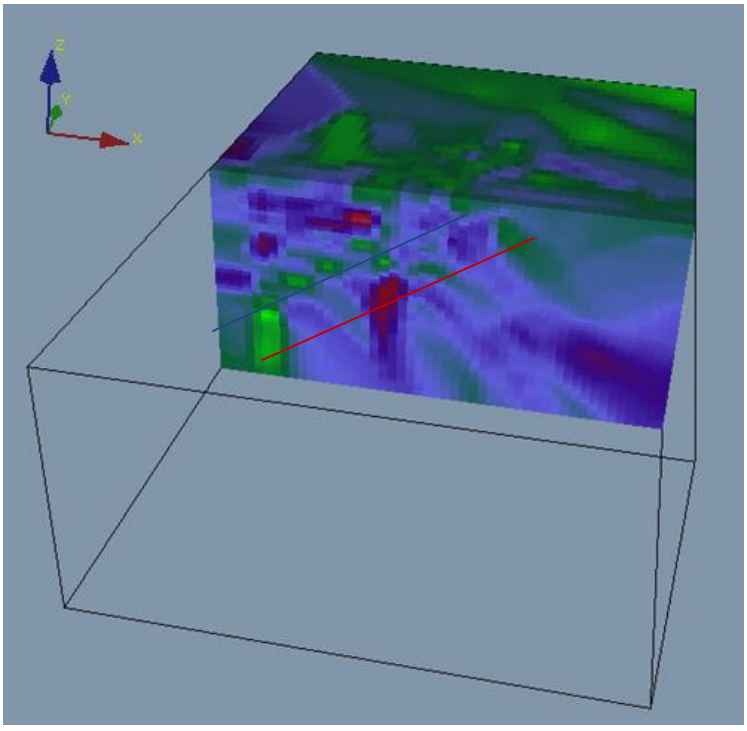


Figure 103: 3D rendered model. Blue line indicates HW contact and red line indicates FW contact. The lighter green colours within the reef indicate lower rock strengths.

An isosurface was applied to rock strengths >220MPa indicating rocks on the higher end of the strength range and decreased penetration rate (Figure 104). This isosurface indicates areas of OY which will exhibit decreased performance in drilling penetration rates. Once these areas are mined, their performance in the plant can be related back to their rock strength for further study.

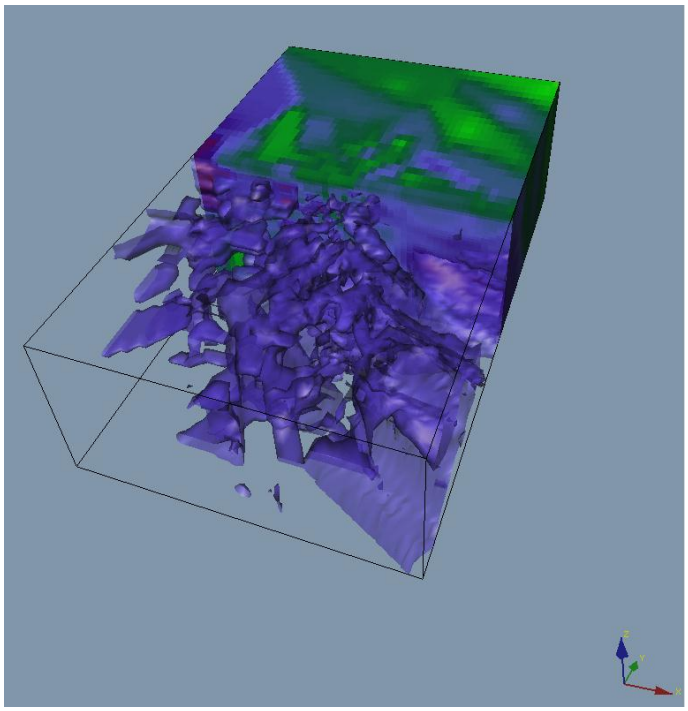


Figure 104: Isosurface set at 220MPa.

Voxler 3 allows simple 3D rendering. Datamine Studio 3 will allow for the application of the rock strength model to be incorporated into pattern by pattern modelling.

4.7 Summary

Chapter 4 has described the results from the exploration database, strength data, drilling results and 3D modelling of rock strength. The results show a good correlation between grain size and rock strength which can be applied to drilling and plant processes. An unforeseen result was the importance of calibration of testing equipment. The uncalibrated results from the point load testing immediately led to a follow up validation study. The next chapter will cover the discussion and conclusions from the above results.

CHAPTER 5: FINANCIAL BENEFITS OF ORE STRENGTH CHARACTERISATION

5.1 Introduction

The following chapter will briefly discuss the potential financial benefit of characterising ore strength and hardness. The information represents an internal investigation on site. The South plant mills offer the opportunity to optimise the feed material hardness to increase the throughput of mill product to the floatation stage. *In situ* ore characterisation would allow for consistent mill performance by correctly blending competent and fine material to the primary crusher. The financial benefits of reef identification using penetration rates are not covered in this chapter.

5.2 South Plant

The South plant business plan targets for 2015 are 4,380,000t milled for the year averaging 365 000t/m at a mean head grade of 2.34g/t 4E. The autogenous mills at South plant rely on a fixed proportion of coarse (>110mm) and fine feed in order to achieve the effective milling performance. The coarse and fine material is stockpiled separately after being separated at an 11mm grizzly (Figure 105). Disruptions to the proportion of coarse and fine feed immediately impacts the quality and quantity of feed to the floatation stage due to the negative changes in output particle size. The milling stage is the most energy intensive process on site and its optimisation can greatly cut energy costs, cost per ton milled and throughput. Ineffective milling due to the incorrect proportions of feed material directly and negatively impacts processing costs.



Figure 105: View from Big Bruce crusher over South Plant conveyor system where coarse and fine crushed material is split at the 110mm grizzly.

The largest issue facing stable mill performance is the depletion of the coarse feed material (Figure 105 and Figure 106). Uncontrolled and unplanned variability in ore strength and hardness directly influences the stockpiles of coarse and fine material. The characterisation of ore strength before material is fed to the primary crusher will allow the planned and stable feed of the required ore strength to achieve the 6:4 ratio.

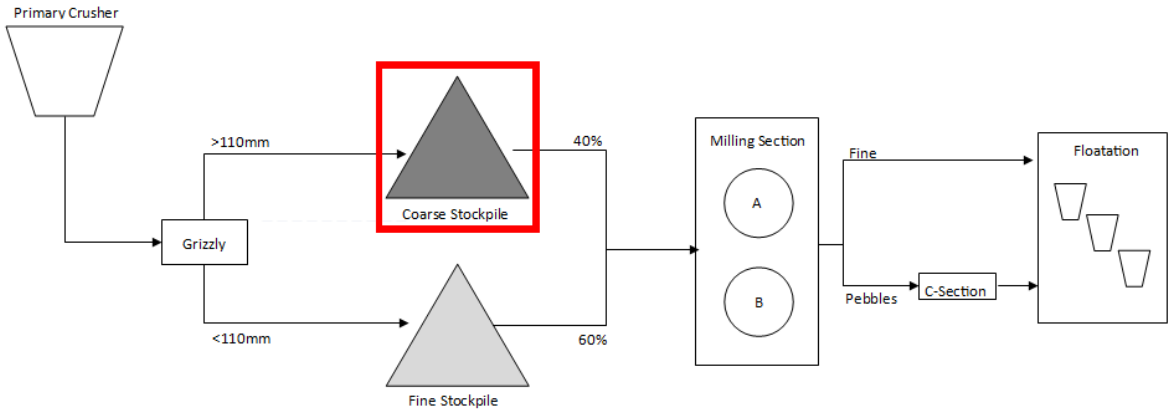


Figure 106: Schematic diagram of South Plant crushing and milling for section A and B. Red block shows coarse material stockpile which can be optimised with improved ore strength feed.

The depletion of coarse material has led to multiple total milling stoppages in 2014 (Table 43).

Table 43: Total downtime per month due to depletion of coarse feed material.

Month	Downtime (hrs)
January	18.5
May	10.5
June	27.3
July	2
August	5.42
October	51.3
November	101.2
December	9.8
Total	**226.02**

The correct ore hardness fed to the primary crusher plays a vital step in achieving the required coarse to fine ratio.

5.3 Financial Benefit Analysis

The following calculations use 2014 results and costs. The calculation assumes that A and B mills were running at 2014 mean output (380.74t/hr) during the total down times of 226.02hrs (Table 44).

Table 44: Total milled tons lost due to depletion of coarse material.

Input	Value
Lost milling time (hrs)	226.02
Milling rate (t/hr)	380.74
Total lost milled tons (t)	**86,054.38**

The calculation results in an additional 86,054.38t milled for 2014 (a 2.58% increase) (Figure 107).

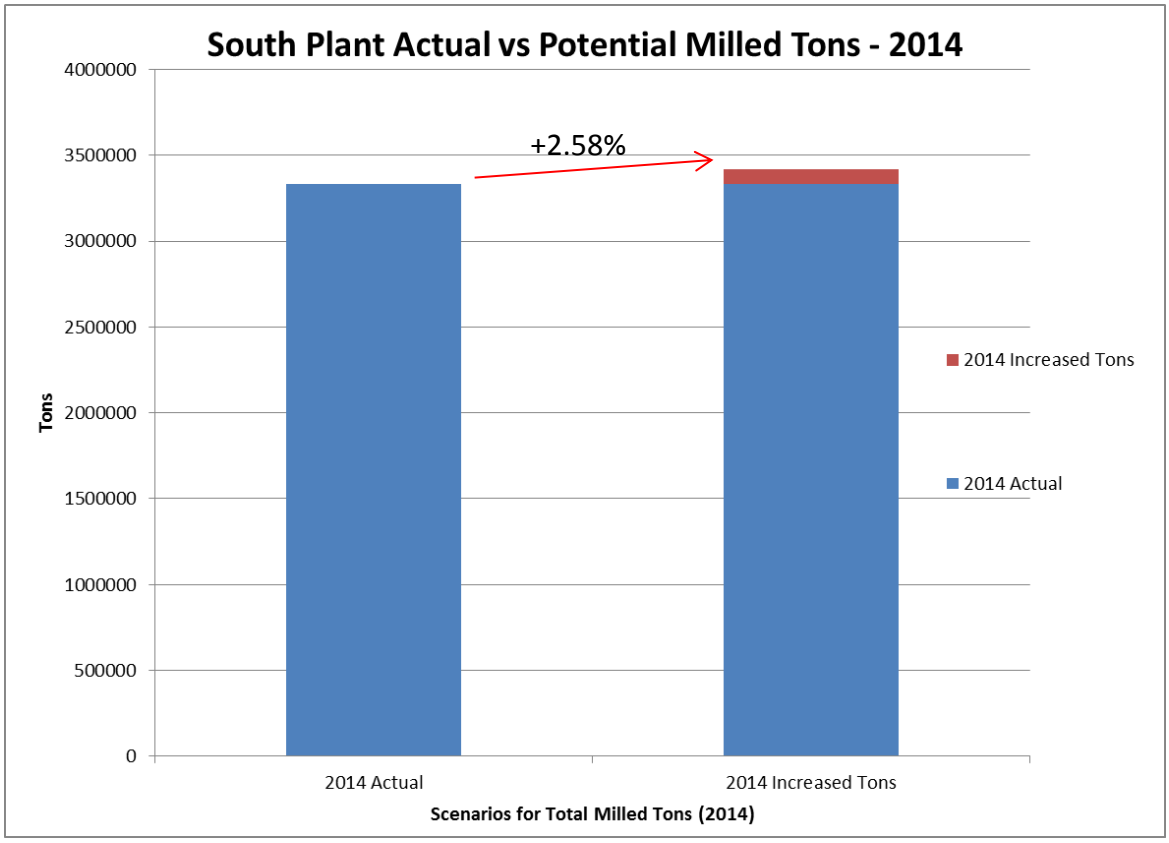


Figure 107: South Plant milled tons for 2014 with potential increase in coarse material due to optimised ore feed.

The following assumptions are made to establish the financial benefit of the additional feed to South Plant (Table 45):

Table 45: The assumptions used for the financial benefit calculation.

Input	Value
Additional Tons with Constant Feed (t)	86054.38
Recovery (%)	71.36
Grade 4E (g/t)	2.53
Basket Price[6] (R/g)	330.54
On-Mine Costs per Milled Ton (R/t)	437

[6] Using the prill split from 2015 Business Plan with an exchange rate of R13/$ and commodity prices as of 10 September 2015.

An additional 86054.38t of ore would have entered the floatation process (Figure 107) had the feed to the mills been constant. Results of the financial analysis with the above values reveal an **additional revenue of R51,353,773.97** for 2014.

The total mining costs per ton milled is R437 which results in a total cost for milling (with the increased tons added) of R37,605,764.06. One concludes that a constant feed to South Plant would **increase operation profits by R13,748 009.91.**

The average cost of drilling for all bit sizes is R44.85 applied to a total of 1 366 193m (2014). Therefore, the added benefit of modelling ore strength and hardness to stabilise and optimise the correct feed to South Plant results in an added value of **R37.6** per meter drilled (average for all bit sizes and rigs).

5.4 Proposed Feed Material Optimisation Plan

The financial benefits of optimising ore feed to South Plant to achieve stable ore feed require that patterns are modelling using ore strength and hardness data from UCS testing (PL derived) and MWD (RockMa) generated data.

The hardness modelling would be required during the mining stage to ensure a timely buffer from mine to mill. The ore loaded would be stockpiled according to rock strength parameters (assuming grade was constant between both stockpiles). The stockpiles would be re-handled to the South Plant primary crusher at the required ratio of 6:4 (fine to coarse) (Figure 108).

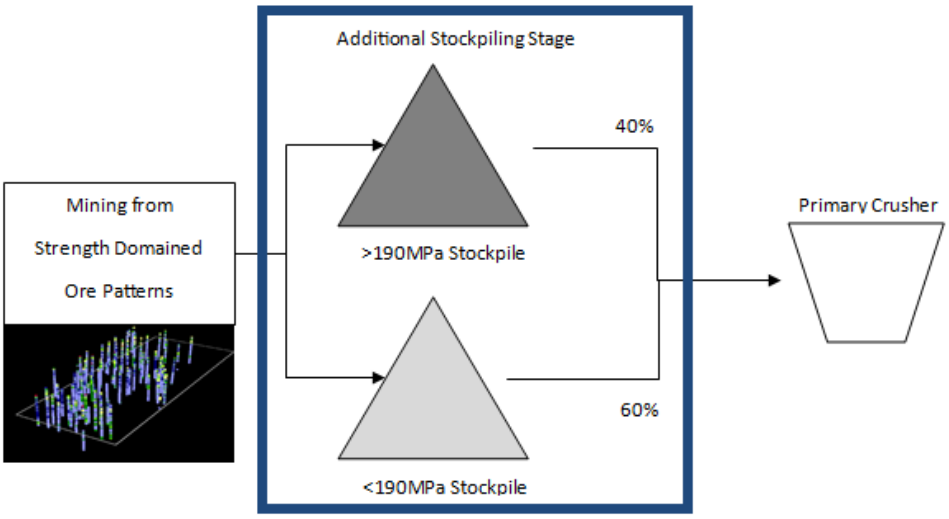


Figure 108: Proposed modelling and stockpiling stage before primary crushing to South Plant using a 190Mpa division.

This would ensure that an additional buffer is created and that the ratio of coarse to fine is maintained before primary crushing.

5.5 Summary

This brief chapter investigated the potential benefit of optimising the feed material according to South Plant autogenous milling requirements. The stabilisation and optimisation of feed material, during the mining stage through the modelling of ore strength and hardness parameters per pattern, with ensure the ratio of coarse to fine material is achieved

CHAPTER 6: DISCUSSION AND CONCLUSION

6.1 Introduction

This chapter discusses the results, the interpretation and application of the findings in the previous chapter in terms of forward usage in a geometallurgical domaining project. The main outcomes are listed and recommendations for future work are made.

6.2 Discussion

The 6 investigations are discussed separately and summarised in the conclusion. The 6 discussion themes are:

- Distributions of texture and grain size per ore type.
- Link the PLI derived UCS data to texture and grain size.
- Compare strength and hardness data.
- Analyse drilling penetration and MWD data usage.
- 3D rock strength model (grain size adjusted).
- Potential financial benefits of ore strength domaining for South Plant Comminution

6.2.1 Textural Distribution

The study identified the major rock types by analysing the available literature and mine databases. The research concludes that rock naming is based on both composition and textural descriptions. A list of major rock types for OY was established through this investigation which would describe the vast majority of rock found in the operational area. Furthermore, the resulting distribution of major rock types conforms to previous studies (Nex *et al.*, 2006; Bye, 2004).

The relationship between composition, texture and grain size was investigated for rock types in both the reef and footwall stratigraphies. Rock composition was shown to offer a broad range of expected rock strength results but did not accurately supply a more detailed understanding of rock strength variations within the same lithologies. Generally, a higher felsic mineral content leads to higher rock strength. Understanding rock strength variation within a single rock type requires descriptions of grain size and texture as they both play integral parts in describing rock strength behaviour (Ozturk *et al*., 2014). The large variety of textural description has led to inappropriate use of textural terms such as homogeneous and recrystallised while textural descriptions left blank (absence of a textural description) are difficult to interpret. The most reasonable approach was to treat blank textures as the rock type's dominant texture. The use of site specific textural descriptions should be discontinued and replaced by globally accepted terms. An investigation into suitably descriptive terms should be carried out on site.

Grain size descriptive terms were far too complex and the study highlighted that simplification of term use does not decrease the usefulness of the data. Duplicate terms such as F - M and M - F are unnecessary. Human error is introduced in grain size descriptions because the exploration core is visually identified using a rudimentary handheld measurement tool. Furthermore, the database includes logging from a plethora of geologists over many years compounding subjectivity concerns regarding descriptions used. Additionally, only the major mineral grain size is recorded in the database. Both norite and feldspathic pyroxenite would be described as cumulus. However, the plagioclase grains are intercumulus in feldspathic pyroxenite. This knowledge is pertinent to avoid incorrect conclusions about the nature of the textural and lithological relationship.

The dominant rock type in the reef is feldspathic pyroxenite (60-80% of the reef) which conforms to previous studies (Bye, 2004). Feldspathic pyroxenite contains the greatest range of grain sizes. A subcategory of feldspathic pyroxenite in the database is pegmatoidal feldspathic pyroxenite which included all occurrences of

grain sizes with the range C – PEG. Unaltered and slightly altered rock types (serpentinised pyroxenite and serpentinised feldspathic pyroxenite) were dominated by the cumulus description. From the descriptive terms used, serpentinised pyroxenite and serpentinised feldspathic pyroxenite can be treated as a single suite due to the difficultly in visual identification.

Altered ores (calc-silicate and parapyroxenites) had a higher occurrence of a recrystallised texture. Parapyroxenites and calc-silicates vary widely (compositionally and texturally) making visual identification difficult in hand specimen and core. Calc-silicate had a low occurrence in the dataset as compared to ZN and SS properties. This is largely due to the presence of the granitic footwall at OY rather than the dolomite footwall in ZN and SS. Grain sizes are difficult to measure in these rock types due to metamorphism, metasomatism and assimilation which disguise lithological distinctions (Kinnaird *et al*., 2010; Holwell *et al*., 2006).

The term granofels is used loosely as the suite includes granite, leucocratic veining and fine grained pyroxenite. The differences in the textural descriptions of granofels can be attributed to the varying composition of the rock. These variations within the suite are not adequately distinguished in the database.

The findings show that descriptions of rock have to be simplified due to the number of rocks types in the database and textural variability over small distances. The simplistic stratigraphic terms of A, B and C reef appear largely redundant as this order within the reef package is contradicted in field. Moreover, field checks at pattern 326/063 highlighted the variation in textures and positions of rock types within a single stratigraphic unit. The simplification and accuracy of texture and grain size descriptions are needed to make data more useful. The sporadic nature of alteration and recrystallisation requires a higher density of data. Gathering data in the field before blasting and before comminution processes are necessary. A proposed logging sheet to describe texture and alteration in chip logging was created for immediate implementation at Mogalakwena Mine

(Appendix 4). This is to be implemented for RC drilling sample descriptions to identify lithological properties for a single blast pattern. Descriptive compositional and textural terms from chip logging are sufficient for predicting drilling performance.

The descriptive terms for grain size and texture are used at the discretion of individual geologists and are therefore subjective. The training of geologists to conform to site best practise is vitally important. The database therefore has inherent inaccuracies which must be understood before conclusions can be drawn. The size of the database reveals a general and relative comparison of rock types. The database is nevertheless useful as it forms the generalised foundation of rock type variety at Mogalakwena Mine.

6.2.2 Rock Strength and Textural Relationship

PLI tests were extracted from the exploration database and converted to UCS. The UCS value was linked to the lithological, textural and grain size description for the sample interval. The major texture and grain sizes for the primary rock types were established and linked to the applicable UCS values. Conversion factors were applied to the tests following previous research (Hayes & Piper, 2003). These conversion factors do not cover the entire reef suite of rock types. However, OY farm is dominated by feldspathic pyroxenite and pyroxenite (upwards of 60% in the reef) and is included in the conversion factor investigation.

Rock types strength ranges at Mogalakwena Mine are classified as high to very high (Heinz, 2009). Other strength test types were not examined due to the limited amount of records in the database.

The initial results show that rock composition has an impact on rock strength. This is seen when comparing feldspathic pyroxenite to pyroxenite mean values. The increased plagioclase content alone increases rock strength (all other properties being the same). Grain size has more influence on rock strength than

texture at OY farm. In unaltered ore types a strong correlation is established between decreasing rock strength and increasing grain size. The practical implementation of this knowledge concludes that the grain size adjusted UCS results can be applied to rock described in the field and more accurate rock strength values can be estimated by geological description alone.

Pyroxenite shows a clear downward trend of UCS with increasing grain size. The importance of the distinction between pyroxenite and the other rock types is the significantly lower UCS range. Identifying pyroxenite and feldspathic pyroxenite within the reef would categorise 80% of the reef. The differences in strength response of the two rocks alone would indicate probable differences in plant response.

Altered ore (calc-silicates and parapyroxenites) showed complex results in the analysis. The influence of metamorphism and high degrees of alteration and recrystallization makes grain size identification more difficult. Therefore, the database for altered rocks should be treated with greater circumspection. The lower accordance of these altered ore types in OY decreases rock type complexity for North Pit and Cut 8.

The dataset of 100 PLI tests carried out at the exploration coreyard validated the findings that grain size affects rock strength when composition is constant. Igneous rocks are generally isotropic and orientation of the sample for testing is not important and was taken into account. The mode of failure in the test work was not considered as the aim of the test work was to replicate the exploration database. Unfortunately, the PL machine used was not calibrated and all UCS results are up to 40% higher than expected when compared to the exploration database results. The error was constant throughout testing and the results are useful for establishing the qualitative grain size and strength relationship. PL tests on pegmatoidal grain sizes were discarded due to the size relationship between the grain size and core diameter (ISRM, 1985). Samples with visible discontinuities were discarded. These issues emphasise the importance of QAQC processes on

PL test work. A follow up validation programme was immediately initiated after the discrepancy in the PL results of the 100 samples.

The feldspathic pyroxenite samples tested showed a strong inverse relationship between grain size and rock strength. Granofels samples were separated into felsic and mafic components and tested separately. Mafic rocks are generally weaker yet the fine grained mafic samples showed higher UCS results. This indicates that texture (specifically grain size) has a larger impact on rock strength than composition. Texture is highly variable in granofels (Nex *et al.*, 2006). Compositional differences for granofels are more important than texture when determining rock strength. Logging does not separate felsic and mafic components in granofels. There is scope for changing the method in logging to fit more complex requirements in geometallurgical characterisation.

Research into the use of XRF data for distinguishing rock types is ongoing. Current visual rock type identification, which can be used as a general early categorisation guide, does not allow for the level of detail required to characterise geometallurgical response within a concentration system. Therefore, c exploration ore and RC chip rock type descriptions can be supplemented with XRF whole rock chemistry in order to determine more detailed geometallurgical and mineralogical characteristics. In the case of feldspathic pyroxenite, AlO content can be used to distinguish between feldspathic pyroxenite and pyroxenite. The CaO content, which is correlated to hardness, should be used to describe composition (Schouwstra and de Vaux, 2013) while a quantitative method of textural description of the rock type will supply textural data before milling. Additionally, CaO is indicative of alteration and the presence of altered minerals such as serpentine, talc and chlorite (Schouwstra & de Vaux, 2013) thus linking mineralogy to the observed rock type as logged by a geologist. The finding by Bye (2005) included the shift from enstatite to diopside from altered to unaltered ores in Sandsloot which is indicative of a more CaO rich chemistry. Additionally, this relationship indicates that CaO is linked to recrystallization processes and therefore to textural changes.

For accurate measurements, it is suggested that the PLI is used independently rather than calculating a resulting UCS value due to the presence of errors (Dhungana, 2013). Samples tested in laboratory settings are of better quality because poor rock is discarded in either drill cores or samples (Laubscher, 1990). The field strength of the *in situ* rock mass will always be less than the laboratory strength of an intact sample of the mass. Generalised geological properties alone should not dictate mechanical properties as strength is correlated to various properties (Dhungana, 2013; Napier-Munn *et al*., 1999; (Ozturk *et al*., 2014). The findings in this research report indicate a relationships between composition, grain size and rock strength. For a higher certainty of the actual UCS for each grain size category, validation is necessary through UCS test work.

The qualitative nature of descriptions in the exploration database will include subjectivity bias. There are inaccuracies in the data and these areas have been highlighted. The descriptions can be used to guide UCS determination if simultaneously applied XRF and chemical data is used. Other properties, mechanical, mineralogical or geochemical, can be added to the greater description of the rock to fine tune the understanding of rock strength and rock type.

6.2.3 Strength and Hardness Relationships

Rock breakage occurs along pre-existing weaknesses (Heinz, 2009). This was observed on unaltered North pit pyroxenite ore during the early stages of coarse crushing and grinding (Gloy & Hey, 2002). Ore response in the crushers and plant is of vital interest at Mogalakwena Mine. Appropriate rock tests need to be performed regularly to accurately predict response. The forecasting of grinding circuit from UCS values is not recommended due to the generally poor correlation between BWI and DWT to UCS (Doll *et al*., 2003). However, UCS can be incorporated within the metallurgical understanding of the ore to forecast other mining processes. Additionally, there is scope to apply ore strength to autogenous milling requirements in the case of South Plant.. Two hardness tests are

applicable, DWT and BWI. There is a material influence of grain size and grain boundaries on grinding tests (Doll *et al*., 2003).

Proving a correlation between DWT and UCS or BWI and UCS would be advantageous. Poor relationships have been widely reported due to the difference in breakage mechanisms of the tests (Barrat & Doll, 2008; Doll *et al*., 2003.; (Napier-Munn *et al*., 1999).

Mean results for BWI, DWT and UCS were used in this study. UCS vs. BWI shows promising results. A directly proportional relationship exists between the two rock tests for major ores at Mogalakwena Mine. The mean values only imply a relationship. Empirical evidence derived from specific ore types separated by compositional variability, texture and grain sized is required to prove such a relationship.

Establishing a correlation between BWI, UCS and DWT samples categorised by grain size will be the next logical step from this study. UCS data will be generated from the RockMa system for each blast pattern and application of the UCS data could include plant performance predictions. The predictive usage showing that such a relationship exists would imply cost savings and optimisation of plant processes.

6.2.4 Drilling Performance and Rock Strength

The results from the analysis comparing rock strength and penetration rate have shown a directly proportional relationship. This was expected as the relationship has been described at length (Heinz, 2009; Bourgoyne *et al*., 1986). Mafic rich reef material (pyroxenite) has the highest penetration rate with hanging wall and footwall rocks showing respectively slower rates.

The application of the UCS and penetration rate understanding on Mogalakwena Mine specific rocks types includes the more accurate scheduling of drilling rigs. Drilling rigs scheduled to drill in norite as opposed to softer reef material will

have a slower penetration rate applied. Mean UCS for different stratigraphy's can be used for accurate scheduling. Drilling responses can help identify stratigraphic boundaries. These uses are a cost effective means to increase geological knowledge and limit costs in poor scheduling.

The investigation of pattern 326/063 showed that reef material can be found within the hanging wall. Faster penetration rates in such areas can be investigated before blasting. This implies an effective reef identification tool which adds more ore to the mine where it would not have been identified.

Drilling rigs vary in performance due to differences in machinery characteristics; bit type, motor wear and rod diameter. Mean drilling performance shows up to 100% difference in performance between rigs. Maximum penetration rate is 30.85m/h while the lowest is 12.83m/h. Mean penetration rate for the fleet is 24.48m/h (Appendix 5). Applying standard penetration rates across the fleet is not accurate. Controllable variables included feed force (WOB) and rotation. Limiting the parameters that vary will increase the accuracy of determining penetration rates per rock type in further studies. Variation of ROP in a single rock type (single composition) could be due to textural or grain size differences. UCS differences must be above 40MPa to eliminate the "noise". Such UCS variation exists in a single rock type if grain size is included. Further study is necessary to link grain size and penetration rates to empirically prove this.

MWD technology has enhanced the utilisation of drilling performance variables. RockMa makes use of drilling parameters to indicate rock strength. The system is currently identifying weathered horizons in the reef package at Cut 8. This alerts the geologists at the mine that the material should not be fed to the plant due to the adverse effects of oxidised ore on flotation. In areas where a weathered zone lies above a fresh zone in a single bench, the RockMa system can be used to identify the depths which need to be mined using flitches. Knowing the depth at which the reef becomes less oxidised is highly valuable for achieving planned recoveries.

This rock strength information can be calibrated and used to update a UCS model for patterns before blasting. Drilling response information can be used with chip logging information (texture and grain size) and XRF data for geometallurgical domaining. It is recommended from this study that actual UCS test work is used to calibrate the RockMa system with the exploration PLI data (converted to UCS) being used as a guide.

In summary, ROP values are not accurate enough to identify rock type due to many other variables which affect performance (Heinz, 2009; Bourgoyne *et al*., 1986). However, accurate stratigraphy knowledge can assist in drill rig scheduling. MWD information (including ROP) can give instruction as to the method of loading and quality of the reef material (oxidised). Calibration will allow the creation of a rock strength model for a single blast pattern at a tighter grid (5x6m) than that created from exploration boreholes (50x50m). Once calibration is complete, the RockMa system may be used to guide rock type identification when linked to XRF and textural descriptions from RC sampling. The concentrator can be alerted to an increase in hardness of feed ore.

6.2.5 Rock Strength Modelling

A geometallurgical model requires accurate sampling of ore variables. Spacing of data points and level of uncertainty needs to be recognised (Deutch, 2013). Increases in complexity reduce the model utility if it is not aligned to mining operational scale. Increased uncertainty in the rock properties will undermine the certainty in the prediction of processing variables (Deutch, 2013). Useful models of comminution need to represent the application of energy to breakage mechanism (crusher or ball mine) (Napier-Munn *et al*., 1999). Similar representation is needed for other mining processes including drilling performance response. Such a model would be used to simulate optimisation of a comminution circuit and drilling performance. A rock strength model (UCS) can

be used to forecast crushing and potentially grinding throughput (Burger *et al*., 2006).

This project made use of some of the guidelines from Deutsch (2013) in establishing the workflow in creating a practical strength model. The variable used was the grain size adjusted UCS value for rock types. Where a grain size adjusted value did not exist, the mean UCS (as recorded in the exploration database) was used. This is not the first UCS model produced for Mogalakwena Mine; however, this model represents the first which incorporates the effects of grain size.

The strength model does not directly represent crushing or milling as this parameter is not suitable (Barrat & Doll, 2008). The link between BWI, DWT and UCS is not fully established at Mogalakwena Mine. The strength model does allow for increased effectiveness in the planning and scheduling of drilling equipment. Rock strength will have a direct influence on drilling performance and bit wear (Heinz, 2009; Bourgoyne *et al*., 1986). Other variables can be overlain and the relationships can be established i.e. CaO and UCS.

The more accurate UCS model created can be immediately applied to drilling operations at the mine. If a relationship between BWI, and another variable which proxies comminution performance, exists, the model's application can be expanded.

6.2.6 Potential Financial Benefits

The financial benefits can be immediately realised through the strength characterisation of feed material to the South Plant. South Plant requires coarse and fine material feed to the autogenous mills. The correct ratio (6:4) of coarse and fine feed material would be achieved by modelling the in pit ore hardness data from the RockMa drilling system. The mine ore would be stockpiled separately using an initial division of 190Mpa which would separate pyroxenite and feldspathic pyroxenite end members. The result of optimised feed material would

be the stabilisation of the fine and coarse stockpiles before the milling stage. The mills would have less standing time due to proactive loading practices pre-empting the requirements of the plant. The calculated financial benefit of optimising feed material hardness would lead to an annual increase of **R51 353 773.97.** The same strategy would not work at North Plant due to the use of the HPGR and ball mills.

The model created would guide planning in the establishment of the correct ratio of soft to hard feed material to South plant. RockMa drilling would validate the hardness model through the MWD strength data produced. The shovel can be placed at the appropriate point to load according to the plant's immediate requirements.

6.3 Conclusion

Mining and plant equipment performance is directly affected by rock properties. Rock strength and hardness share two related characteristics which determine the breakage features of ore in various scenarios. Equipment at various stages must be aligned to the characteristics of the ore body.

Different rock types have differing rock strengths due to a variety of determinants. Three rock properties were examined to determine the rock strength of the most abundant ore types at Mogalakwena Mine, namely; composition, texture and grain size.

The major ore types were identified by their proportion in the exploration database and confirmed by company reports. The major ore types were separated into their most abundant textures and grain sizes. This allowed for the identification of simplified and representative textural and grain size populations within each major ore bearing rock type. Using the texture and grain size populations identified describe 90% occurrences of each rock type.

The large UCS database, as calculated from PLI test work, was linked to the textural and grain size distributions allowing for more detailed rock strength ranges. Unaltered rock types showed a clear inverse relationship between grain size and rock strength. The relationship was validated using a smaller data set. In general, grain size has more influence on rock strength than textural variation. Altered ores and granofels had a more complex relationship due to the complexity in composition and higher degree of variation in texture. Two distinct strength results were identified when granofels was separated into two components; fine-grained mafic and medium-grained felsic component. The area investigated did not contain enough strength data for calc-silicate. The results also highlight that PLI testing must be carried out with accuracy and the correct training of the operator is important due to the significance of the data created.

The project also highlighted the potential for combining plant specific hardness tests to the rock strength data. The differences in UCS of other rocks fall within a small range and this conforms to the differences in plant throughput. However, the dataset used to link BWI, DWT and UCS relied on means only.

It is widely proven that the drill rig penetration rate is affected by rock strength. Penetration rates have been proven to change across stratigraphic units and major rock types. More accurate rock strength domains applied to the mine will increase the accuracy of drill rig scheduling. Qualitative MWD data as gathered through the RockMa system identifies areas of substantial weakness (oxidised ore) and strength (norite and granofels). Penetration rates alone can identify the reef which will assist in establishing the HW - reef contact and the identification for additional blast hole sampling. Penetration rates do vary per machine and whether a sweeper is installed. Areas of weakness can be delineated to be loaded as flitches. Identifying pyroxenite and calc-silicate is the area of largest value for modelling comminution. Pyroxenite is the weakest of the reef rocks and is identified by penetration rates. The data set could not correlate grain size to penetration rate.

The basic model created provides the first grain size adjusted UCS geotechnical model for Mogalakwena Mine. The level of detail in data, although low, matches the scale of operation and selectivity ability. Its use can extend to drill rig scheduling, blast indexing and, potentially, crusher and milling performance prediction. The additional datasets can be overlain over the base UCS model; such as BWI and DWT results for patterns. Processing issues in the plant can be traced to specific patterns which will not include grain size adjusted UCS information.

A system to link rock property identification including texture and grain size was created to add to the SABLE database for chip logging. This information will assist in creating the link between grain size and penetration rate. The dataset will provide a high level of data support due to its size. Additionally, the findings can be applied to other geometallurgical research that is being done at Mogalakwena Mine.

The financial benefits can be immediately realised through the strength characterisation of feed material to the South plant. This would be achieved through feeding a 6:4 ratio of soft to hard (terms used loosely) material as determined through modelling the ore hardness data from the RockMa system.

The result of optimised feed material would be the stabilisation of the fine and coarse stockpiles before the milling stage. The mills would have less standing time due to proactive loading practices pre-empting the requirements of the plant.

In summary, the project has achieved the following:

- Illustrated the relationship between grain size and UCS in unaltered rocks.
- Justification for alteration, grain size and texture in chip logging.
- Justification for installation of sweeper installation on drilling rigs.
- Model of grain size adjusted UCS.
- RockMa reef identification for use in Geology Department.

- Separation of granofels into felsic and mafic component for logging.
- Importance of training and simplicity in logging and PLI testing.

The financial benefits were not analysed in this project. It is intrinsically suggested in the research outcome that cost saving will be realised in:

- Accurate scheduling of drilling rigs to minimise standing time.
- Blasting indexing related to rock type rather than stratigraphy.
- Energy efficiency of comminution due to optimised milling times (this is assuming the BWI and UCS data sets are correlated).

Value addition will be realised in:

- MWD strength information generation.
- Strength modelling more accurately reflects rock characteristics.
- Stabilisation of feed material to South Plant.

The project has shown that interdisciplinary communication and information sharing can provide a framework for problem identification and solution. Solutions offer cost saving or value addition opportunities.

6.4 Recommendations

The following recommendations for Mogalakwena Mine can be made using the results from this investigation:

- Export function for RockMa strength data immediately necessary.
- Calibration of RockMa strength data with large exploration database.
- PLI derived UCS can never replace actual UCS test work.
- QAQC on PLI testing at exploration department needed.
- Apply grain size and texture logging to chips.
- Simplification of look ups for texture and grain size.

- Metallurgical tests on ore hardness must include grain size description.
- Granofels to be separated for strength using composition and not texture.
- Drill rig scheduling based on penetration rates for varying rock types.
- Ore strength domaining for stabilisation of feed to South Plant to realise increased financial benefits.

REFERENCES

Adeyemo, A.T. & Olaleye, B.M., 2012. Establishing Relationships between some Engineering Properties of Granitic Rock Types in Selected Quarries in South-West, Nigeria. *Jornal of Emerging Trends in Applied Sciences*, 3(6), pp.934-37.

Afolabi, A.S., Nkobane, M.P. & Abdulkareem, A.S., 2012. Development of PGMs and Chrome Extraction Circuit from UG2 Ore. In *Proceedings of the World Congress of Engineering*. London, 2012.

Akram, M. & Bakar, Z.A., 2007. Correlation between Uniaxial Compressive Strength and Point Load Index for Salt-Range Rocks. *Pakistan Journal of Engineering and Applied Science*, 1.

Allen, S.W., 1996. *General Geology and History of the Potgietersrus Prospect*. Technical Report fo Anglo Platinum. Unpublished.

Armitage, P.E.B., McDonald, I., Edwards, S.J. & Manby, G.M., 2002. *PGE Minerlaisation in the Platreef and Calc-Silicate Footwall at Sandsloot, Potgiersrus District, South Africa*.

Atals Copco, 2012. *Blast hole Drilling in Open Pit Mining*. 3rd ed. Texas, USA: Ulf Linder.

Bar-Cohen, Y. & Zacny, K., eds., 2009. *Drilling in Extreme Environments: Penetration and Sampling on Earth and other Planets*. 1st ed. Weinheim: Wiley-VCH.

Barrat, D. & Doll, A., 2008. *Testwork Programs that Deliver Multiple Data Sets of Comminution Parameters for use in Mine Planning and Project Engineering*. Canada.

Bell, F.G., 1983. *Fundamentals of Engineering Geology*. 1st ed. London: Butterworth & Co.

Bourgoyne, A.T., Milheim, K.K., Chenevert, M.E. & Young, F.S., 1986. *Applied Drilling Engineering*. 2nd ed. TX: Richardson.

Brady, B.H.G. & Brown, E.T., 2006. *Rock Mechanics: For Underground Mining*. 3rd ed. Dordrecht, The NEtherlands: Springer.

Broch, E. & Franklin, J.A., 1972. The Point Load Strength Test. *International Journal of Rock Mechanics and Mining Science,* 9, pp.669-97.

Burger, B. *et al*., 2006. *Batu Hijau Model for Throughput Forecast, mining and Milling Optimisation and Expansion Studies*. Brisbane: Newmont Mining Corporation.

Bye, A.R., 2003. *The Development and Application of a 3D Geotechnical Model for mining Optimisation, Sandsloot Open Pit Platinum mine, South Africa*. Doctoral Thesis. Durban: University of Natal.

Bye, A., 2004. *PPRust North Geotechnical Review*. Internal report. Mogalakwena Mine.

Bye, A., 2005. *Geotechnical, Metallurgical and Blasting Information for Blast 138-055*. Internal Angla Platinum Report. PPL.

Cairncross, B. & Dixon, R., 1995. Minerals of South Africa. *Geological Magazine,* 134(02), p.290.

Cawthorn, R.G., Barton, J.M. & Viljoen, M.J., 1985. Interaction of Floor Rocks with the Platreef on Overysel, Potgietersrus, Northern Transvaal. *Economic Geology*, 80, pp.988-1006.

Chibaya, A., 2013. *Geometallurgical Analysis - Implications on Operating Flexibility*. MSc Report. Johannesburg: Unpublished University of the Witwatersrand.

Cohen, H.E., 1983. Energy Usage in Mineral Processing. *Transactions - Institution of Mining and Metallurgy*, pp.160-63.

Deutch, C.V., 2013. Geostatistical Modelling of Geometallurgical Variables - Problems and Solution. In *The Second AUSIMM International Geometallurgy Conference*. Brisbane, 2013. AUSIMM.

Dhungana, S., 2013. *Properties of Rocks*. Sushil Dhungana.

Doll, A.D., Barrat, D.J. & Wood, K., 2003. *Comparison of UCS to Bond Work Indices*. Vancouver.

Gloy, G., 2005. *PPRust North Exploration Project: Mineralogical Investigation of Zwartfontein Boreholes*. Johannesburg: Anglo Platinum Management Services (Pty) Ltd Anglo Platinum Research Centre – Mineralogical Research Department.

Gloy, G. & Hey, P.V., 2002. *PPRust North Expansion Project: Mineralogical Investigation of Altered and Unaltered A-Reef and B-Reef Drillcore Samples from Overysel*. Johannesburg: ARC - Mineralogical Research Department.

Gokhale, B.V., 2010. *Rotary Drilling and Blasting in Large Surface Mine*. 1st ed. CRC Press.

Hayes, S. & Piper, P.S., 2003. *Point Load Tests on Various Rock Types at Potgietersrus Platinum Mine for Determination of Rock Strength*. Johannesburg: Groundwork Consulting (Pty) Ltd.

Heinz, W.F., 2009. *Diamond Drilling Handbook*. 4th ed. Halfway House: W.F. Heinz.

Holwell, D.A. & McDonald, I., 2010. A Review of the Behaviour of Platinum Group Elements within Natural Magmatic Sulfide Ore Systems. *Platinum Metals Review*, 1, p.54.

Holwell, D.A., McDonald, I. & Armitage, P.E.B., 2006. Platinum-group mineral assemblages in the Platreef at the Sandsloot Mine, northern Bushveld Complex, South Africa. *Mineralogical Magazine*, 70(1), pp.83-101.

ISRM, 1985. Suggested Method for Determining Point Load Strength. *International Journal of Rock Mechanics, Mining Sciences and Geomechanics*, pp.51-60.

Jager, A.J. & Ryder, J.A., 1999. *A Handbook on Rock Engineering Practice for Tabular Hardrock Mines*. 1st ed. Johannesburg: The Safety in Mines Research Advisory Committee (SIMRAC).

Johnson, M.R., Anhaeusser, C.R. & Thomas, R.J., 2006. *The Geology of South Africa*. Johanesburg: Geological Society of South Africa and COuncil for Geoscience.

Kennedy, D.C., 1994. Datamine Modelling as a Tool for Ore Reserve Evaluation and Mine Design, and the Need for Standardization in Data Generation. In *XVth CMMI Congress*. Johannesburg, 1994. SAIMM.

Kinnaird, J.A. *et al*., 2010. Along-strike and down-dip variations in multiphase sills of the Platreef, Bushveld Complex. In *11th International Platinum Symposium*. Ontario, 2010. Ontario Geological Survey.

Little, M.J., 2006. *Geotechnical Strategy and Tactics at Anglo Platinum's PPRust Open Pit Operation, Limpopo Province, South Africa*. Masters Disertation. Johannesburg: University of Witswatersrand.

Maier, W.D. *et al*., 2007. Petrogenesis of Contact-style PGE Mineralisation in the Northern Lobe of the Bushveld Complex: Comparison of Data from the Farms Rooipoort, Townlands, Drenthe and Nonnenwerth. *Mineralium Deposita*.

McDonald, I., Holwell, D.A. & Armitage, P.E.B., 2005. *Stratigraphy and Platinum-Group Element Mineralization in the Northern Lobe of the Bushveld Complex, South Africa*. Cardiff University and University of Greenwich.

McLean, E. & Watt, J., 2009. Processing Strategies for Hidden Valley Operations. In *Tenth Mill Operators' Conference*. Adelaide, 2009.

Mwanga, A., Rosenkranz, J. & Lamberg, P., 2015. Testing of Ore Comminution Behaviour in the Geometallurgical Context - A Review. *Minerals*, 5, pp.276-97.

Napier-Munn, T.J., Morrell, S., Morrison, R.D. & Kojovic, T., 1999. *Mineral Comminution Circuits: Their Operation and Optimisation*. Indooroopilly, Australia: Julius Kruttschnitt Mineral Research Centre.

Nex, P., Kinnaird, J., Jones, B. & Colloty, A., 2006. *Platreef Rock Type Definitions and Descriptions*. Anglo American Platinum.

Osgouei, R.E., 2007. *Rate of Penetration Estimation Model for Directional and Horizontal Wells*. Masters Thesis. The Graduate School of Natural and Applied Sciences of Middle East Technical University.

Ozturk, C.A., Nasuf, E. & Kahraman, S., 2014. Estimation of Rock Strength from Quantitative Assessment of Rock Texture. *The Journal of the Southern African Institute of Mining and Metallurgy,* 114, pp.471-80.

Palmstrom, A., 1995. *RMi - A Rock Mass Characterization System for Rock Engineering Purposes*. PhD Thesis. Norway: Oslo University.

Paterson, M.S. & Wong, T., 2005. *Experimental Rock Deformation - The Brittle Field*. 2nd ed. The Netherlands: Springer.

Pells, P.J.N., 1975. *Australian Geomechanics Journal*, 24, pp.54-56.

Prikryl, R., 2001. Some microstructural aspects of strength variation in rocks. *International Journal of Rock Mechanics*, 38, pp.671-82.

Radzivhoni, C., Spichiger, S., Muzondo, T. & Harney, D.M.W., 2014. *Geometallurgical Sampling: The practice at Mogalakwena Platinum Mine, South Africa*. Anglo American Platinum.

Roberts, J.R. & Reinecke, P., 2003. *Mineralogy and Floatation Response of the PPL North Pit 'A-Reef' Pyroxenite*. Germiston: Anglo Platinum Management Services (Pty) Ltd Anglo Platinum Research Centre.

Saliu, M.A., Akindoyeni, A.F. & Okewale, I.A., 2013. Correlation between Blast Efficiency and Uniaxial Compressive Strength. *International Journal of Engineering and Technology*, 3(8).

Schouwstra, R.P. & de Vaux, D.V., 2013. *Geometallurgical Domaining of Mogalakwena Ores Based on Chemistry: Some Preliminary Metallurgical Data*. Johannesburg: Technical Solutions - Research.

Walraven, F., Armstrong, R.A. & Kruger, F.J., 1990. A Chronostratigraphic Framework for the North-Central Kaapval Craton, the Bushveld Complex and Vredefort Structure. *Tectonophysics*, 23-48(171).

White, J.A., 1994. The Potgietersrus Prospect - Geology and Exploration History. In *XVth CMMI Congress*. Johannesburg, 1994. SAIMM.

Ziemski, M. *et al*., 2010. An Integrated Geology-Mine-Plat and Eco-Efficiency Simulator for Anglo Platinum's Evaluation and Operational Improvement Initiatives. In *XXV International Mineral Processing Congress (IMPC) 2010 Proceedings*. Brisbane, Australia, 2010.

APPENDIX